Final Report

GUIDELINES FOR USE OF MODIFIERS IN SUPERPAVE MIXTURES

EXECUTIVE SUMMARY

and

VOLUME 1 OF 3 VOLUMES: EVALUATION OF SBS MODIFIER

UF Project No.:	4910-4504-718-12
State Job No.:	99052793
Contract No.:	BC-354 (RPWO#1)

Submitted to:

Florida Department of Transportation
605 Suwannee Street
Tallahassee, FL 32399

by

Principal Investigator: Reynaldo Roque, Professor
Co-Principal Investigators: Bjorn Birgisson, Assistant Professor; Mang Tia, Professor
Researcher: Booil Kim; Zhanwu Cui

Department of Civil and Coastal Engineering
College of Engineering
University of Florida
365 Weil Hall
P.O. Box 116580
Gainesville, FL 32611-6580
Tel: (352) 392-9537, extension 1458
Fax: (352) 392-3394

UNIVERSITY OF FLORIDA

January 2004

Technical Report Documentation Page

1. Report No.	2. Government Accession No.	3. Recipient's Catalog No.
Final Report, 3 volumes		

Comment: Print all on scanner printer, but must print Metric Conversion page on scanner printer . . .

4. Title and Subtitle	5. Report Date
Guidelines for Use of Modifiers in Superpave Mixtures: Executive Summary and Evaluation of SBS Modifier	January 2004
	6. Performing Organization Code
7. Author(s)	8. Performing Organization Report No.
Reynaldo Roque, Bjorn Birgisson, Mang Tia, Booil Kim and Zhanwu Cui	4910-4504-718-12
9. Performing Organization Name and Address	10. Work Unit No. (TRAIS)
University of Florida Department of Civil and Coastal Engineering 365 Weil Hall / P.O. Box 116580 Gainesville, FL 32611-6580	
	11. Contract or Grant No.
	BC354, RPWO #1
12. Sponsoring Agency Name and Address	13. Type of Report and Period Covered
Florida Department of Transportation Research Management Center 605 Suwannee Street, MS 30 Tallahassee, FL 32301-8064	Final Report, Vol. 1 of 3 Sept. 15, 1999 – Sept. 15, 2003
	14. Sponsoring Agency Code

15. Supplementary Notes

Prepared in cooperation with the Federal Highway Administration

16. Abstract

A laboratory investigation was conducted to evaluate the effects of SBS polymer modification on the cracking resistance and healing characteristics of Superpave mixtures. Asphalt mixtures with low and high design asphalt contents using unmodified and SBS modified asphalt cements were produced in the laboratory. Tests performed with the Superpave IDT included resilient modulus tests, creep tests, repeated load fracture tests, healing tests, strength tests at two loading rates, as well as longer-term creep tests to failure. The test results showed that the benefit of SBS modifiers to mixture cracking resistance appeared to be derived primarily from a reduced rate of micro-damage accumulation. The reduced rate of damage accumulation was reflected in a lower m-value without a reduction in fracture limit. However, SBS modifier does not appear to influence healing or aging of asphalt mixture. Therefore, it was shown that the benefits of the SBS modifier were clearly identified by using the HMA fracture model, which accounts for the combined effects of m-value and fracture energy limit on cracking resistance. It was also determined that the residual dissipated energy as determined from Superpave IDT strength tests appears to be uniquely associated with the presence and benefit of SBS modification, and may provide a quick way to make relative comparisons of cracking performance. Longer-term creep tests showed that time to crack initiation appeared to provide another parameter uniquely related to the effects of SBS modification. Cost analyses indicate that the construction cost of AC layer would be reduced by using SBS modifier. Consequently, the use of SBS modified mixtures was clearly justified. In conclusion, the key to characterizing the effects of SBS modifier on the cracking resistance of asphalt mixture is in the evaluation of the combined effects of creep and failure limits.

17. Key Words	18. Distribution Statement
Superpave, SBS Modifier, Asphalt Mixture, Cracking, Indirect Tension, Polymer	No restrictions. This document is available to the public through the National Technical Information Service, Springfield, VA, 22161

19. Security Classif. (of this report)	20. Security Classif. (of this page)	21. No. of Pages	22. Price
Unclassified	Unclassified	131	

Form DOT F 1700.7 (8-72)

Reproduction of completed page authorized

DISCLAIMER

"The opinions, findings and conclusions expressed in this publication are those of the authors and not necessarily those of the Florida Department of Transportation or the U.S. Department of Transportation.

Prepared in cooperation with the State of Florida Department of Transportation and the U.S. Department of Transportation."

SI* (MODERN METRIC) CONVERSION FACTORS

APPROXIMATE CONVERSIONS TO SI UNITS

Symbol	When You Know	Multiply By	To Find	Symbol
		LENGTH		
in	inches	25.4	millimeters	mm
ft	feet	0.305	meters	m
yd	yards	0.914	meters	m
mi	miles	1.61	kilometers	km
		AREA		
in^2	square inches	645.2	square millimeters	mm^2
ft^2	square feet	0.093	square meters	m^2
yd^2	square yards	0.836	square meters	m^2
ac	acres	0.405	hectares	ha
mi^2	square miles	2.59	square kilometers	km^2
		VOLUME		
fl oz	fluid ounces	29.57	milliliters	ml
gal	gallons	3.785	liters	l
ft^3	cubic feet	0.028	cubic meters	m^3
yd^3	cubic yards	0.765	cubic meters	m^3
NOTE: Volumes greater than 1000 l shall be shown in m^3.				
		MASS		
oz	ounces	28.35	grams	g
lb	pounds	0.454	kilograms	kg
T	short tons (2000 lb)	0.907	megagrams	Mg
		TEMPERATURE (exact)		
°F	Fahrenheit temperature	5(F-32)/9 or (F-32)/1.8	Celcius temperature	°C
		ILLUMINATION		
fc	foot-candles	10.76	lux	l
fl	foot-Lamberts	3.426	candela/m^2	cd/m^2
		FORCE and PRESSURE or STRESS		
lbf	poundforce	4.45	newtons	N
psi	poundforce per square inch	6.89	kilopascals	kPa

APPROXIMATE CONVERSIONS FROM SI UNITS

Symbol	When You Know	Multiply By	To Find	Symbol
		LENGTH		
mm	millimeters	0.039	inches	in
m	meters	3.28	feet	ft
m	meters	1.09	yards	yd
km	kilometers	0.621	miles	mi
		AREA		
mm^2	square millimeters	0.0016	square inches	in^2
m^2	square meters	10.764	square feet	ft^2
m^2	square meters	1.195	square yards	yd^2
ha	hectares	2.47	acres	ac
km^2	square kilometers	0.386	square miles	mi^2
		VOLUME		
ml	milliliters	0.034	fluid ounces	fl oz
l	liters	0.264	gallons	gal
m^3	cubic meters	35.71	cubic feet	ft^3
m^3	cubic meters	1.307	cubic yards	yd^3
		MASS		
g	grams	0.035	ounces	oz
kg	kilograms	2.202	pounds	lb
Mg	megagrams	1.103	short tons (2000 lb)	T
		TEMPERATURE (exact)		
°C	Celcius temperature	1.8C + 32	Fahrenheit temperature	°F
		ILLUMINATION		
lx	lux	0.0929	foot-candles	fc
cd/m^2	candela/m^2	0.2919	foot-Lamberts	fl
		FORCE and PRESSURE or STRESS		
N	newtons	0.225	poundforce	lbf
kPa	kilopascals	0.145	poundforce per square inch	psi

* SI is the symbol for the International System of Units. Appropriate rounding should be made to comply with Section 4 of ASTM E380.

(Revised August 1992)

ACKNOWLEDGMENTS

The authors would like to acknowledge and thank the Florida Department of Transportation (FDOT) for providing technical and financial support and materials for this project. Special thanks go to engineers and technicians of the Bituminous Section of the State Materials Office for their contributions in terms of their expert knowledge, experience, and construction advice throughout the course of this work. Their efforts are sincerely appreciated and clearly made a decisive impact on the quality of the research.

TABLE OF CONTENTS

page

ACKNOWLEDGMENTS ii
LIST OF TABLES v
LIST OF FIGURES vii
EXECUTIVE SUMMARY xi

CHAPTERS
1 INTRODUCTION 1
1.1 Background 1
1.2 Objectives 2
1.3 Scope 3

2 LITERATURE REVIEW 4
2.1 Fatigue Cracking 4
2.2 Material Properties from Superpave IDT 6
2.3 Fatigue Analysis 7
2.3.1 Traditional Fatigue Approach 7
2.3.2 Continuum Mechanics Approach 9
2.3.3 Fracture Mechanics Approach 9
2.4 Healing 12
2.5 Modifiers 14

3 MATERIALS AND METHODS 21
3.1 Materials 21
3.1.1 Aggregates 21
3.1.2 Asphalt Binders 22
3.2 Asphalt Mixture Design 23
3.2.1 Selection of Traffic Level 24
3.2.2 Batching and Mixing 24
3.2.3 Compaction 25
3.3 Test Specimens 27
3.4 Test Procedures 29
3.4.1 Standard Superpave IDT 31
3.4.1.1 Resilient modulus test 31
3.4.1.2 Creep test 33
3.4.1.3 Strength test 36
3.4.2 Repeated Load Fracture Test 37
3.4.3 Strength Tests at Slower Loading Rates 38
3.4.4 Longer-Term Creep Tests to Failure 38
3.4.5 Healing Test 39

4 EVALUATION OF FATIGUE CRACKING 41
4.1 Standard Superpave IDT 41
4.1.1 General Properties 41
4.1.2 Temperature Sensitivity 44
4.2 Repeated Load Fracture Test 48
4.3 Strength Tests at Slower Loading Rates 51
4.4 Longer-Term Creep Tests to Failure 54
4.5 HMA Fracture Model 56
4.6 Long Term Aging Effect 58
4.7 Aggregate Structure Effect 61

5 EVALUATION OF HEALING 64
5.1 Healing Test 64
5.2 Determination of Healing Parameters 65
5.3 Healing Rates 68
5.4 Damage Recovery 71

6 COST ANALYSIS FOR USE OF SBS MODIFIER 79
6.1 Pavement Design 79
6.2 Calculation of Energy Ratio 81
6.3 Cost Analysis 85

7 FINDINGS AND CONCLUSIONS 94
7.1 Findings 94
7.2 Conclusions 96

APPENDIX
A AGGREGATE BATCH WEIGHT SHEETS 98
B ASPHALT MIX DESIGN AND VOLUMETRIC PROPERTIES OF MIXTURES 101
C INDIRECT TENSILE TEST (IDT) DATA 114
D HEALING TEST RESULTS 116
E AC LAYER THICKNESS FOR COST ANALYSIS 123

REFERENCES 129

LIST OF TABLES

Table page

2.1 Classification of Polymer 15

3.1 Aggregate Blend Proportions 22

3.2 Asphalt Binder Properties 23

3.3 Traffic Levels and Gyratory Compaction Effort 24

3.4 Test Samples 27

4.1 Superpave IDT Results (Coarse 1, STOA) 42

6.1 Design Layer Thickness and Calculated Stresses 80

6.2 Factorial Design for Parametric Study 82

6.3 Energy Ratios Calculated for Conventional Pavement Structures 82

6.4 Energy Ratios Calculated for Full Depth AC Pavement 83

6.5 Energy Ratios Calculated for HMA Overlay 84

6.6 Cost of AC Layer to Meet ER_{min} in Conventional Pavement 86

6.7 Cost of AC Layer to Meet ER_{min} in HMA Full Depth Pavement 88

6.8 Cost of AC Layer to Meet ER_{min} in HMA Overlay Pavement 88

6.9 Costs of AC Layer With the Equivalent ER 92

A.1 Cumulative Batch Weight (IDT Samples) 99

A.2 Cumulative Batch Weight (MTD Samples) 100

B.1 Volumetric Properties for Asphalt Mix Design (Coarse 1) 102

B.2 Volumetric Properties for Asphalt Mix Design (Fine 1) 108

C.1 Superpave IDT Results (Coarse 1, LTOA) 115

C.2 Superpave IDT Results (Fine 1, STOA) 115

E.1 Tensile Stress at the Bottom of AC Layer to Meet ER_{min} for Conventional Pavement 124

E.2 AC Layer Thickness to Meet ER_{min} for Conventional Pavement 125

E.3 AC Layer Thickness to Meet ER_{min} for HMA Full Depth Pavement 126

E.4 AC Layer Thickness to Meet ER_{min} for HMA Overlay 127

E.5 AC Layer Thickness and Tensile Stress of Unmodified AC Layer to Meet ER of Modified Mixture 128

LIST OF FIGURES

Figure page

2.1 Schematic locations of shear and tensile stress zones in the asphalt concrete pavement 5

2.2 Classification of polymers based on link-structure 17

2.3 SBS modifier structure 18

3.1 Aggregate gradations (Coarse 1 and Fine 1) 22

3.2 Batching 25

3.3 Mixing 26

3.4 Compacting 26

3.5 Slicing the sample 29

3.6 Gage point attachment 30

3.7 Marking the loading axis 30

3.8 Power model of the creep compliance 34

3.9 Determination of fracture energy and dissipated creep strain energy to failure 37

3.10 Typical behavior and initial failure in creep 39

4.1 Fracture energy and m-value from Superpave IDT 43

4.2 Temperature sensitivity of resilient modulus 44

4.3 Temperature sensitivity of tensile strength 45

4.4 Temperature sensitivity of failure strain 46

4.5 Temperature sensitivity of fracture energy 46

4.6 Temperature sensitivity of creep compliance 47

4.7 Temperature sensitivity of m-value 47

4.8 Temperature sensitivity of D_1 48

4.9 Determination of initial resilient deformations (δ_i) and original resilient deformation (δ_o) 49

4.10 Fracture test results (STOA, Coarse 1, and 10° C) 50

4.11 Creep compliance of coarse-graded mixtures (10° C, STOA) 51

4.12 Comparison of tensile strength at different loading rates 52

4.13 Comparison of failure strain at different loading rates 53

4.14 Determination of the residual dissipated energy (6.1% SBS modified mixture) 53

4.15 Comparison of residual dissipated energy 54

4.16 Creep test results (DCSE vs. time) 55

4.17 Comparison of $DCSE_f$ between creep and strength test 56

4.18 Comparison of measured and predicted N_f 57

4.19 Relative effect of SBS modifier for different asphalt contents on predicted N_f across all temperatures 58

4.20 Fracture test results (LTOA, Coarse 1, and 10° C) 59

4.21 Comparison of measured and predicted N_f of LTOA mixtures 59

4.22 Comparison of predicted N_f between STOA and LTOA mixtures 60

4.23 Comparison of D_1 between STOA and LTOA mixtures 61

4.24 Comparison of predicted N_f of coarse and fine-graded mixtures 62

4.25 Relationship between predicted N_f and creep compliance 63

4.26 Relationship between predicted N_f and fracture energy 63

5.1 Healing test results, loading (1000 cycles with 75 psi) & healing at 15° C 64

5.2 Comparison of healing rate at 15° C (after 1000 loading cycles at 75 psi) 65

5.3 Relationship between total accumulated damage and healing rate (1000 cycles loading with 75 psi & healing at 15° C) 66

5.4 Healing test at different DCSE for modified mixtures with 6.1% AC (loading with 55 psi & healing at 20° C) 67

5.5 Healing rates in terms of DCSE with different $DCSE_{applied}$ on same mixtures (6.1SBS, loading with 55 psi & healing at 20° C) 67

5.6 Healing rates in terms of $DCSE/DCSE_{applied}$ with different $DCSE_{applied}$ on same mixtures (6.1SBS, loading with 55 psi & healing at 20° C) 68

5.7 Normalized healing (after 1000 cycles of loading with 75 psi at 15° C) 69

5.8 Comparison of normalized healing rates at 15° C 69

5.9 Temperature sensitivity of normalized healing rate 71

5.10 Resilient deformations during loading and healing 72

5.11 Series of repeated loading for determining the damage recovery rate 74

5.12 Typical healing test results for determining the rate of damage recovery (72SBS, 500 lb of cyclic loads at 20° C) 75

5.13 Normalized damage recovery rates of mixtures at three temperatures 76

5.14 Temperature sensitivity of normalized damage recovery rate 77

5.15 Relationship between normalized damage recovery rate and D_1 78

5.16 Relationship between normalized damage recovery rate and m-value 78

6.1 Comparison of construction cost of AC layer depending on mixture properties for conventional pavement and low traffic level 87

6.2 Comparison of construction cost of AC layer depending on pavement structure and traffic level for the mixtures with $DCSE_f = 1.0$ (KJ/m^3) and $D_1 = 14 \times 10^{-7}$ (l/psi) 91

B.1 Volumetric properties with number of gyrations at 4% air voids (Coarse 1) 103

B.2 Volumetric properties with asphalt contents at $N_d = 75$ (Coarse 1) 104

B.3 Volumetric properties with asphalt contents at $N_d = 100$ (Coarse 1) 105

B.4 Volumetric properties with asphalt contents at $N_d = 125$ (Coarse 1) 106

B.5 Percentage of Gmm (Coarse 1) 107

B.6 Volumetric properties with number of gyrations (Fine 1) 109

B.7 Volumetric properties with asphalt contents at N_d = 75 (Fine 1) 110

B.8 Volumetric properties with asphalt contents at N_d = 100 (Fine 1) 111

B.9 Volumetric properties with asphalt contents at N_d = 125 (Fine 1) 112

B.10 Percentage of Gmm (Fine 1) 113

D.1 Healing test (6.1% unmodified asphalt, Coarse 1, 2000 lb cyclic load at 0° C) 117

D.2 Healing test (6.1% modified asphalt, Coarse 1, 2000 lb cyclic load at 0° C) 117

D.3 Healing test (7.2% modified asphalt, Coarse 1, 2000 lb cyclic load at 0° C) 118

D.4 Healing test (6.1% unmodified asphalt, Coarse 1, 1200 lb cyclic load at 10° C) 118

D.5 Healing test (7.2% unmodified asphalt, Coarse 1, 1000 lb cyclic load at 10° C) 119

D.6 Healing test (6.1% modified asphalt, Coarse 1, 1200 lb cyclic load at 10° C) 119

D.7 Healing test (7.2% modified asphalt, Coarse 1, 1200 lb cyclic load at 10° C) 120

D.8 Healing test (6.1% unmodified asphalt, Coarse 1, 500 lb cyclic load at 20° C) 120

D.9 Healing test (7.2% unmodified asphalt, Coarse 1, 500 lb cyclic load at 20° C) 121

D.10 Healing test (6.1% modified asphalt, Coarse 1, 400 lb cyclic load at 20° C) 121

D.11 Healing test (7.2% modified asphalt, Coarse 1, 400 lb cyclic load at 20° C) 122

EXECUTIVE SUMMARY

A comprehensive project was undertaken to evaluate the effects of SBS polymer on the cracking resistance of Superpave mixtures. Additional research was also performed to evaluate the binder rheology to predict the cracking performance of SBS modifier mixtures, and to evaluate the effect of ground tire rubber on the cracking resistance of Superpave mixtures. This summary provides a brief description of accomplishments, key findings, and recommendations resulting from this work.

The primary accomplishments may be summarized as follows:

- Laboratory mixture tests, as well as specific mixture properties and parameters were identified that reveal the beneficial effect of SBS polymer modification on pavement cracking performance.
- It was determined that the HMA fracture mechanics model developed at the University of Florida appears to accurately reflect, quantitatively, the beneficial effects of SBS polymer modification on the cracking performance of asphalt mixtures.
- Two relatively simple laboratory test procedures were identified to uniquely characterize the presence of SBS polymer modification in mixtures, which is important from the standpoint of quality assurance.
- It was determined that the effect of SBS modification must be evaluated on the basis of tests performed on modified asphalt mixture. The primary beneficial effects of the SBS polymer was not revealed in Superpave binder test results. It appears that SBS modifiers behave differently when introduced into mixtures than in bulk form.
- A methodology was developed to evaluate the cost-effectiveness of different mixtures, including modified mixtures, that considers the effect of the key mixture properties identified in this study, as well as the effect of traffic and pavement structure on pavement cracking performance.

- It was determined that the use of SBS modifiers in surface structural mixtures clearly appears to be cost effective for most pavement structures in Florida. Cost analyses indicated that the construction cost of the AC layer alone would be reduced by up to 30% by using SBS modifiers.
- It was determined that the use of SBS modifiers appears to be justified as a replacement for ground tire rubber (GTR) in open graded friction course (OGFC) mixtures. SBS modifiers provide much greater benefit than GTR in terms of pavement cracking performance. GTR appears to provide no benefit other than to allow the use of higher asphalt content in open graded mixtures. Furthermore, it was determined that SBS modifiers provide greater benefit to open graded mixtures than to dense graded mixtures, which implies that SBS modifiers would result in even greater performance benefits in OGFC mixtures than in surface structural mixtures.

Some secondary accomplishments and findings resulting from the work may be summarized as follows:

- Laboratory testing and analysis procedures were developed to measure healing in asphalt mixtures.
- Healing studies revealed that SBS modification does not appear to improve or to adversely affect the healing characteristics of asphalt mixtures. It was determined that healing was affected by the characteristics of the aggregate structure.
- SBS modification did not appear to influence the rate of aging of asphalt mixtures.
- It was determined that existing relationships between binder properties and mixture properties are unsuitable for use at intermediate in-service temperatures where cracking is thought to occur. Therefore, these relationships should not be used to evaluate the effects of using a modified binder on the cracking performance of asphalt mixtures.

The following conclusions may be derived from the accomplishments and findings summarized above:

- The key to characterizing the presence and beneficial effects of SBS modifier on the cracking resistance of asphalt mixture is in the evaluation of the combined effects of creep and failure limits. This may be accomplished in one of two ways: 1) by performing a short-term creep test followed by a strength test to obtain the mixture's m-value and fracture Energy, whose combined effects can be evaluated using the HMA fracture mechanics model developed at the University of Florida; and 2) by performing a longer-term creep test to assure cracking initiation by creep. The fracture Energy limits and m-value can also be determined from this test. In addition, the time to crack initiation provides a parameter that can be used directly to evaluate the relative cracking resistance of mixtures without further modeling. However, the longer-term creep test will generally be more time-consuming than a short-term creep and strength test.
- The residual (or post-peak) fracture Energy appears to provide a quick way to make relative comparisons of mixture cracking performance that a suitable for use with SBS modified asphalt mixtures.
- It appears that the use of SBS modified asphalt mixture in structural surface course layers would reduce construction costs and improve the cracking performance of pavement in Florida.
- The use of SBS modifiers appears to be justified as a replacement for ground tire rubber (GTR) in open graded friction course (OGFC) mixtures. Whereas GTR provides no added benefit in terms of mixture cracking performance, the results of this study clearly show that SBS modifiers significantly enhance mixture cracking performance, particularly for open graded mixtures.

Therefore, the Florida Department of Transportation (FDOT) should seriously consider specifying the use of SBS modified asphalt mixtures in structural surface course layers whenever the budget allows for their use. FDOT should also seriously consider specifying the use of SBS modified binder instead of GTR in open graded friction course mixtures.

CHAPTER 1
INTRODUCTION

1.1 Background

Superpave mix design has gained considerable popularity among various states across the country, including Florida. Superpave mix design has the following major advantages over the traditional Hveem and Marshall mix design procedures:

- Additional requirements that help to select aggregates having consensus properties.
- Selection of binders using fundamental properties that incorporates or takes into account a broader range of in-service temperatures.
- Gyratory compaction that more closely simulates field compaction and traffic conditions.

However, the Superpave mix design procedure being implemented today essentially remains a volumetric design procedure. Validated performance-based mechanical property tests for asphalt mixtures are not yet available. The volumetric design procedure assumes that the number of gyrations applied by the Superpave gyratory compactor represents the traffic conditions to which the mixture will be subjected. The design asphalt content is determined as the asphalt content required to obtain 4% air voids at the design number of gyrations for a particular level of traffic and environment. No other mechanical testing is currently required to determine whether or not the mixture is appropriate.

Therefore, Superpave mix design has essentially placed much stricter requirements on the shear resistance of the mixtures at higher temperatures, but there are no appropriate checks to guarantee cracking resistance of mixtures. Observations made over the past few years in the use of Superpave design procedure have indicated that mixtures produced with conventional asphalt binders, particularly those intended for use on high traffic volume facilities, may not have adequate resistance to cracking as a result of lower design asphalt content for such road facilities.

This observation is a direct result of the Superpave design procedure since the higher the number of gyrations (which simulates higher traffic volume) the lower the design asphalt content, thus increasing its susceptibility to cracking. Furthermore, recent experience in Florida indicated that coarse-graded Superpave mixtures could be difficult to compact and might result in pavements with relatively high permeability. The combination of high permeability and low asphalt content indicates that such mixtures may also have low fracture resistance.

The above observations indicate that it may not be possible to produce Superpave mixtures with conventional asphalt cement for certain levels of traffic and environment to have both adequate rutting and cracking resistance. According to results of recent research on modifiers, one way to achieve the above objective of producing a mixture with sufficient fracture resistance as well as desirable rutting resistance is through the use of asphalt modifiers.

The discussion presented above indicates that there is a need to identify the mixture properties that control cracking in the field and laboratory. Furthermore, there is a need to evaluate in depth the effect of modifiers on cracking properties of asphalt mixture: that is, introducing modifier may increase cracking resistance and/or introducing modifier may increase binder content without loss of rutting resistance.

1.2 Objectives

The overall objective of this study was to achieve a better understanding of how SBS polymer modification affects the cracking resistance of asphalt mixtures. A clearer understanding of these effects will lead to better guidelines for their use, as well as improved methods to characterize their benefit and to evaluate their potential benefit in specific mixtures and loading environments. More specific objectives of the study may be summarized as follows:

- Identify specific mixture properties and/or behavioral characteristics that uniquely characterize the presence of SBS polymer modification. This is important from the standpoint of quality control and field evaluation of mixtures, where the exact presence of SBS polymers may be unknown.
- Identify laboratory test methods and evaluation procedures that can be used to realistically evaluate the effects of SBS polymer modification on the cracking performance of asphalt mixtures and pavements.
- Evaluate the effect of SBS polymer modification on micro-damage healing in asphalt mixtures.
- Evaluate the cost effectiveness and establish guidelines for use of SBS modifiers in asphalt pavements.

1.3 Scope

This study focused primarily on the effects of Styrene Butadiene Styrene (SBS) block copolymer on the cracking performance of asphalt mixtures. This polymer type has been perhaps the mostly widely accepted and used for enhancing the cracking performance of asphalt pavements. The specific modified binder used in this study was provided by CITGO Asphalt Refining Company.

The aggregate used for this study was limestone, and aggregate gradation was coarse gradation (C1) and fine gradation (F1), which passes below and over the Superpave restricted zone, respectively. Mixtures were produced for two traffic levels (traffic level 2 and 6) using the Superpave Mix Design procedure.

The test method was based on the Superpave Indirect Tensile Test (IDT). In addition, fracture and healing tests were conducted to evaluate the cracking and healing properties of both unmodified mixtures and SBS modified asphalt mixtures.

CHAPTER 2
LITERATURE REVIEW

A literature review was conducted to understand: (1) fatigue cracking, which is the primary distress mode being addressed in this study; (2) fatigue and healing models, which have been developed to describe fatigue and healing of asphalt mixtures; (3) and modifiers, which may have the potential to improve fatigue cracking of asphalt mixtures. Through the literature review, it was possible to identify reliable and practical ways for evaluation in this study.

2.1 Fatigue Cracking

Fatigue cracking is one of the main distress modes in asphalt pavement. Much research has been done to help mitigate fatigue cracking. This study evaluated the effect of SBS modifier on the cracking of asphalt mixture. Consequently, it is necessary to understand the mechanism of fatigue cracking.

There are three major mechanisms taking place in asphalt concrete pavement when multi-level vehicular loads are applied at various intervals: fatigue, time-dependent behavior, and healing (Kim et al., 1994). Among them, fatigue causes cracking, so-called fatigue cracking, but the others retard cracking. It had been traditionally thought that fatigue cracking occurs at the bottom of asphalt layer when the damage accumulated by repeated loads is higher than the failure limit of asphalt mixture. In addition to conventional fatigue cracking concept, several researches have hypothesized that fatigue cracking could be propagated by tensile or shear stresses or combinations of both occurring at the bottom or the surface of asphalt concrete layer. Myers (1997) found that the high tensile stresses underneath the ribs of radial truck tires could cause surface-initiated cracking. Thus, fatigue cracking can form and grow in any location of the pavement structure where sufficiently large tensile or shear stresses or a combination of both

occur. The tensile and shear stress zones in the pavement structure are shown in Figure 2.1. Once fatigue cracking is initiated, it develops into what is commonly referred to us alligator cracking, which occurs where longitudinal cracks are connected with transverse cracks.

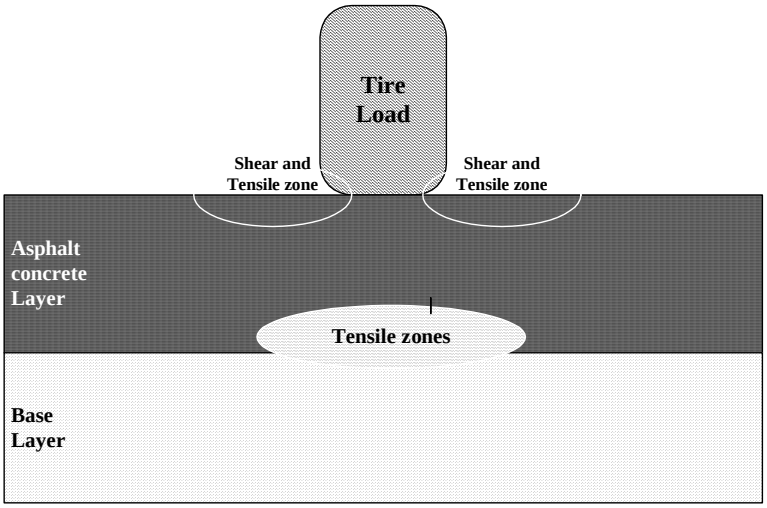

Figure 2.1 Schematic locations of shear and tensile stress zones in the asphalt concrete pavement (after Lytton et al. 2001)

Fatigue cracking is usually affected by a number of factors. Heavy wheel loads, thin pavements, or those with weak underlying layers, increase the tensile stresses and may result in fatigue cracking. Poor construction, poor drainage, insufficient cracking resistance of asphalt mixture, and under-designed pavement structure all contribute to this kind of problem. In addition, the magnitude and position of the load, in combination with pavement temperature gradients, may have a significant effect on the surface initiated cracking (Myers, 2000).

One way to overcome fatigue cracking is to use asphalt mixture that is stiff enough to withstand normal deflection and has proper strength to resist the applied tensile and shear stresses. And, it may also be possible to improve fatigue cracking performance through the use of asphalt modifier.

2.2 Material Properties from Superpave IDT

Compared to the other asphalt mixture tests, the Superpave Indirect Tensile Test (IDT) has several advantages: fundamental and diverse materials properties can be obtained; it is a relatively simple test procedure; and it has wide application in measuring materials properties. In addition to these, since much experience has been accumulated at University of Florida using the IDT, most of the tests in this study were performed using the IDT. Therefore, there is a need to identify and review the engineering and/or mechanical significance of material properties measured from IDT.

From the evaluation of the SHRP Indirect Tensile Testing System developed by Roque et al. (1997), it was known that SHRP IDT can provide reasonable and accurate asphalt mixture properties at an in-service temperature where cracking is generally presumed to occur. These mixture properties include resilient modulus, creep compliance, m-value, failure strain, tensile strength, and fracture energy. These properties are related to fatigue cracking directly and/or indirectly.

Resilient modulus indicates the stiffness of asphalt mixture at small strain or short loading times, and it is necessary to predict the response of pavement subjected to wheel loads. As described above, because resilient modulus is measured at small strain, it just gives the ratio of the applied stress and the measured strain for short loading time. Failure strain and tensile strength are the strain and stress at failure, so they are useful to evaluate whether a particular loading condition will induce pavement failure, and can be used as relative failure criteria of asphalt mixture. Fracture energy, which is the area under the stress-strain curve of strength test of IDT up to failure, is also useful to evaluate the fracture toughness for asphalt mixtures.

As a time-dependent property, creep compliance is suitable for the evaluation of permanent deformation, and it also gives the stiffness of asphalt mixture at relatively large strain and long loading time. The m-value, along with the fracture energy, is related to the fracture resistance of asphalt mixture. In other words, Zhang (2000) showed in her study that the rate of damage accumulation appears to be reflected in the creep response, and the fracture energy could be used as a threshold controlling crack performance. Therefore, there is a need to perform IDT to obtain the mixture properties described above that can be used as parameters to evaluate fracture resistance of different mixtures.

2.3 Fatigue Analysis

Fatigue is the result of damage accumulation and eventual failure due to repeated loading. In general, the study of asphalt concrete fatigue can be divided into three approaches. The first is a traditional fatigue approach, which is a regression analysis between phenomenological observation and laboratory data from the materials tested. The second is a continuum mechanics approach, which is a constitutive model calibrated to the material properties of asphalt concrete, then fitted to fatigue test data. And the last is a fracture mechanics approach, which is based on the crack growth rate.

2.3.1 Traditional Fatigue Approach

The oldest type of this model was developed by Monismith et al. (1981) using a simple exponential relationship:

$$N_f = a\,(1/\varepsilon_0)^{\,b} \tag{2.1}$$

where N_f is the fatigue life, ε_0 is the initial applied tensile strain, and a, b are constants derived of fitting the data. This method allows evaluating the relative performance of the mixtures but can

be applied only to the specimens tested. Thus, Monismith et al. (1985) adjusted the original fatigue model as follows:

$$N_f = a\,(1/\varepsilon_0)^{\,b}\,(1/S_0)^{\,c} \tag{2.2}$$

where N_f is fatigue life, ε_0 is an initial applied tensile strain, S_0 is a initial mixture stiffness, and a, b, and c are constants derived by fitting the data. In seeking a more general approach independent of loading mode, fatigue life was compared to dissipated energy, which is the product of stress and strain.

Many researchers, including Chomton and Valayer (1972), van Dijk (1975), van Dijk and Visser (1977), and Tayebali et al. (1992), have investigated the relationship between cumulative dissipated energy and fatigue life as follows.

$$W_N = A\,(N_f)^{\,z} \tag{2.3}$$

where N_f is a fatigue life, W_N is the cumulative dissipated energy to failure, and A and z are constants derived by fitting the data. In practice, Tayebali et al. (1994) calibrated the above model to the shape of traditional approach as follows:

$$N_f = d\,(\Psi)^{\,b}\,(w_0)^{\,g} \tag{2.4}$$

where Ψ is a shaping factor, which accounts for the mode of loading and the variation in stiffness of the material throughout the test, w_0 is energy dissipated during the initial cycle, and d, b, and g are constants derived by fitting the data. However, because of the lack of constitutive properties, the dissipated energy prevents material state description, or relating a material response (stiffness loss or material compliance) to energy dissipation (Lytton et al., 2001).

2.3.2 Continuum Mechanics Approach

H. J. Lee and Y. R. Kim (1998) presented a viscoelastic constitutive model of asphalt mixtures that accounts for the rate-dependent damage growth and healing. They developed a constitutive model calibrated to the material properties of asphalt concrete, then fitted to fatigue test data to develop a predictive relationship for similar materials. This model is based on an elastic-viscoelastic correspondence principle and a rate-type internal state evolution law, which is employed to describe the damage growth and microdamage healing. This approach categorized the constitutive properties into three functions as follows:

$$\sigma = I\,(\varepsilon^{R})\,[F + G + H] \tag{2.5}$$

where I is the initial pseudo stiffness, F is the damage function representing the change in the slope of each transformed hysteresis loop of stress versus pseudo strain, G is the hysteresis function delineating loading versus unloading paths, and H is a healing function representing the change in the pseudo stiffness due to rest periods. In this model, tensile uniaxial cyclic tests were performed under controlled-strain mode with different strain amplitudes to determine model parameters. The application of this model in design and practice is limited by the lack of fundamental properties related to the evolution of damage and healing. The only measurable property is pseudo stiffness, and this is difficult to relate to mixture properties (Little et al., 1999).

2.3.3 Fracture Mechanics Approach

The fracture mechanics approach assumes that material has inherent flaws inside, and thus, when external loads are applied, stress is concentrated over a small area around the flaw. Fracture mechanics deals with the propagation of cracking, generally in terms of crack growth rate.

Paris (1963) developed the relationship between fatigue crack growth rate and the stress state in the material. It has been generally known as Paris' law:

$$\frac{da}{dN} = A(\Delta K)^n \tag{2.6}$$

where da/dN is the crack growth rate, ΔK is the change in stress intensity factor, and A and n are mixture parameters determined from laboratory data. Several researchers have conducted fracture tests to obtain parameters A and n for asphalt mixture.

Jacobs et al. (1996) used asphalt concrete specimens (50 mm × 50 mm × 150 mm) under tension and compression repeated loading condition. He concluded that the exponent in Paris' law, n, can be estimated from the slope of the compliance curve of the asphalt mixture, and the constant A can be estimated from a combination of the maximum tensile strength, fracture energy, and the mixture stiffness.

Read and Collop (1997) used the Indirect Tensile Fatigue Test (ITFT) as a routine practical method for evaluating fatigue cracking and introduced a linear elastic fracture mechanics (LEFM) approach to characterize crack propagation. The comprehensive evaluation of the ITFT showed that it is experimentally sensible, simple, inexpensive, and commercially viable so that it is suitable to characterize fatigue performance.

On the other hand, Schapery (1984) developed a fundamental law for the time-dependent fracture of non-linear viscoelastic media. Little et al. (1999) postulated an allied fundamental law for the material healing properties, as reversal of fracture using Schapery's fundamental fracture equation. The absolute crack speed is the difference between the fracture speed ($\dot{f}$) and the healing speed ($\dot{h}$). Thus, Lytton rearranged the fracture and healing equations to obtain the combined fracture and healing model:

$$\frac{dc}{dt} = \dot{c}_f - \dot{c}_h$$

$$= \frac{K_f \alpha \left(D_{1f} E_R J_V\right)^{\frac{1}{m_t}}}{\left(2\Gamma_f - D_{of} E_R J_V\right)^{\frac{1}{m_t}}} - \frac{K_h \alpha \left(D_{1h} E_R H_V\right)^{\frac{1}{m_c}}}{\left(2\Gamma_h - D_{oh} E_R H_V\right)^{\frac{1}{m_c}}} \tag{2.7}$$

In the model, K_f and K_h are constants, which are functions of m (≈ 1/3); α is the length of the process zone ahead of the crack tip; D_{1f} and D_{0f} are components of tensile compliance; D_{0h} and D_{1h} are components of compressive compliance to time t_α that is required for a crack to move (or heal) through the distance α; E_R is the reference modulus used to make the equation dimensionally correct; J_V and H_V are the viscoelastic J-integral and H-integral, respectively, which is the change of the dissipated energy per unit of crack growth and healing area from one tensile and compressive load cycle to the next; m_f and m_c are creep compliance slopes in logarithm scale; Γ_f and Γ_f is the surface energy density of a crack surface in fracture and healing. This model assumes that fracture is the only method of energy dissipation in the asphalt concrete analyzed. This model depends on fundamental mechanical properties such as creep compliance and surface energy density that are measurable in the laboratory. These fundamental relationships allow secondary analysis of mixtures based on typically measured properties, like creep and relaxation moduli, and direct chemical evaluations such as surface energy of asphalt and aggregate surface (Lytton et al. 2001).

Zhang (2000) used the Superpave Indirect Tension Test to develop a suitable crack growth law for generalized loading conditions. She introduced a dissipated creep strain energy limit as a fatigue failure limit that controls crack performance. She also introduced an HMA fracture model, which accounts for the combined effects of m-value, fracture energy, and loading conditions to determine the number of repeated loading cycles to failure or to a certain length of crack. From the research, the following main findings were made:

- Dissipated creep strain energy at failure ($DCSE_f$) is a threshold controlling crack performance
- $DCSE_f$ is a fundamental material property, independent of loading at a given temperature.
- DCSE/cycle and number of cycles to failure can be calculated as follows:

$$\text{DCSE/cycle} = 1/20 * \sigma_{AVG}^2 * D_1 * m * 100^{(m-1)} \quad (2.8)$$

$$\text{Number of cycles to failure } (N_f) = DCSE_f / (\text{DCSE/cycle}) \quad (2.9)$$

where σ_{AVG} is the average stress near crack tip, D_1 and m are material parameters obtained from creep compliance tests.

- Crack propagation can be described as a step function, which consists of crack initiation (i.e., dissipated creep strain energy is less than threshold) and crack propagation (i.e., dissipated creep strain energy is greater than threshold) at each step.
- Micro-damage will be healed while macro-damage will not be healed as rest period and/or temperature increase.

2.4 Healing

The difference of fatigue lives between laboratory and field can be attributed to the difference in loading condition, including rest periods, multi-level loading, sequence of multi-level loading. During rest periods, the relaxation of stresses due to viscoelasticity and the healing (recovery) of micro-damage occur simultaneously in asphalt concrete. Both of these enhance the fatigue life of asphalt pavement.

Since Bazin and Saunier (1967) reported the recovery of tensile strength during rest period, a lot of research has been conducted to evaluate the healing mechanism of asphalt cement. Wool and O'Connor (1981) identified healing stages in their diffusion model as follows: (1) surface rearrangement, (2) surface approach, (3) wetting, (4) diffusion, and

(5) randomization. Kim and Wool (1983) described the diffusion model in their minor chain concept: "By the end of the wetting stage, potential barriers associated with the inhomogeneities at the interface disappear, and the stages of diffusion and randomization are the most important ones because chains are free to move across the interface and the characteristic strength of a polymer material appears in these stages" (pp. 1119).

Button and Little (1987) conducted controlled displacement crack propagation testing in asphalt concrete mixes modified with various additives. They found an increase in work done to open the crack after rest periods due to both relaxation in the uncracked body and chemical healing at the micro-crack and macro-crack interface. Kim and Little (1990) introduced a healing index, HI, to represent the healing capacity of specific asphalt concrete as a function of rest time as follows:

$$HI = \frac{\Phi_A^R - \Phi_B^R}{\Phi_A^R} \tag{2.10}$$

where Φ_A^R is the pseudo energy density after the rest period and Φ_B^R is the pseudo energy density before the rest period.

This healing index has been used as an important criterion in their healing research since introduced by Kim and Little. Little et al. (1999) also performed controlled-strain fatigue testing to evaluate the effect of factors on healing index. They described that healing index is strongly affected by the source of the bitumen, additives to the bitumen, the temperature of testing, the length of the rest period, and the number of rest periods introduced during the fatigue process. Especially for the effect of additives, they found that the polymer additive might have a positive effect on retarding crack growth but a negative effect on healing.

Zhang (2000) conducted fracture tests using the Indirect Tensile Test and showed healing before and after a critical point that is able to distinguish micro-damage and macro-damage; micro-damage is healable and macro-damage is not healable. Grant (2001) developed a method to determine the amount of healing and the rate of healing of asphalt mixture in terms of recovered dissipated creep strain energy (DCSE) per unit time. He also showed that healing is very dependent on temperature and that damage is accumulated across temperature.

Most research conducted so far, relating to healing of asphalt mixtures, have focused on the effect of asphalt binder. In addition, there is little data related to the differences in healing between different asphalt mixtures. Thus, healing tests must be performed both unmodified and modified asphalt mixture to evaluate the effect of modifier on healing performance.

2.5 Modifiers

It may not possible to produce asphalt mixtures that have both adequate rutting and cracking resistance for certain traffic levels and environments, particularly for mixtures slated for use on higher volume roads. In order to achieve appropriate resistance to rutting, the Superpave volumetric mixture design procedure simply reduces the amount of asphalt binder required without regard for the effect of the reduced asphalt binder on the cracking performance of asphalt mixture. One way to maintain the desirable characteristics of the strong aggregate structures that resist rutting, yet have sufficient resistance to cracking is through the use of modifiers. From the more technical perspective, modifiers are added to asphalt mixtures for the following reasons:

- To obtain stiffer mixtures at high service temperature for enhancing resistance to rutting;
- To obtain softer mixtures at low service temperature to minimize thermal cracking;
- To improve fatigue resistance;

- To improve the asphalt / aggregate bonding for reducing the incidence of stripping or moisture damage;
- To improve the resistance to abrasion which also reduces other forms of surface disintegration;
- To rejuvenate aged asphalt binders; and
- To improve the overall performance of asphalt pavement.

One of the most extensively used modifiers is polymer (Sebaaly, 1997). A polymer is a large molecule that is formed by chemically reacting many (poly) smaller molecules (monomers) to one another in long chains or branched chains. Depending on the monomers, the way the molecules are linked, and the chemical process used in its manufacture, polymer can possess a wide variety of properties. The physical properties of polymer can also vary markedly depending on its chemical composition and the length of the chains (Usmani, 1997).

Polymer can be classified in many different ways, as shown in the Table 2.1. Among them, one way of classifying polymers is to divide them into homopolymers and copolymers

Table 2.1 Classification of Polymer

Based on	Classifications
Origin	• Natural polymer • Synthetic polymer
Structure	• Homopolymer • Random copolymer • Alternating copolymer • Block copolymer
Chain	• Linear • Branched • Cross linked
Thermal property	• Thermoplastics • Thermosets
Deformation property	• Elastomers • Plastomers

based on the polymer structure. Polymers made up of only one kind repeating unit in the polymer molecular chain is called homopolymers, while polymers made up of two or more different repeating units is defined as copolymers. Within the copolymers, the repeating units on the copolymer chain may also be arranged in different ways of order along the main chain; the main chain of the polymer may have branches on it. So, types of copolymers are shown as follows:

- Random Copolymer ---- The repeating units are arranged randomly on the chain backbone. If we represent the repeating units by A and B, then the random copolymer might have the structure shown below.

----- AABBABABBAAABAABBA----

- Alternating Copolymer---- There is an ordered (alternating) arrangement of the two repeating units along the polymer chain.

---- ABABABABABAB----

- Block Copolymer ---- The chain consists of relatively long sequences (blocks) of repeating unit.

---- AAAAA ----BBBBBBBBB ---- AAAAAAAAA ---BBBB ----

Another way of classifying polymers based on the polymer structure is to divide them into linear polymers, branched polymers, and cross-linked polymers as shown in Figure 2.2 (Usmani, 1997). Each of these three types of polymers has their own properties and uses in the manufacturing and application of polymer materials.

Another important way of classifying the polymer materials is to classify them by thermal-mechanical property. According to this method, polymers are classified as thermoplastics and thermosets. Thermoplastics, when reacted with appropriate ingredients, can

usually withstand several heating and cooling cycles without suffering structural breakdown. When heated, a thermoset undergoes a chemical change to produce a cross linked solid polymer. They can be shaped into desired forms by the application of heat and/or pressure, but are incapable of undergoing repeated cycles of softening and hardening (Ebewele, 1993).

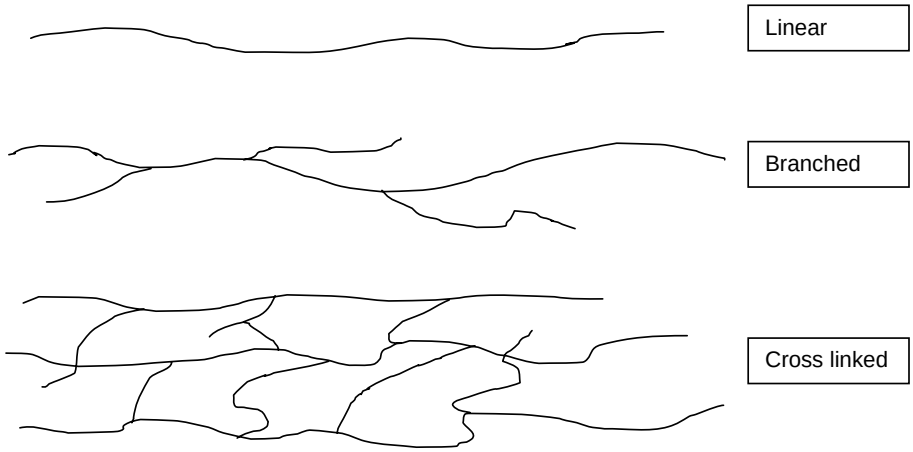

Figure 2.2 Classification of polymers based on link structure.

Among the polymer materials, elastomers have some special properties. Elastomers exhibit high extensibility (up to 1000%) from which they recover rapidly on the removal of the imposed stress. Elastomers generally have low initial modulus in tension, but when stretched they stiffen.

Research indicates that thermoplastic elastomers are frequently used to modify the asphalt materials. Thermoplastic elastomers are generally block copolymer of the $(SB)_nX$ type, where 'S' represents the polystyrene block, 'B' the polybutadiene block, and 'X' the coupling agent. Because of the mutual incompatibility of polybutadiene and polystyrene, a separation takes place between the "soft" (polybutadiene) and the "hard" (polystyrene) blocks, resulting in a

morphological arrangement in which the polystyrene domains are dispersed in a continuous elastomeric matrix (Diani et al., 1997)

A typical thermoplastic elastomer is SBS (Styrene Butadiene Styrene) block copolymer, shown in Figure 2.3.

S (Styrene) repeating unit

$$- CH_2 - \underset{\underset{C_6H_5}{|}}{CH}$$

B (Butadiene) repeating unit

$$CH_2 - CH - CH - CH_3$$

SBS Block Copolymer: – **SSSSSBBBBBBSSSSSBBBBBB** –

Figure 2.3 SBS modifier structure.

The main effect of the modification with SBS copolymers is a dramatic reduction of the bitumen thermal sensitivity, which is the main technological drawback of neat bitumen. SBS modified binders add substantially to the strength of modified bitumen at high temperature, and the polybutadiene chains contribute to the flexibility of the binder at low temperature. The elastomeric lattice between asphalt molecules and SBS polymer improves the elastic characteristics of the binder without increasing the stiffness of binders at low service temperature (Collins, 1991).

Crumb rubber is also a kind of polymer, which is often referred to as a thermoset. A thermoset is a rigid, tightly cross-linked polymer that is degraded rather than melted by heating (Rouse, 1997). A typical crumb rubber is ground tire rubber (GTR). When GTR and asphalt are mixed at high temperature, rubber particles may swell to at least twice their original volume due to chemical and physical interaction between asphalt and rubber particles. This leads to a

significant increase in the viscosity of the mixtures. Many researchers have reported that the resulting rubber modified binder can lower the temperature susceptibility, increase resistance to permanent deformation at high temperature and age hardening.

Most research related to modifiers have focused on the characterization of modified asphalt binder or relative comparison of straight and modified asphalt mixture properties. Little work has been done towards evaluating crack propagation and healing characteristics of polymer modified mixtures compared to straight asphalt mixtures. Recently, some research has focused on the modification of polymer for asphalt mixtures. Among them, Aglan (1997) showed that the fracture resistance superiority of the SBS modified asphalt mixture based on the specific energy of damage from the analysis of controlled-stress fatigue tests conducted at room temperature (70° F). And from the scanning electron microscopic analysis, he also observed profound ridges in binder-rich areas of SBS modified asphalt mixture, which is produced by the micro-stretching of the binder on the fracture surface and results in improvement of adhesion and cohesion.

Jones et al. (1998) revealed that Superpave binder specification could not characterize modified asphalt adequately. In other words, they showed that the five mixtures, which were mixed with five different modified binders including polymer modifier, and all with a PG graded of 76-22 performed differently during tests including Superpave IDT strength and creep tests. Some of the elastomer showed a higher tensile strength at intermediate temperature (25° C), but almost the same at low temperatures (−18° C to 4° C) as those of control mixture and the other modified mixtures. Similarly, Khattak and Baladi (1998) measured engineering properties of polymer modified asphalt mixtures to evaluate the effect of polymer modification on asphalt mixtures. SBS and SEBS modified mixture, which were designed throughout Marshall mix

design procedure, showed the increased fatigue life and tensile strength at 25° C while the elastic properties at –5° C were not affected by the addition of polymer.

Wegon and Brûlé (1999) were trying to observe the structure of the polymer modified binder directly in the asphalt mixture using UV-light by illuminating the surface of cut and polished specimens as thin or plane sections. They observed that the structure of the pure polymer modified binder in most case has shown not to be the same as the structure of the polymer modified binder in the asphalt mixture. They also observed the polymer phase as small spots or as smaller or larger irregular globules in a continuous asphalt phase. The study showed that an interaction exists between the polymer phase and the aggregate in the asphalt mixtures, indicating that it would be most sensible to evaluate the performance of the polymer modified asphalt mixture from tests on the actual asphalt mixtures rather than binders.

More recently, Khattak and Baladi (2001) developed fatigue and permanent deformation model for polymer modified mixtures, and showed that the laboratory fatigue life and permanent deformation were strongly related to the rheological properties of polymer modified binders and the engineering properties of the polymer modified mixtures.

CHAPTER 3
MATERIALS AND METHODS

This chapter provides information on the type of materials and procedures for the production of asphalt mixture specimens in the laboratory. Testing procedures and instrumentation are also described.

3.1 Materials

3.1.1 Aggregates

White Rock (crushed limestone) was used in this study. The limestone is mined from Miami, South Florida by White Rock Quarries, Inc. White rock is one of the major aggregates currently used in the state of Florida, because of its abundance, and is approved by the Florida Department of Transportation (FDOT) for road construction and rehabilitation projects. It is also a standard aggregate that the FDOT uses for its FC-2 friction course mixture. Several coarse and fine gradations of the Limestone aggregate were developed for the production of the HMA mixtures by the FDOT. The coarse and fine gradations were designed to pass below and above the Superpave restricted zone, respectively. The aggregate components provided were a coarse aggregate, S1A; a fine aggregate, S1B; and screenings. Granite mineral filler from Georgia was also used in the mixtures.

One of the coarse gradations, C1, was selected for the main aggregate gradation in this study, which was used for all the tests conducted. A fine gradation, F1, was selected for the sub-aggregate gradation to evaluate the effect of SBS polymer on the cracking of mixtures with different aggregate gradation. Figure 3.1 shows the gradation chart of the mixtures including the restricted zone and control points. The blend proportion of the aggregates is shown in Table 3.1.

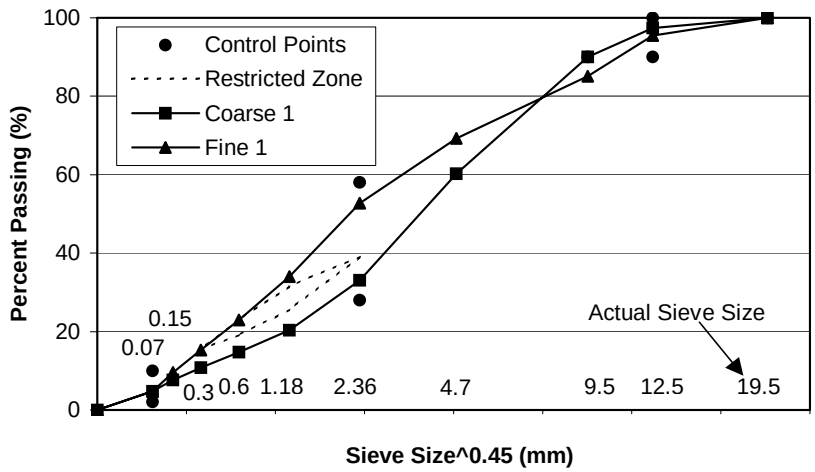

Figure 3.1 Aggregate gradations (Coarse 1 and Fine 1).

Table 3.1 Aggregate Blend Proportions

	S1A (%)	S1B (%)	Screenings (%)	Filler (%)
C1	10.20	63.27	25.51	1.02
F1	20.30	25.37	53.29	1.03
Bulk Specific Gravity	2.43	2.45	2.53	2.69

3.1.2 Asphalt Binders

Two binders were involved in this study; one control and one SBS polymer modified asphalt. According to the information provided by the manufacturer, the control asphalt binder graded as a PG 67-22 or AC 30, while the modified asphalt binder graded as a PG 76-22. SBS polymer (3%) was blended with the control asphalt in the process of high shear milling to produce the SBS modified asphalt. The characteristics of asphalt binder are shown in Table 3.2. All of these asphalt binders were provided by CITGO Asphalt Refining Company.

Table 3.2 Asphalt Binder Properties

		Control Asphalt	SBS Modified Asphalt*
Asphalt Grade		PG 67-22	PG 76-22
Un-aged Asphalt			
Viscosity (20 rpm) @ 135° C, Pa-s	ASTM D4402	0.51	1.315
Viscosity (20 rpm) @ 165° C, Pa-s	ASTM D4402	0.155	0.368
Dynamic Shear (10 rad/sec) G*/sinδ and δ kPa	AASHTO TP5	1.27 and 85.8 @ 67° C	1.386 and 71.6 @ 76° C
RTFO Aged Residue	AASHTO TP240		
Dynamic Shear (10 rad/sec) G*/sinδ, kPa	AASHTO TP5	2.864 @ 67° C	3.025 @ 76° C
PAV Aged Residue @ 100° C	AASHTO PP1		
Dynamic Shear (10 rad/sec) G*sinδ, kPa	AASHTO TP5	2754 @ 25° C	2879 @ 25° C 1432 @ 31° C
Creep Stiffness and m-value, 60 sec	AASHTO TP1	155.0 and 0.362 @ −12° C	131 and 0.355 @ −12° C 263 and 0.298 @ −18° C

* Control asphalt was used as base asphalt in manufacturing SBS modified asphalt

3.2 Asphalt Mixture Design

The laboratory asphalt mixtures produced for testing and evaluation were designed with the Superpave Volumetric Mix Design procedure, which bases its selection for design asphalt content on a set of criteria on the volumetric properties of the mixture (VMA, VFA, density) at 4% air voids. Apart from the above procedure that determines the design asphalt content, the aggregates need to fulfill a set of criteria for the consensus and source properties that aim to prevent the use of substandard aggregates in producing asphalt mixture.

3.2.1 Selection of Traffic Level

The Superpave design method for compacted asphalt mixtures specifies the number of gyrations to which a sample must be compacted with the Superpave Gyratory compactor. The number of gyrations for these traffic levels as specified in Florida Department of Transportation is presented in Table 3.3. Two traffic levels, namely level 2 and 6, were selected for the mixture design. Traffics between level 2 and level 6 cover more than 90% of traffics running on arterial road, interstate highway, and turnpike in Florida.

Table 3.3 Traffic Levels and Gyratory Compaction Effort

Traffic Level (millions of EASL's)	N_{ini}	N_{des}	N_{max}
1 (< 0.3)	6	50	75
2 (0.3-1.0)	7	75	115
3 (1-3)	7	75	115
4 (3-10)	7	75	115
5 (10-30)	8	100	160
6 (30-100)	9	125	205
7 (> 100)	9	125	205

3.2.2 Batching and Mixing

Aggregate batching sheets, which are attached in Appendix A, were prepared for 4500 g samples and 1500 g samples based on the JMF's for the aggregates. Figure 3.2 shows a picture of the batching operation. The 4500 g samples (batched) were heated in an oven at the mixing temperature for approximately 2 hours. The mixing tools and asphalt used were also heated at the mixing temperature. According to manufacturer recommendation, the mixing temperature of the unmodified mixture and modified mixture are 300° F and 340° F, respectively. The aggregates were then removed from the oven and mixed until the aggregates were well coated (approximately 3-5 minutes) with asphalt binder. For the asphalt mix design, the asphalt content

Figure 3.2 Batching.

was the estimated asphalt content of P_b, and $P_b \pm 0.5$; and for the mixture test, the asphalt content was the design asphalt content. Figure 3.3 shows a picture of mixing operation. The mixed samples were then spread out in pans and heated in an oven for 2 hours at a temperature of 275° F for short-term oven aging (FDOT, 2001). Each of the mixtures was stirred after 1 hour to obtain a uniformly aged sample. In addition to the 4500 g samples, 1500 g samples were prepared to determine the theoretical maximum density (TMD) of the various mixes according to AASHTO T209-94.

3.2.3 Compaction

After short-term oven aging, the 4500 g samples were then removed and quickly compacted using the Superpave gyratory compactor (Pine). Figure 3.4 shows the Pine model Superpave gyratory compactor used. The samples were compacted with a ram pressure of 600 KPa at a gyratory angle of 1.25° to a maximum number of gyrations of 205, corresponding to

Figure 3.3 Mixing.

Figure 3.4 Compacting.

N_{max} for Superpave Traffic Level 6. The compaction data of the samples were used in determining the design asphalt content for the various traffic levels. That is, volumetric properties of the mixture such as air voids (AV), voids in mineral aggregates (VMA), and voids filled with asphalt (VFA) were calculated at these asphalt contents and then each was plotted as a function of asphalt content at $N_{des.}$ The design asphalt content was obtained by interpolating the air void versus asphalt content curve to obtain to asphalt content at 4% air void. The other volumetric properties were then obtained at this design asphalt content. The details of asphalt mix design are presented in Appendix B.

3.3 Test Specimens

Four types of asphalt mixtures were produced for coarse graded aggregate structures as shown in Table 3.4. Design asphalt contents were determined as 6.1% for traffic level 6, and 7.2% for traffic level 2 using unmodified asphalt binder. The modified mixtures were produced to have the same asphalt content as the unmodified asphalt mixtures. This approach assured that only the effect of the modifier would affect the test results. All four mixtures were batched and mixed in the laboratory in the same way as for the mixture design process. Manufacturer-recommended mixing temperatures were used for the SBS polymer modified mixture, and all

Table 3.4 Test Samples

Samples	Binder		Aggregate Type/Gradation	Designation
	Content	Type		
6.1	6.1%	Straight	Limestone/C1	Control sample
7.2	7.2%	Straight	Limestone/C1	Unmodified higher binder content
6.1SBS	6.1%	Modified	Limestone/C1	Modified Same binder content
7.2SBS	7.2%	Modified	Limestone/C1	Modified higher binder content

mixtures were Short Term Oven Aged (STOA) in accordance with the Florida Department of Transportation specification 334-4.2.1 (2001), then compacted to 7% (± 0.5%) air voids. The mixtures were Long Term Oven Aged (LTOA) in accordance with Superpave specifications to evaluate the aging effects of the modifier. The other four types of asphalt mixtures with fine graded aggregate structures were also produced to evaluate the effect of SBS polymer on the cracking resistance for different aggregate gradation. These mixtures will be further described in Chapter 4.7.

One hundred fifty mm diameter specimens were compacted by the Superpave gyratory compactor. After waiting for the specimen to fully cool down, the bulk specific gravity of the compacted specimen was measured, and the air void percentage for each specimen was calculated. The target air voids of the gyratory pill was of 7.5%, because the air void of the sliced specimen taken from the middle of the pill is generally 0.5% less than that of the compacted specimen. A cutting device, which has a cutting saw and a special attachment to hold the pills (Figure 3.5), was used to slice the pill into specimens of desired thickness. Two two-inch samples or three one-inch samples could be attained from each specimen. Because the saw uses water to keep the blade wet, the specimens were dried for one day at room temperature to achieve the natural moisture content.

The bulk specific gravity was taken for each specimen to obtain its air void percentage. Specimens had to be in the range of 7 ± 0.5 % air voids to be considered for testing. Specimens were placed in the humidity chamber for at least two days to negate moisture effects in testing. The two-inch thick specimens were used for the standard Superpave IDT (Resilient Modulus, Creep Compliance, and Tensile Strength tests), strength tests at slower loading rates, and longer-

Figure 3.5 Slicing the sample.

term creep tests. The one-inch thick samples were used for the repeated load fracture tests and healing tests.

Gage points were attached to the samples using a steel template and vacuum pump setup and a strong adhesive (Figure 3.6). Four gage points were placed on each side of the specimens at distance of 19 mm (0.75 in.) from the center, along the vertical and horizontal axes. A steel plate that fit over the attached gage points was used to mark the loading axis with a marker. This helped with placement of the sample in the testing chamber and assured proper loading of the specimen (Figure 3.7).

3.4 Test Procedures

All tests were performed using the Superpave Indirect Tensile Test (IDT). Standard Superpave IDT tests were performed on all mixtures to determine resilient modulus, creep

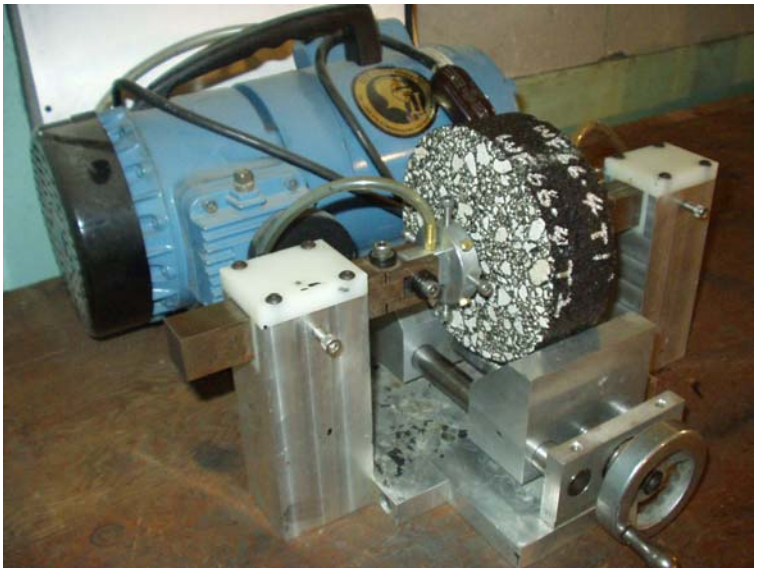

Figure 3.6 Gage point attachment.

Figure 3.7 Marking the loading axis.

compliance, m-value, D_1, tensile strength, failure strain, fracture energy, and dissipated creep strain energy to failure (Roque, 1997). A significant number of additional tests were also performed including: (1) repeated load fracture tests to evaluate measured crack growth behavior (Roque, 1999); (2) strength tests at slower loading rates (2.5 mm/min) to evaluate differences in the post-fracture behavior of modified mixture; (3) longer-term creep tests to failure to evaluate the potential of this type of test to uniquely characterize SBS polymer modification; and (4) healing tests to evaluate the healing behavior of mixtures. The strength tests at slower loading rates and longer-term creep tests to failure are modifications of tests described by Roque et al. (Roque, 1997). Crack growth as predicted by Hot-Mix-Asphalt (HMA) Fracture Mechanics Model (Zhang 2001), which is based on the dissipated creep strain energy limit obtained from Superpave IDT, was used to evaluate the cracking resistance of mixtures in this study.

3.4.1 Standard Superpave IDT

Standard Superpave IDT tests were performed on all mixtures to determine resilient modulus, creep compliance, m-value, D_1, tensile strength, failure strain, fracture energy, and dissipated creep strain energy to failure. The tests were performed at three different temperatures: 0, 10, and 20° C.

3.4.1.1 Resilient modulus test

The resilient modulus is defined as the ratio of the applied stress to the recoverable strain when repeated loads are applied. The test was conducted according to the system developed by Roque et al. (1997) to determine the resilient modulus and the Poisson's ratio. The resilient modulus test was performed in load control mode by applying a repeated haversine waveform load to the specimen for a 0.1 second followed by a rest period of 0.9 seconds. The load was

selected to keep the horizontal strain in the linear viscoelastic range, in which horizontal strain is typically 150 to 350 micro-strains. The procedures for resilient modulus test are as follows:

(1) The specimens compacted are cut parallel to the top and bottom faces using a water-cooled masonry saw to produce 2-inch thick specimens having smooth and parallel faces.

(2) Four brass gage points are affixed with epoxy to each trimmed smooth face of the specimen.

(3) Test samples are stored in a humidity chamber at a constant relative humidity of 60 percent for at least 2 days. And specimens are cooled at the test temperature for at least 3 hours before testing.

(4) LVDTs (Linear Variable Differential Transducers) are mounted and centered on the specimen to the gage points for the measurement of the horizontal and vertical deformations. (LVDT was exchanged with extenthometer later. Extenthometer has exactly same function with LVDT, but less affected by temperature)

(5) A constant pre-loading of approximately 10 pounds is applied to the test specimens to ensure proper contact with the loading heads before test loads are applied.

(6) The specimen is then tested by applying a repeated haversine waveform load for five seconds to obtain horizontal strain between 150 to 350 micro-strains. If the horizontal strains are higher than 350 micro-strains, the load is immediately removed form the specimen, and specimen is allowed to recover for a minimum of 3 minutes before reloading at different loading level.

(7) When the applied load is determined, data acquisition program begins recording test data. Data are acquired at a rate of 150 points per seconds.

(8) The resilient modulus and Poisson's ratio are calculated by the following equations, which were developed based on three dimensional finite element analysis by Roque and Buttlar (1992). The equation is involved in the Superpave Indirect Tensile Test at Low Temperatures (ITLT) program, which was developed by Roque et al. (1997).

$$M_R = \frac{P \times GL}{\Delta H \times t \times D \times C_{cmpl}}$$

$$\nu = -0.1 + 1.480 \times (X/Y)^2 - 0.778 \times (t/D)^2 \times (X/Y)^2$$

where M_R = resilient modulus

P = maximum load

GL = gage length

ΔH = horizontal deformation

t, D = thickness, diameter

C_{cmpl} = $0.6354 \times (X/Y)^{-1} - 0.332$

v = Poisson's ratio

(X/Y) = ratio of horizontal to vertical deformation.

3.4.1.2 Creep test

Creep compliance is a function of time-dependent strain over stress. The creep compliance curve was originally developed to predict thermally induced stress in asphalt pavement. However, because it represents the time-dependent behavior of asphalt mixture, it can be used to evaluate the rate of damage accumulation of asphalt mixture. As shown in Figure 3.8, D_0, D_1, and m-value are mixture parameters obtained from creep compliance tests. Although D_1 and m-value are related to each other, D_1 is more related to the initial portion of the creep compliance curve, while m-value is more related to the longer-term portion of the creep compliance curve.

The m-value has been known to be related to the rate of damage accumulation and the fracture resistance of asphalt mixtures. In other word, the lower the m-value, the lower the rate of damage accumulation. However, mixtures with higher m-value typically have higher DCSE limits. The creep compliance is a time dependant strain, ε(t), divided by a constant stress. That

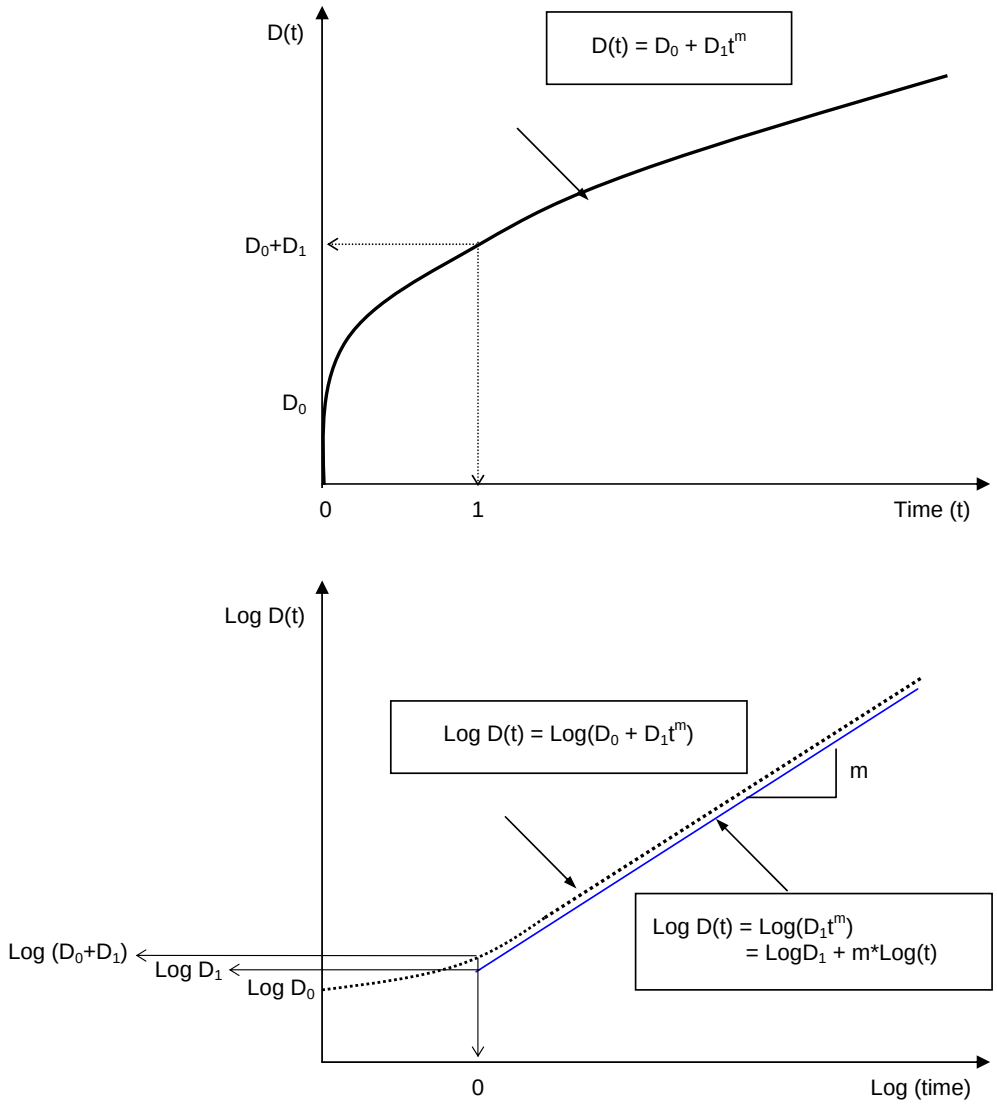

Note: D(t) = Creep compliance at time, t; D_0, D_1, m = Power model constants

Figure 3.8 Power model of the creep compliance.

is, the inverse of the creep compliance, which is called creep stiffness, is a kind of stiffness. According to the analysis conducted by Roque et al. (1997), M_R is higher than creep compliance stiffness at 1 second.

The Superpave Indirect Tensile Test at Low Temperatures (ITLT) computer program was used to determine creep properties of the mixtures. The test was conducted in a load control mode by applying a static load. The load was selected to keep the horizontal strain in the linear viscoelastic range, which is below a horizontal strain of 500 micro-strain. The test procedure was presented by Roque et al. (1997). The procedures for indirect tensile creep test consist of the following steps.

(1) The preparation of test samples, the mounting LVDT, and the pre-loading are same as those for resilient modulus test. (LVDTs have been replaced with extensometers)

(2) Applying a static load and then holing it for 1000 seconds. If the horizontal strains are not between 150 and 200 micro-strains at 30 seconds, the load is immediately removed from the specimen, and specimen is allowed to recover for a minimum 3 minutes before reloading at a different level.

(3) When the applied load is determined, the data acquisition program records the loads and deflections at a rate of 10 Hz for the first 10 seconds, 1 Hz for the next 290 seconds, and 0.2 Hz for the remaining 700 seconds of the creep test.

The computer program, ITLT, was used to analyze the load and deflection data to calculate the creep compliance properties. Creep compliance and Poisson's ratio are computed by the following equations.

$$D(t) = \frac{\Delta H \times t \times D \times C_{cmpl}}{P \times GL}$$

$$\nu = -0.1 + 1.480 \times (X/Y)^2 - 0.778 \times (t/D)^2 \times (X/Y)^2$$

where $D(t)$ = creep compliance at time t, 1/psi

P = ΔH, t, D, C_{cmpl}, GL, v, P, and (X/Y) are same as described above.

3.4.1.3 Strength test

Failure limits such as tensile strength, failure strain, and fracture energy were determined from strength tests using the Superpave IDT. These properties are used for estimating the cracking resistance of the asphalt mixtures. The strength test was conducted in a displacement control mode by applying a constant rate of displacement of 50 mm/min until the specimen failed. The horizontal and vertical deformation, and the applied load are recorded at the rate of 20 Hz during the test. The maximum tensile strength is calculated as the following equation.

$$S_t = \frac{2 \times P \times C_{sx}}{\pi \times b \times D}$$

where S_t = maximum indirect tensile strength

P = failure load at first crack

C_{sx} = $0.948 - 0.01114 \times (b/D) - 0.2693 \times v + 1.436\,(b/D) \times v$

b, D = thickness, diameter

v = Poisson's ratio.

From the strength test and the resilient modulus test, fracture energy and dissipated creep strain energy can be determined. Fracture energy is a total energy applied to the specimen until the specimen fractures. Dissipated creep strain energy (DCSE) is the absorbed energy that damages the specimen, and dissipated creep strain energy to failure is the absorbed energy to fracture ($DCSE_f$). As shown in the Figure 3.9, fracture energy and $DCSE_f$ can be determined as described below. The ITLT program also calculates fracture energy automatically.

$$\mathrm{M_R} = \frac{S_t}{\varepsilon_f - \varepsilon_0} \Rightarrow \varepsilon_0 = \frac{\mathrm{M_R}\varepsilon_f - S_t}{\mathrm{M_R}}$$

Elastic Energy (EE) = $\frac{1}{2} S_t(\varepsilon_f - \varepsilon_0)$

Fracture Energy (FE) = $\int_0^{\varepsilon_f} S(\varepsilon)d\varepsilon$

Dissipated Creep Strain Energy ($DCSE_f$) = $FE - EE$

where S_t = tensile strength

ε_f = failure strain

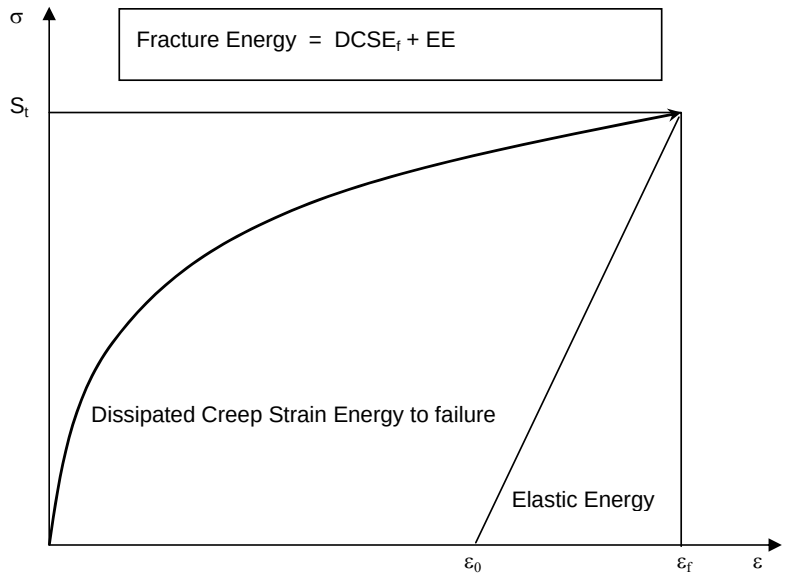

Figure 3.9 Determination of fracture energy and dissipated creep strain energy to failure.

3.4.2 Repeated Load Fracture Test

As described in Chapter 3, mixtures were prepared for the fracture and healing test using Superpave Gyratory Compactor to produce 4500 g, 150-mm diameter specimens, to air voids of 7% (±0.5%). The specimens were then sliced into three fracture test specimens having approximately 25-mm thickness. The previous fracture test conducted in University of Florida by Zhang (2000) was performed on specimens with an 8-mm diameter hole drilled in the center of each specimen. This hole was designed to concentrate stresses so that cracks would initiate at the center of the specimen. However, the fracture test in this study was conducted without a designed hole to eliminate the effect of the hole on the micro damage propagation and healing

properties. The test temperature was 10° C, and specimens were placed in an environmental chamber and allowed to reach temperature stability over three hours. A 10-lb seating load was applied to the specimen. The same load used for the M_R test was used. The fracture test was continued for the desired time until it was manually stopped. During the test, the data is collected manually. This allowed more data points to be recorded when the rate of deformation changed, indicating that cracking had initiated. When the data button is pushed, the program recorded M_R readings over 5 cycles of loading. The test was stopped once the rate of deformation was observed to increase drastically, indicating imminent catastrophic failure.

3.4.3 Strength Tests at Slower Loading Rates

After compacting the specimens to 7% air voids, the specimens were sliced to approximately 50-mm thickness for this test. The test temperature was 10° C, and specimens were placed in an environmental chamber and allowed to reach temperature stability over three hours. A 10-lb seating load was applied to the specimen. The test procedure was the same as the standard indirect tensile strength test but the loading rate was much slower (2.5 mm/minute) than that of the standard strength test (50 mm/minute). The slower rate of loading was used to determine whether it might be possible to see the differences in the post-fracture behavior between the unmodified and the modified mixtures.

3.4.4 Longer-Term Creep Tests to Failure

The procedure of this test was exactly same as the standard indirect tensile creep test, but the loading time is not limited (e.g., 100 seconds or 1000 seconds). The test was continued until the sample failed. In general, creep can be described in terms of three stages, and the rate of creep increases rapidly at the point when the sample reaches initial failure as shown in Figure 3.10 (William et al, 1989). Therefore, the test was performed beyond the failure point, and then

stopped to capture the failure limit of the mixture in creep response. This test was performed to evaluate the potential of using creep response through failure to uniquely characterize SBS polymer modification.

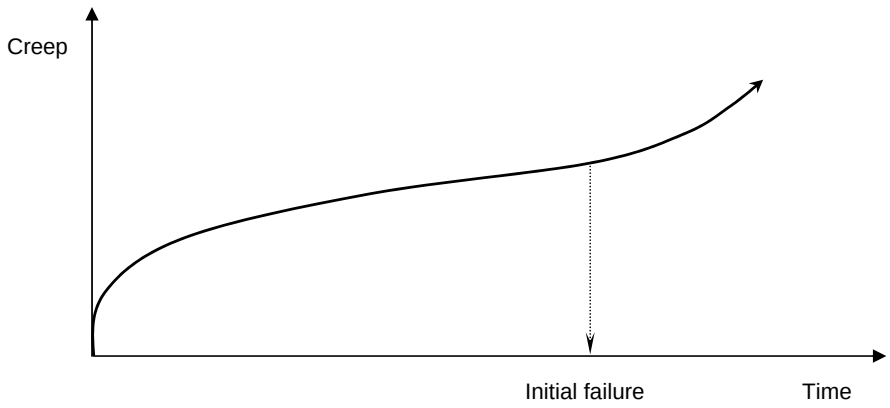

Figure 3.10 Typical behavior and initial failure in creep.

3.4.5 Healing Test

One hundred fifty mm diameter samples (4500g) were prepared with 7% (±0.5%) air voids for this test. The specimens were then sliced into three fracture test specimens having approximately 25-mm thickness. Previous healing tests conducted at University of Florida (Grant, 2001) were performed on specimens with an 8-mm diameter hole drilled at its center. This hole was designed to concentrate stresses so that cracks would initiate at the center of the specimen. However, the healing test in this study was conducted without a designed hole to eliminate the effect of the hole on the healing properties. The healing test consists of repeated load fracture tests and a series of M_R test at selected times during the damage and healing process. That is, the sample was damaged with repeated cyclic loading, and then allowed to heal or recover. During the healing period, the M_R test was conducted at 2 minutes, 4 minutes, 6 minutes, 10 minutes, 20 minutes, 40 minutes, and 60 minutes to measure the resilient

deformation. The resilient deformation can be then transformed to stiffness or dissipated creep strain energy (DCSE). The healing tests were conducted at 0, 10, and 20° C. The procedures for healing test consist of the following steps.

(1) The preparation of test samples, the mounting LVDT, and the pre-loading are same as those for resilient modulus test;

(2) Apply the repeated loads, consisting of a 0.1 second haversine load followed by a 0.9 seconds rest period, for 1000 load replications;

(3) Remove the load for healing of micro-cracks;

(4) Run M_R test at 2 minutes, 4 minutes, 6 minutes, 10 minutes, 20 minutes, 40 minutes, and 60 minutes from removing the load.

CHAPTER 4
EVALUATION OF FATIGUE CRACKING

4.1 Standard Superpave IDT

4.1.1 General Properties

Standard Superpave IDT tests were conducted at 10° C to obtain asphalt mixture properties. Results are presented in Table 4.1. As expected, the mixtures had higher resilient modulus at lower binder contents, but SBS modification had relatively little effect on resilient modulus at either binder content. Modification had no effect on resilient modulus at 7.2% binder content and reduced the resilient modulus by about 20% at 6.1% binder content. This seems to indicate that the polymer has little effect on response at small strain or short loading times, which implies that polymer modification does not reduce the mixture's effectiveness from a structural point of view.

Conversely, the SBS modifier dramatically reduced the creep compliance of mixtures at both low and high asphalt contents. Thus, the SBS polymer appears to have a much greater influence on the time-dependent response, and perhaps specifically the creep response, than on the elastic response of the mixture. The lower rate of creep response is more clearly reflected in the much lower m-value of the modified mixtures at both asphalt contents, as shown in Figure 4.1. Prior research, which resulted in the development of HMA fracture mechanics model, clearly showed that there is a direct relationship between the rate of creep and the rate of micro-damage accumulation in asphalt mixtures.

The results presented in Table 4.1 also indicate the polymer had almost no effect on tensile strength, failure strain, fracture energy (FE), dissipated creep strain energy to failure ($DCSE_f$), or creep parameter D_1. Therefore, it appears that the benefit of the polymer is

Table 4.1 Superpave IDT Results (Coarse 1, STOA)

Sample	Property							
	Resilient Modulus (Gpa)	Creep compliance at 1000 seconds (1/Gpa)	Tensile Strength (Mpa)	Fracture Energy (kJ/m^3)	Failure Strain (10^{-6})	m-value	D_1	
Temperature: 0° C								
6.1	15.42	0.77	2.67	1.50	809.9	0.51	1.93E-07	
7.2	11.74	1.66	2.54	2.00	1184.4	0.52	2.99E-07	
6.1SBS	14.28	0.90	3.00	2.40	1219.1	0.45	2.63E-07	
7.2SBS	13.03	1.08	2.89	2.70	1349.3	0.44	3.48E-07	
Temperature: 10° C								
6.1	11.56	5.90	1.87	4.00	2467.6	0.61	6.04E-07	
7.2	7.18	13.44	1.69	4.90	3756.3	0.62	1.21E-06	
6.1SBS	9.26	3.04	1.95	3.80	2291.2	0.45	7.69E-07	
7.2SBS	7.37	5.20	1.93	5.10	3725.7	0.47	1.33E-06	
Temperature: 20° C								
6.1	5.80	20.37	1.61	7.20	7430.0	0.61	1.61E-06	
7.2	4.72	50.98	0.90	7.20	9634.1	0.63	3.68E-06	
6.1SBS	6.04	9.33	1.69	5.30	5098.5	0.52	1.55E-06	
7.2SBS	4.98	12.41	1.59	9.70	9838.5	0.48	4.10E-06	

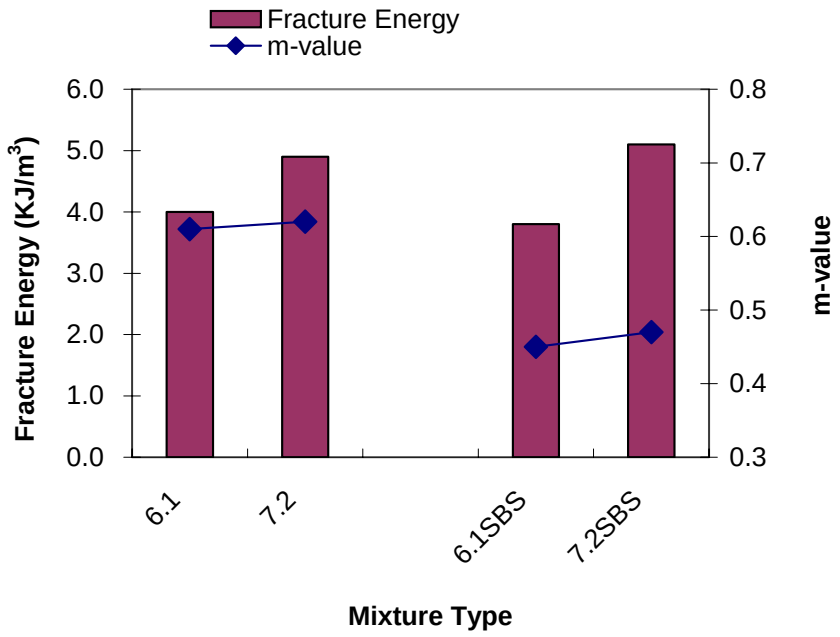

Figure 4.1 Fracture energy and m-value from Superpave IDT.

primarily, and almost exclusively, reflected in the reduced m-value, which indicates a reduced rate of micro-damage accumulation. Fracture and longer-term creep test results presented later will further confirm this point.

Unfortunately, lower m-values are not uniquely related to the addition of polymers. For example, age-hardening a mixture will reduce its m-value, but it will also reduce its FE and $DCSE_f$, which would counteract and likely overwhelm any benefit gained by reducing the m-value in this way. The benefit of the polymer comes from the fact that the m-value is reduced without affecting FE or $DCSE_f$. It is thought that the network, or secondary structure of the polymer phase, reduced the m-value, which is related to the viscous response of the mixture. However, the polymer does not have sufficient time to affect FE during the strength test (around 4 to 5 seconds). Therefore, further research was conducted to evaluate other tests and/or

interpretation procedures that may be used to uniquely characterize the effect of the SBS polymer.

4.1.2 Temperature Sensitivity

Standard Superpave IDT tests were also conducted at 0° C and 20° C to identify the temperature sensitivity of Superpave IDT properties and present the mixture properties for further analysis. Results are presented in Appendix A. As shown in Figure 4.2, at all range of temperatures tested, the mixtures at lower binder contents exhibited the higher resilient modulus than those at higher binder content, but SBS modification had relatively little effect on resilient modulus at either binder content. This seems to indicate that the polymer has little effect, while the amount of asphalt binder has a relatively bigger effect, on response at small strain or short loading times across all of the temperatures tested. Figure 4.2 also indicates that temperature sensitivities of resilient modulus of mixtures are almost identical, as shown in the exponential constant that ranges from –0.0489 to –0.043. It appears that temperature sensitivity of the

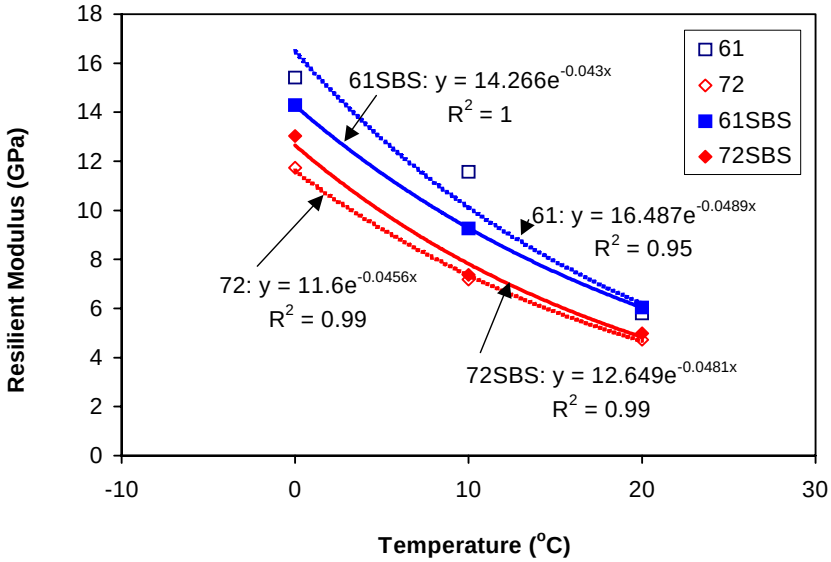

Figure 4.2 Temperature sensitivity of resilient modulus.

response at small strain or short loading time is likely not affected by the modification of binder for this particular asphalt mixture.

The results presented in Figure 4.3 to 4.5 also indicate the polymer had almost no effect on the temperature sensitivity of tensile strength, failure strain, fracture energy (FE), or dissipated creep strain energy to failure ($DCSE_f$). Therefore, it appears that regardless of the modification of the binder, the temperature sensitivity of the response at short loading time is almost identical for a particular base asphalt and mixture type.

On the other hand, the SBS polymer dramatically reduced the creep compliance at all temperatures between 0 and 20° C. In addition, the SBS polymer reduced the temperature sensitivity of creep compliance, which can be represented as the slope of exponential curve in creep compliance versus temperature, at both low and high asphalt contents, as shown in Figure 4.6. The reduced creep compliance and temperature sensitivity of the modified mixtures (6.1SBS and 7.2SBS) are primarily from the reduced m-value shown in Figure 4.7, while those

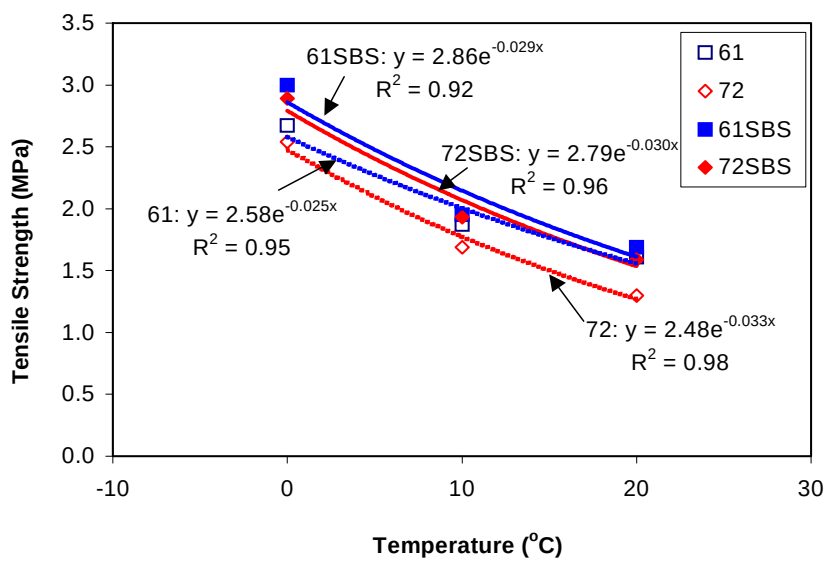

Figure 4.3 Temperature sensitivity of tensile strength.

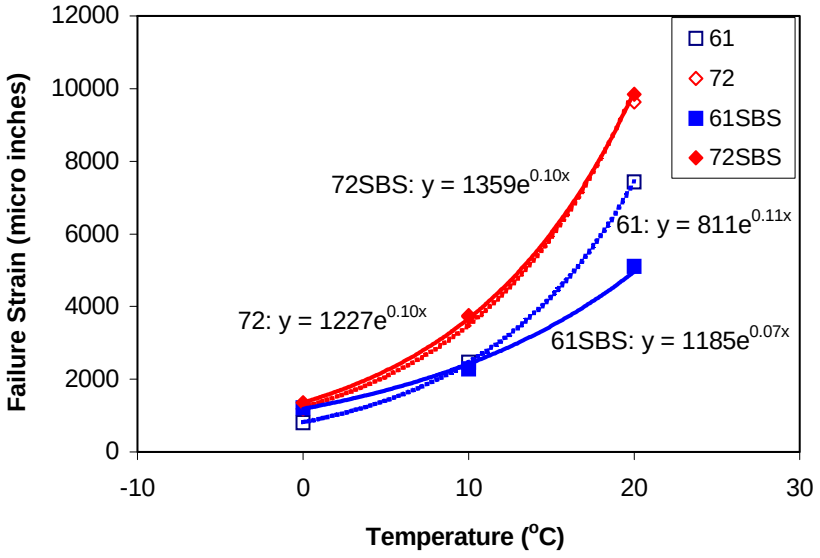

Figure 4.4 Temperature sensitivity of failure strain.

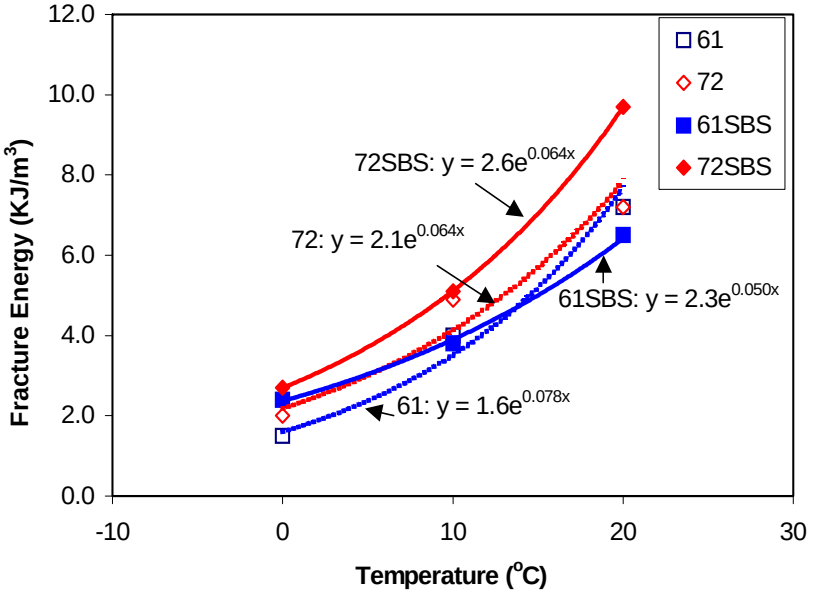

Figure 4.5 Temperature sensitivity of fracture energy.

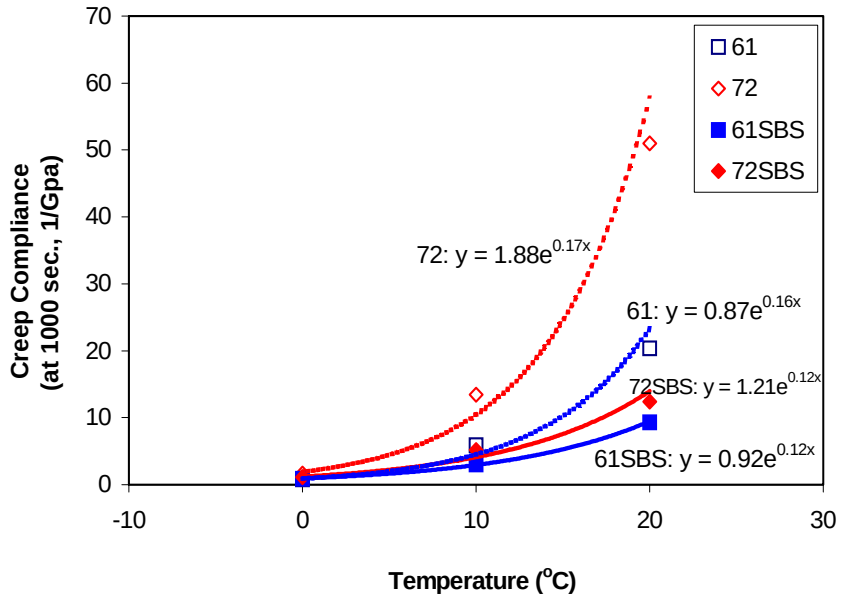

Figure 4.6 Temperature sensitivity of creep compliance.

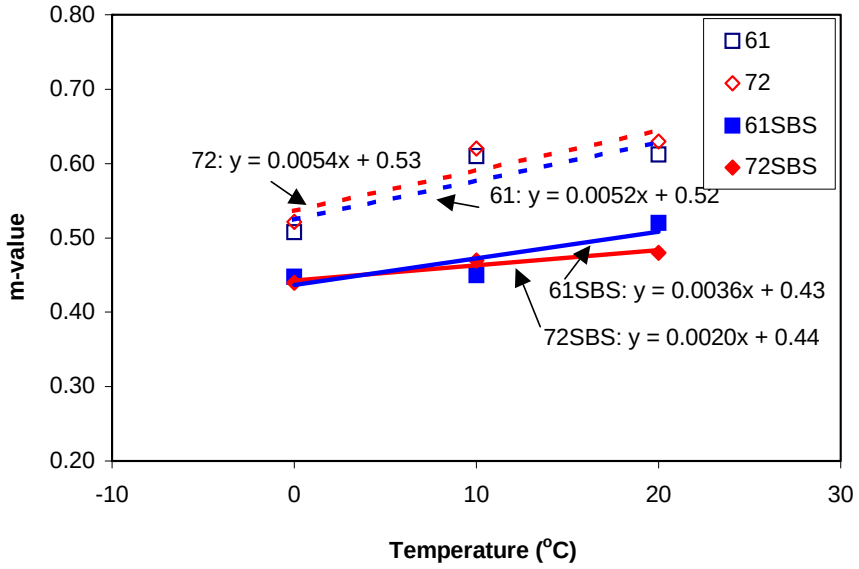

Figure 4.7 Temperature sensitivity of m-value.

of the low binder content mixtures (6.1 and 6.1SBS) are primarily results of the reduced D_1 shown in Figure 4.8. Thus, it appears that among the creep parameters represented in power model, m-value reflects primarily the binder characteristics, while D_1 reflects the structural characteristics of mixture.

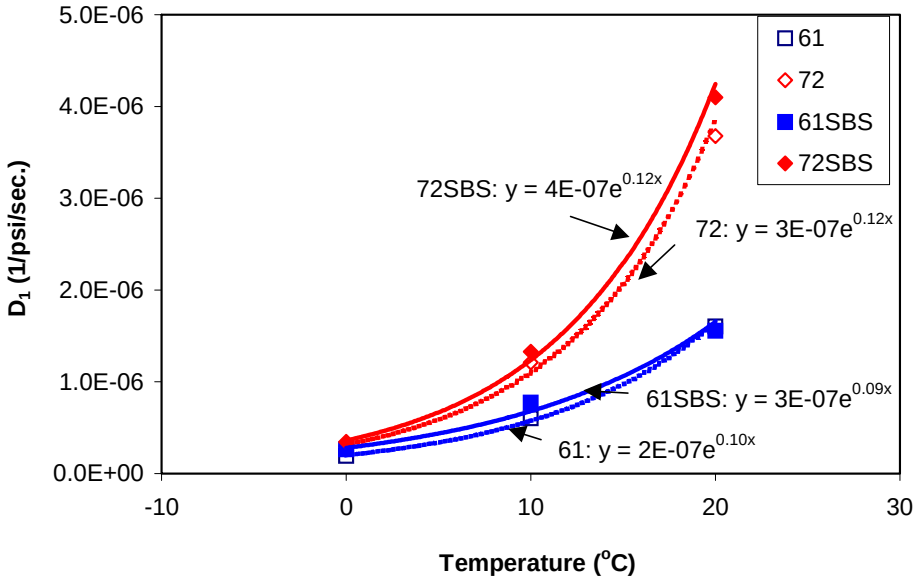

Figure 4.8 Temperature sensitivity of D_1.

4.2 Repeated Load Fracture Test

There were implications that SBS modifier seemed to improve cracking resistance as determined from mixture properties obtained from the Superpave IDT. Superpave IDT results the fundamental material properties from which fracture can be predicted, but it was felt that greater confidence would be achieved by performing actual fracture tests. Fracture tests are necessary to simulate closely the fracture state, and thus to identify the effect of SBS modifier and the binder content on rate of micro-damage development and rate of macro-crack growth.

Tests were performed and analyzed according to the procedures described by Roque et al. (1999).

After conducting and analyzing of fracture tests, the resulting resilient deformation was plotted versus number of load repetitions. Figure 4.9 shows the horizontal resilient deformation (δ_H) during the fracture test. There was a jump in first part of the resilient deformation of all samples. This jump is caused by steric softening and probably by increases in temperature, which reduces the stiffness of the asphalt mixture resulting in higher resilient deformation. However, this jump in resilient deformation has no physical meaning from the damage point of view (Zhang, 2000). One way of eliminating the effect of the initial increase in resilient deformation is to shift the initial resilient deformation (δ_i) to the original resilient deformation (δ_o). The original resilient deformation can be determined by extrapolating the linear portion of the crack growth back to determine the intercept at zero load cycles, as shown in the Figure 4.9.

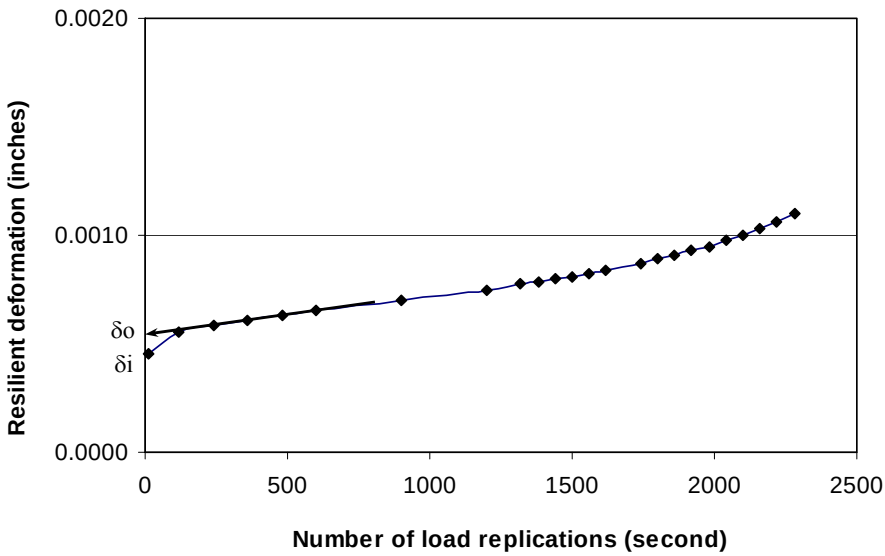

Figure 4.9 Determination of initial resilient deformations (δ_i) and original resilient deformation (δ_o).

Figure 4.10 shows normalized resilient deformation (δ_H/δ_o) as a function of load repetitions. As explained by Roque et al. (1999), an increase in normalized resilient deformation is directly related to the development of damage in the mixture. When the rate of change of δ_H/δ_o is linear (early in the test), the mixture is undergoing micro-damage development. The initiation of macro-damage (macro-crack) occurs when the rate of change of δ_H/δ_o no longer linear.

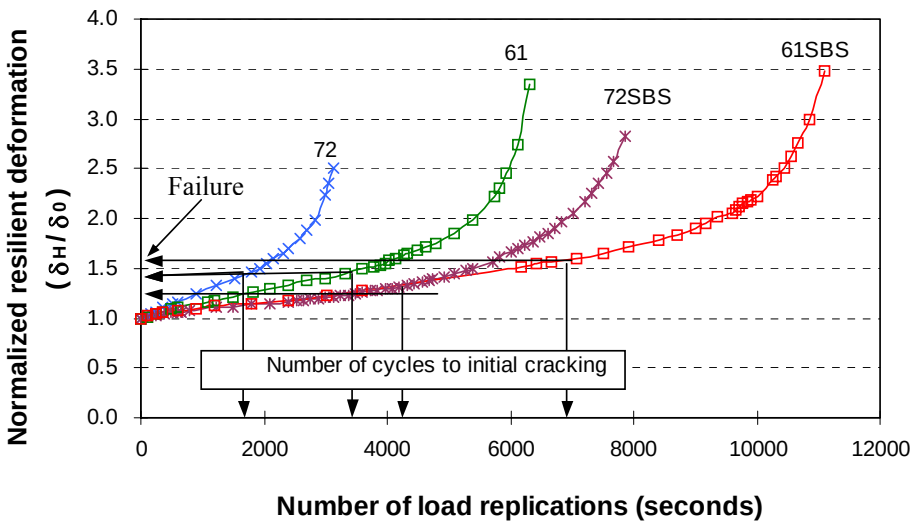

Figure 4.10 Fracture test results (STOA, Coarse 1, and 10° C).

The results presented in Figure 4.10 clearly show that the SBS polymer reduced the rate of micro-damage development and consequently increased the number of load repetitions required for crack initiation. This is consistent with the lower m-value determined for the modified mixtures. The Figure also shows that δ_H/δ_o prior to crack initiation was about the same for all mixtures, modified or unmodified. This is consistent with the fact that the failure limits (FE and $DCSE_f$) were relatively unaffected by the SBS modifier. It should also be noted that the

mixtures with lower binder content, which have lower creep than the mixtures with higher binder content (Figure 4.11), exhibited greater resistance to fatigue-type crack growth (modified and unmodified). This trend is consistent with the test results of the long-term oven aged mixture and the fine-graded mixtures, which will be further presented later in this chapter. Therefore, it appears that fatigue-type crack growth observed in fracture test is better represented in the viscoelastic response measured in creep tests than in the critical responses measured in strength tests.

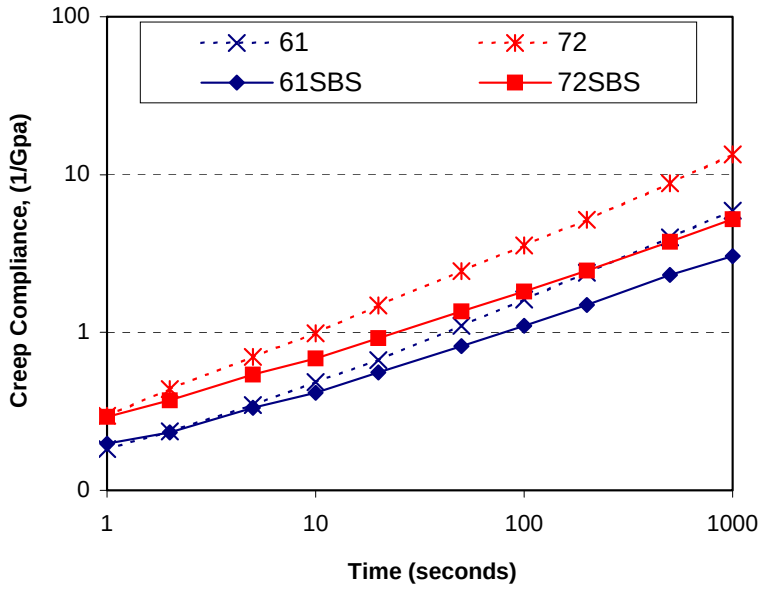

Figure 4.11 Creep compliance of coarse-graded mixtures (10° C, STOA).

4.3 Strength Tests at Slower Loading Rates

It was hypothesized that the effects of the SBS modification may become evident if the strength test were performed at a slower rate of loading. A rate of 50 mm/min is used in the standard Superpave IDT strength test, which allows little or no time for stress relaxation or creep to develop prior to failure. Therefore, even if there is a polymer network present in the mixture,

the high stresses developed in this test will simply break through this network immediately when the strength of the mixture is exceeded. This is why there is little or no difference in failure limits between modified and unmodified mixtures tested at this loading rate. A slower rate of loading will result in lower stresses such that the SBS polymer network may be able to carry these stresses even after the mixture has failed.

Figures 4.12 and Figure 4.13 clearly show the effects of slower loading rate (2.5 mm/min) on mixture tensile strength and failure strain. Unfortunately, even this loading rate was not slow enough to create the intended effect. The resulting properties were not significantly different for the polymer mixture. Although it was thought that the effects would be evident if slower loading rates were used, this approach was deemed impractical because the loading rate required to uniquely distinguish the polymer effect would be different for each mixture, binder and polymer used. Therefore, the decision was made to evaluate the use of longer-term creep tests performed until crack initiation occurs. This approach is presented in the next section of this paper.

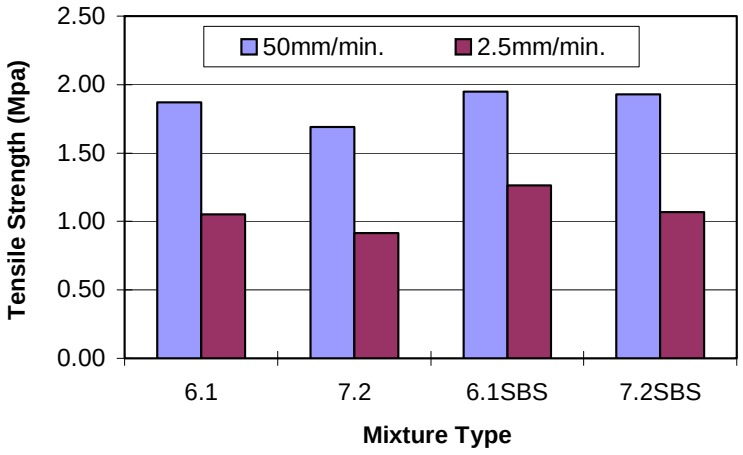

Figure 4.12 Comparison of tensile strength at different loading rates.

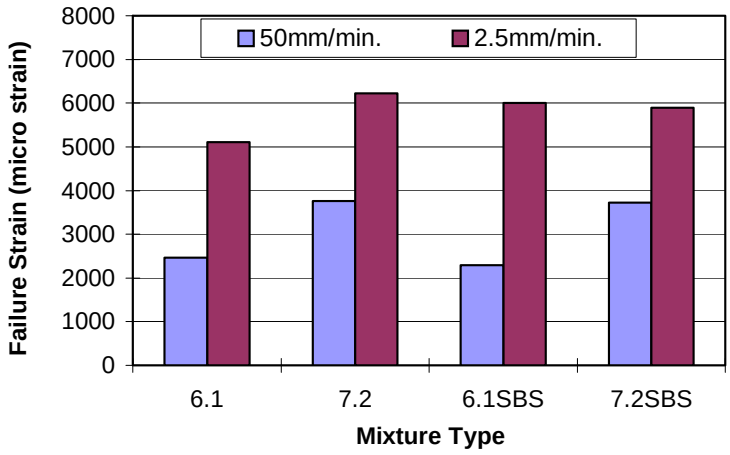

Figure 4.13 Comparison of failure strain at different loading rates.

However, an evaluation of the dissipated energy required to fail the specimen after crack initiation revealed that a parameter defined as the residual dissipated energy was significantly enhanced by the presence of the SBS polymer. Figure 4.14 illustrates schematically how the residual dissipated energy is obtained as the energy between crack initiation and the point when

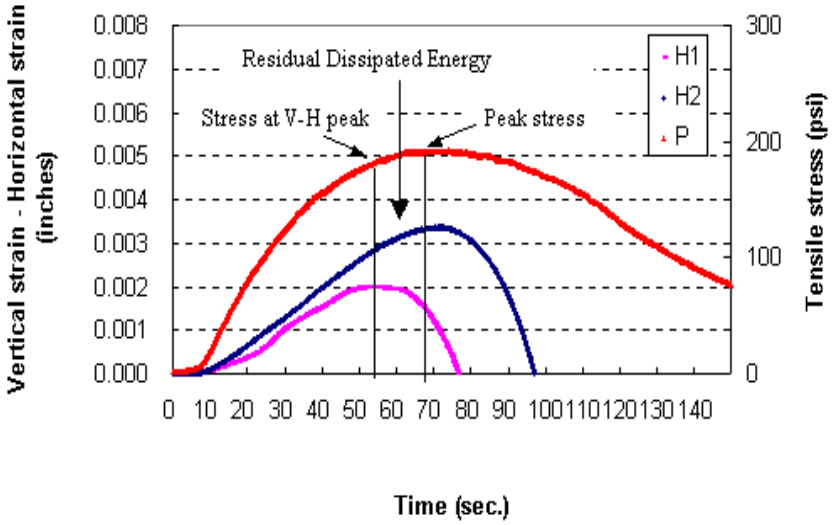

Figure 4.14 Determination of the residual dissipated energy (6.1% SBS modified mixture).

the maximum load is reached during testing. Figure 4.15 shows that the residual dissipated energy was significantly higher for the SBS-modified mixture for both asphalt contents and for both rates of loading. It appears that this may be a useful parameter for uniquely characterizing SBS-modified mixtures.

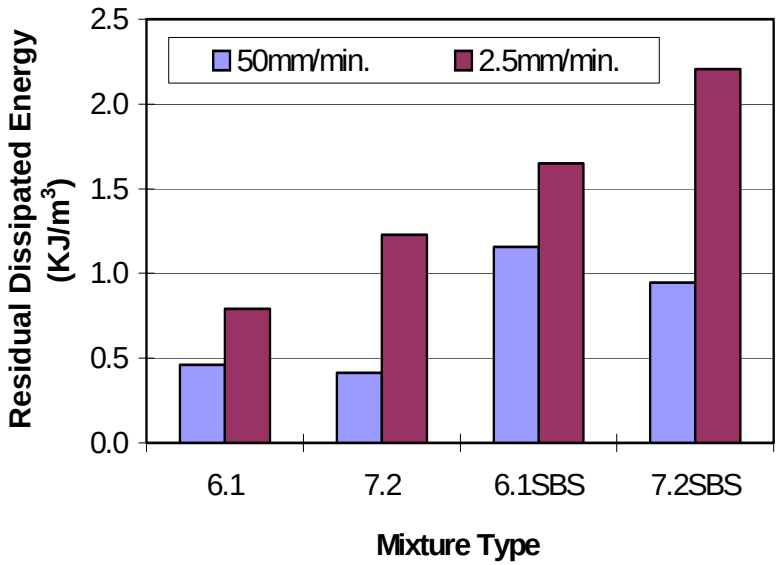

Figure 4.15 Comparison of residual dissipated energy.

4.4 Longer-Term Creep Tests to Failure

Research performed in recent years related to the development of an HMA fracture model has clearly indicated that microdamage is directly related to the development of creep, and that the initiation of cracking in asphalt mixture can be defined in terms of the dissipated creep strain energy threshold ($DCSE_f$). This implies that the mechanism of crack initiation and propagation for sub-critical loading conditions is associated with the development of creep, regardless of the loading pattern used to induce creep. Therefore, it was hypothesized that the effects of SBS polymer modification on cracking could be uniquely identified by performing

creep tests to crack initiation. The DCSE of creep test was calculated by simply multiplying the creep strain by the stress applied during the test. The results of longer-term creep tests presented in Figure 4.16 clearly show the following:

- SBS modifiers reduced the rate of DCSE accumulation.
- The $DCSE_f$ was about the same for modified and unmodified mixtures, which agrees with the results of strength tests as well as with the idea that the SBS polymer primarily reduced the rate of micro-damage, but does little to increase the threshold energy required to crack the mixture.

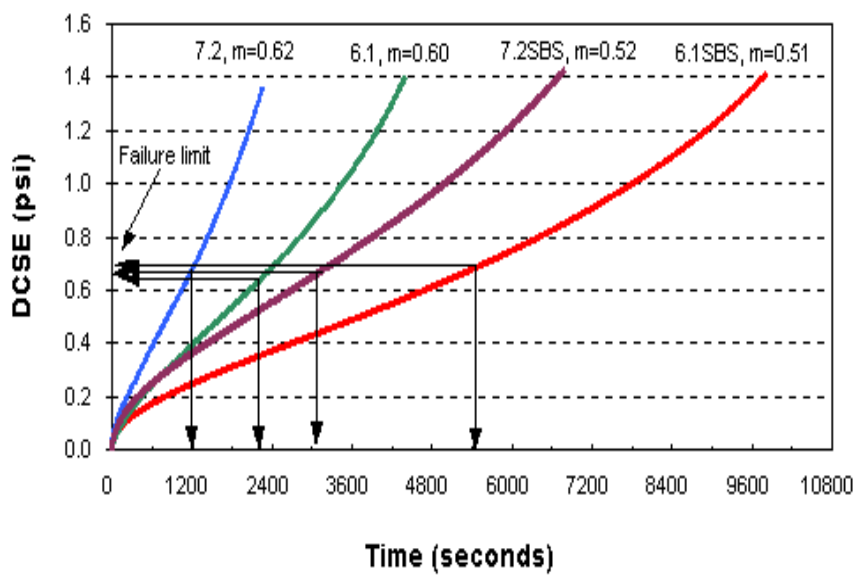

Figure 4.16 Creep test results (DCSE vs. time).

These results seem to indicate that the time to crack initiation as determined from this type of test may be suitable for uniquely characterizing the presence and benefit of SBS modification in asphalt mixture.

Figure 4.17 also shows that this test provides an alternative way to determine the $DCSE_f$ of asphalt mixtures. As shown in the Figure, the $DCSE_f$ obtained from creep tests was almost identical to the value determined from independent strength tests performed on the same mixtures. $DCSE_f$ was determined from the creep tests as the energy to the point where the rate of DCSE became nonlinear.

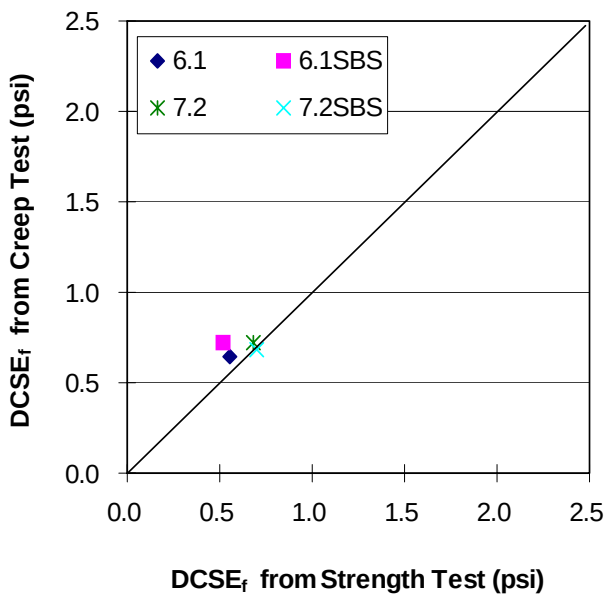

Figure 4.17 Comparison of $DCSE_f$ between creep and strength test.

4.5 HMA Fracture Model

Figure 4.18 shows that the number of cycles to initiate cracking (N_f) predicted from the HMA fracture model is in good agreement with that measured from the fracture tests in the laboratory. N_f was calculated using the equation (2.8) and (2.9); that is, D_1, m-value, and $DCSE_f$ in Table 4.1, were used in the equations with of σ_{AVG} of 230 psi to calculate N_f. From the comparison shown in Figure 4.18, the validity of the concepts associated with the HMA fracture

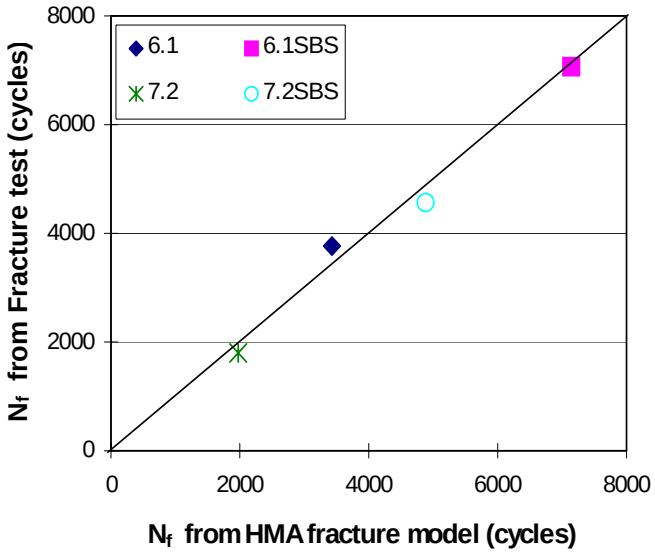

Figure 4.18 Comparison of measured and predicted N_f.

model were confirmed. These results also show that the HMA fracture model, which accounts for the combined effects of m-value, fracture energy, and loading conditions, is also suitable to uniquely identify the presence and benefits of SBS modifier.

From the tests and analyses performed so far, it was known that SBS polymer modification could improve the cracking performance of asphalt mixtures, and that the HMA fracture model accurately reflected the beneficial effects of SBS polymer modification on the cracking performance of asphalt mixtures. Thus, using the number of cycles to failure predicted from the HMA fracture model, the relative effect of SBS modifiers for different asphalt contents was evaluated in Figure 4.19. The relative effect was calculated in terms of the percentage of the predicted N_f of modified mixtures to unmodified mixtures. As expected, the relative effect of SBS modifiers was increased more at higher binder contents and temperatures. This implies that

the effect of SBS polymer would be increased in mixtures with higher asphalt contents such as open graded friction courses.

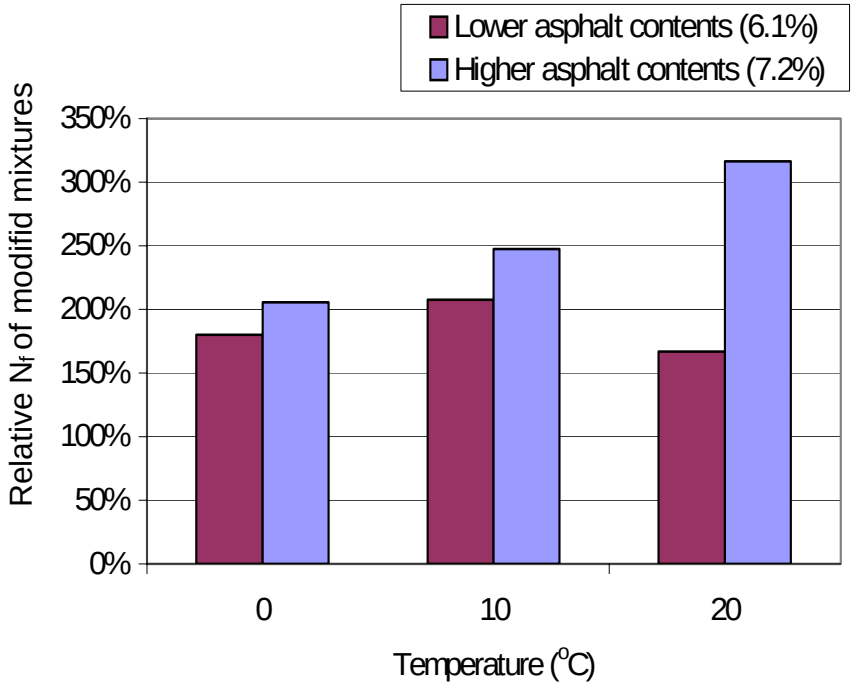

Figure 4.19 Relative effect of SBS modifier for different asphalt contents on predicted N_f across all temperatures.

4.6 Long-term Aging Effect

Standard Superpave IDT tests and repeated load fracture test were also conducted to evaluate the effect of long-term oven aging on the fatigue cracking of the same mixtures. Figure 4.20 shows the fracture test results of long-term oven aged samples performed at 10° C. The number of cycles to failure measured from fracture test and predicted from HMA fracture model was plotted in Figure 4.21. As shown in the figure, the results are in good agreement. Thus, the concepts associated with the HMA fracture model are also applicable for the long-term oven

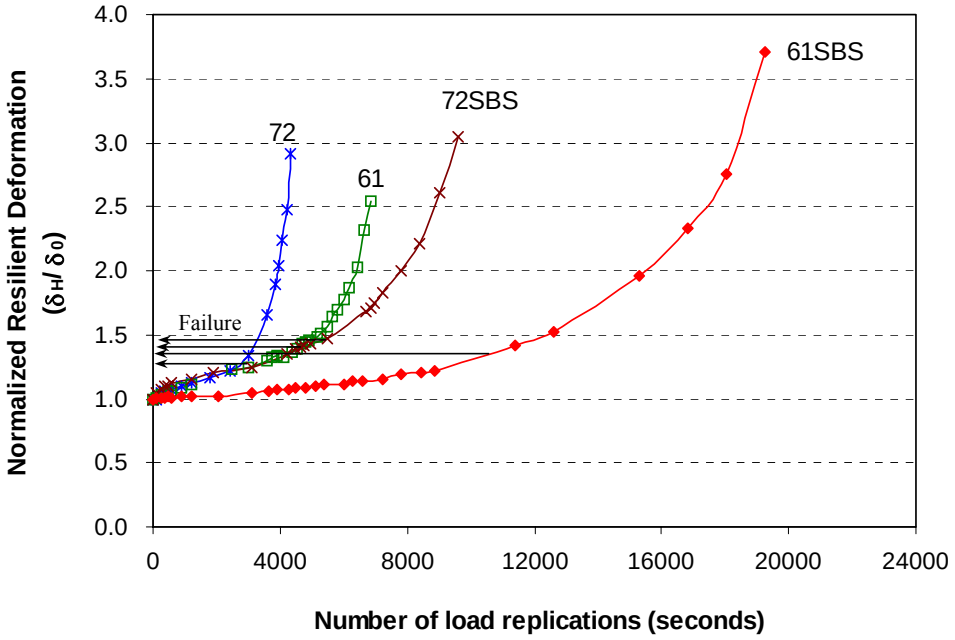

Figure 4.20 Fracture test results (LTOA, Coarse 1, and 10° C).

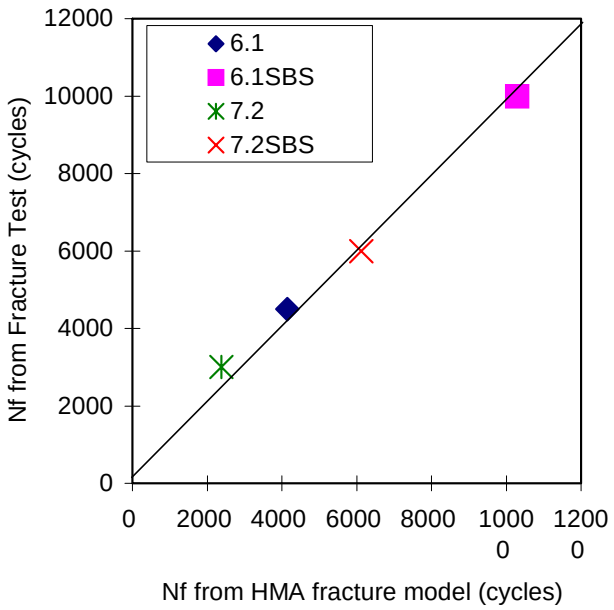

Figure 4.21 Comparison of measured and predicted N_f of LTOA mixtures.

aged asphalt mixtures. On the other hand, Figure 4.22 shows a result that appears to be counter-intuitive. That is, the figure shows that N_f of the LTOA is higher than that of the STOA for all mixtures. This is not consistent with the general trend of cracking, where aging makes mixtures more brittle, resulting in more cracking. However, aging also makes mixture stiffer, and the increased stiffness (or reduction in creep) results in the increased number of cycle to failure in fracture test. This increased stiffness seems to be reflected in the decreased D_1 of the LTOA mixtures (Figure 4.23). Other mixture properties of the LTOA mixtures as measured from standard IDT were almost same with those of the STOA (Appendix C). From the results above, it is evident that fatigue-type crack growth observed in fracture test and predicted from HMA fracture model is greatly affected by the stiffness in creep test, which is well represented in D_1.

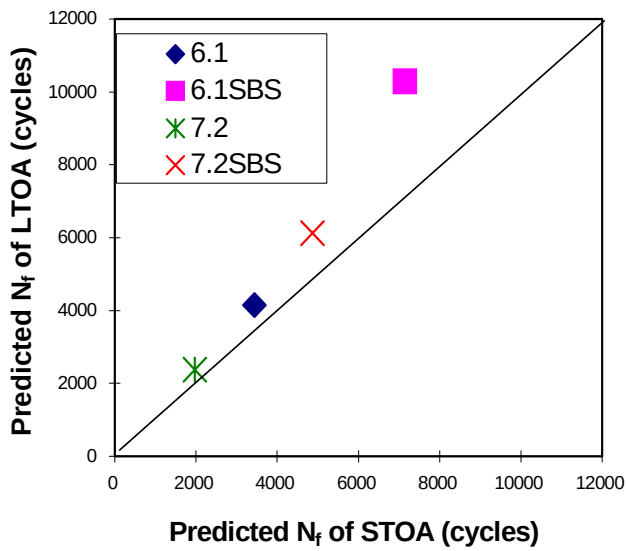

Figure 4.22 Comparison of predicted N_f between STOA and LTOA mixtures.

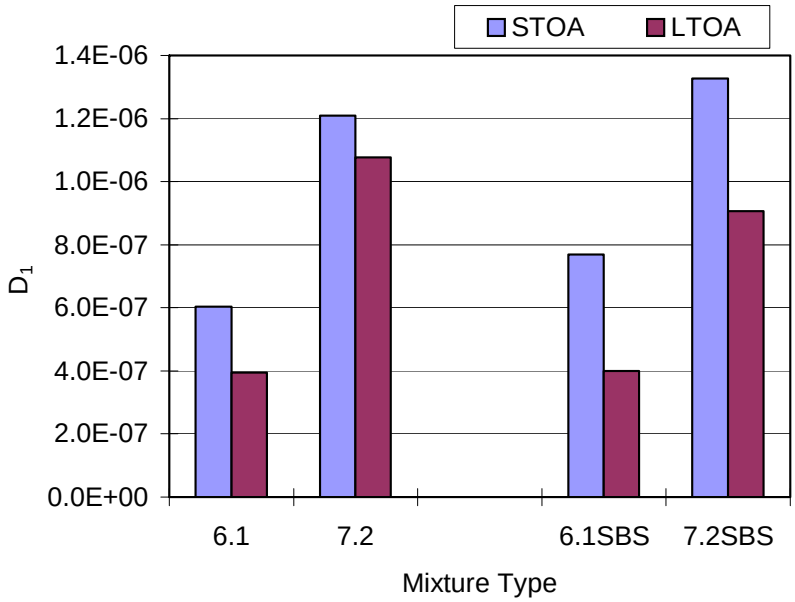

Figure 4.23 Comparison of D_1 between STOA and LTOA mixtures.

4.7 Aggregate Structure Effect

Standard Superpave IDT tests were conducted to evaluate the effect of SBS modification on different aggregate structure, resulting from different aggregate gradation. Fine 1 gradation, which passes above the restricted zone of Superpave gradation chart, was used for this study. The results of Standard Superpave IDT for fine gradation mixture are presented in Appendix C. Figure 4.24 shows number of cycles to failure (N_f) predicted from HMA fracture model using the properties measured from Standard Superpave IDT tests for coarse and fine graded mixtures. In the figure, N_f of fine gradation mixtures is higher than that of coarse gradation mixtures with unmodified binder. SBS modification increased N_f much more with coarse gradation than with fine gradation. Therefore, the test result shows that the effect of modifiers largely varies with aggregate structure, which is a function of aggregate gradation.

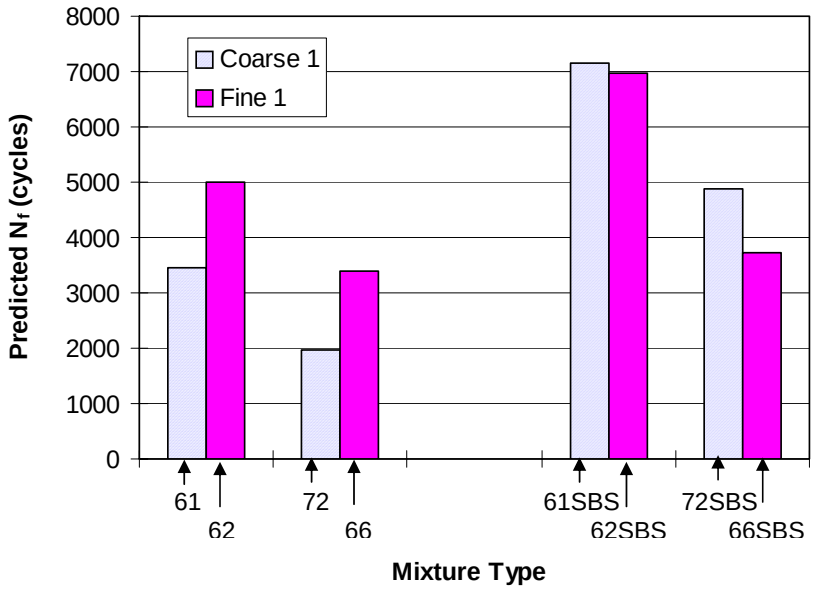

Figure 4.24 Comparison of predicted N_f of coarse and fine graded mixtures.

For all mixtures tested at 10° C, the relationship between N_f predicted from HMA fracture model and material properties measured from Standard Superpave IDT was evaluated. Creep compliance represents the time-dependent stiffness and creep behavior (viscoelastic), while fracture energy, which is a function of tensile strength and failure strain, represents the failure limit of the mixture. Therefore, from Figure 4.25, which shows the relationship between N_f and creep compliance measured at 1000 seconds, and Figure 4.26, which compares N_f with fracture energy, it appears that the fatigue cracking of all mixtures tested in this study is more strongly related with creep stiffness than fracture energy. In other words, creep responses such as m-value and D_1 or failure strain at longer-term creep are more suitable to simulate fatigue cracking development than the responses obtained from short loading time tests such as fracture energy, tensile strength, and failure strain from strength test, which allow little or no time for creep (time-dependency).

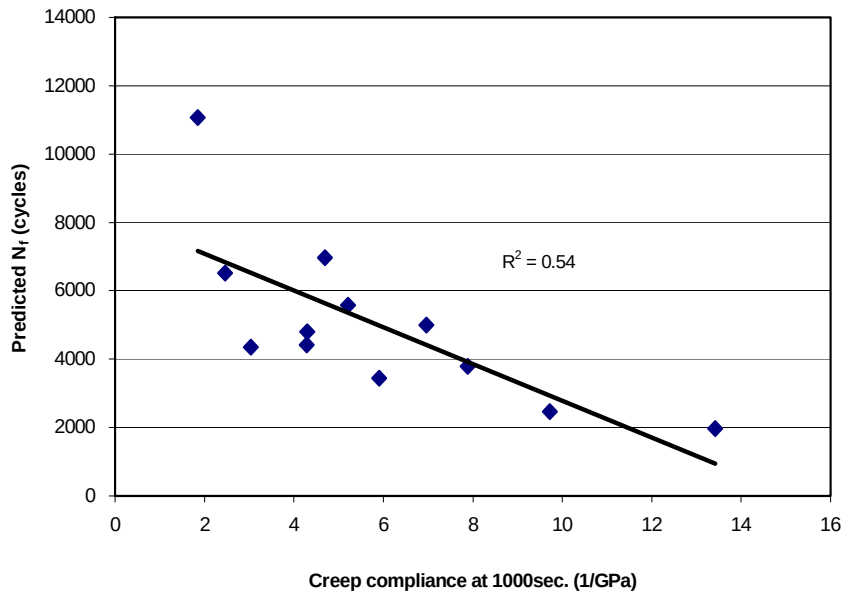

Figure 4.25 Relationship between predicted N_f and creep compliance.

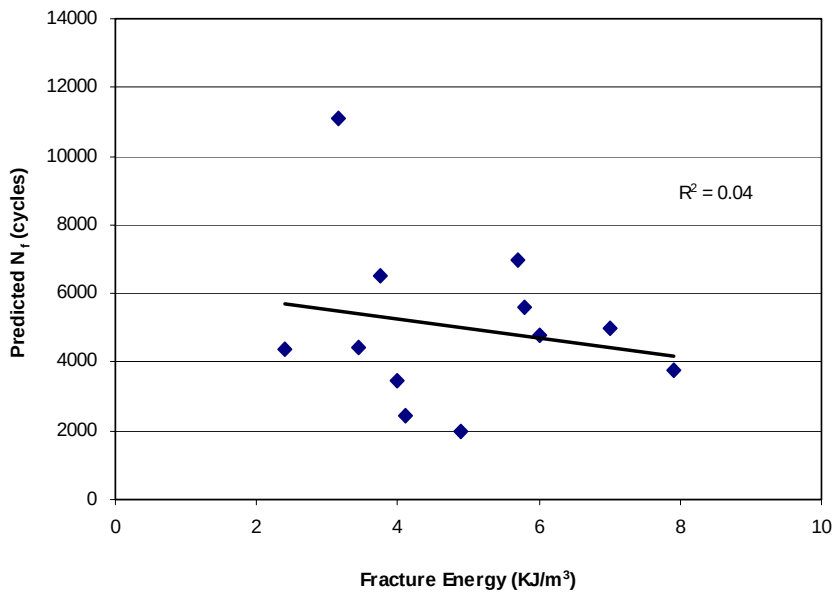

Figure 4.26 Relationship between predicted N_f and fracture energy.

CHAPTER 5
EVALUATION OF HEALING

5.1 Healing Test

A method was developed to determine the rate of healing of asphalt mixture in terms of recovered dissipated creep strain energy (DCSE) per unit time. Figure 5.1 shows the results of healing tests, in which micro-damage was accumulated by applying cyclic loads and then healing was monitored with time after loading was stopped. The accumulated DCSE during cyclic loading was determined using the procedure developed by Zhang (2000). The DCSE associated with healing was determined by developing relationships between changes in normalized resilient deformation (δ_H/δ_0) and DCSE (Grant, 2001). In order to obtain the healed DCSE, horizontal resilient deformation (δ_H) was measured by periodically performing resilient modulus

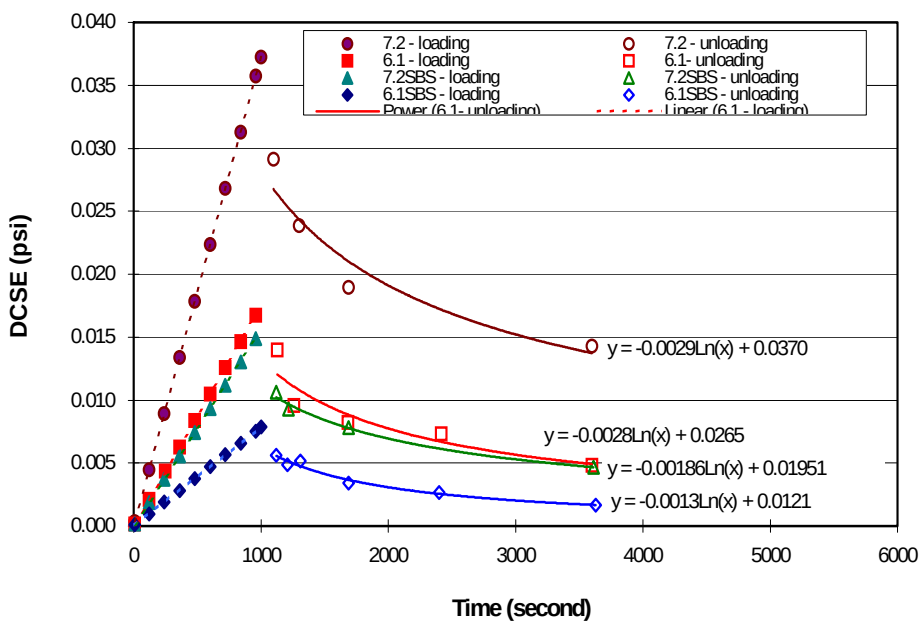

Figure 5.1 Healing test results, loading (1000 cycles with 75psi) and healing at 15° C.

tests during the healing process. As seen in Figure 5.1, a continuous reduction in δ_H/δ_0 was clear evidence of healing.

5.2 Determination of Healing Parameters

As shown in Figure 5.1, healing was observed to be nonlinear, where the rate of healing reduced with time. Therefore, a logarithmic function was selected to obtain a single parameter that could be used to express the nonlinear rate of healing. Regression analysis was performed to obtain best-fit parameters for the logarithmic functions, and then the healing rate was expressed as the slope of these logarithmic functions as shown in Figure 5.1. Figure 5.2 shows the healing rates of mixtures in terms of DCSE. For this particular set of test conditions, the SBS-modified mixtures appear to have a lower healing rate than the unmodified mixtures. However, with the same amount of loading (1000 cycles at 75 psi), the total accumulated DCSE of the SBS-modified mixtures is lower than that of unmodified mixtures, because of the lower rate of

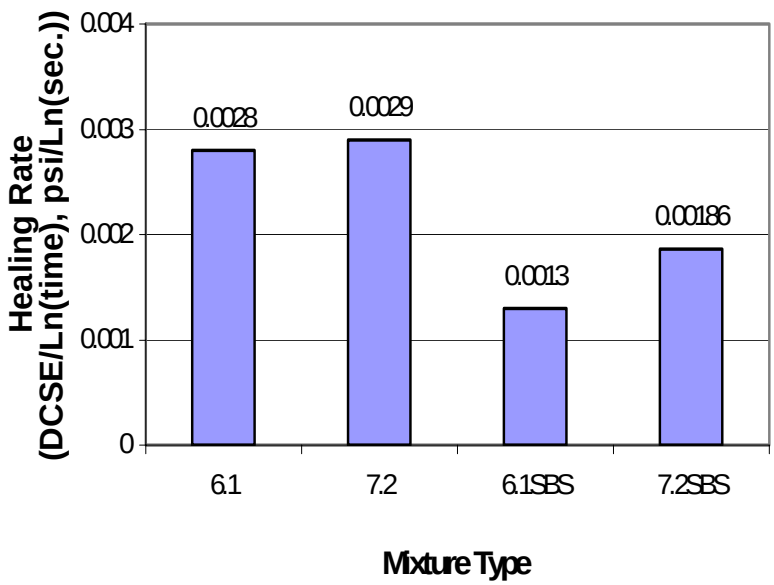

Figure 5.2 Comparison of healing rate at 15° C (after 1000 loading cycles at 75 psi).

damage (DCSE) accumulation as described in Chapter 4.1. Because the total accumulated DCSE may affect the healing rate, it is not certain that the decreased healing rate of modified mixtures would be due to the lower DCSE or due to the healing characteristic of modified mixtures. Therefore, there is a need to normalize the healing rate by the total accumulated DCSE. As shown in Figure 5.3, the healing rate appears to be proportional to the total accumulated DCSE ($DCSE_{applied}$), for all mixtures tested.

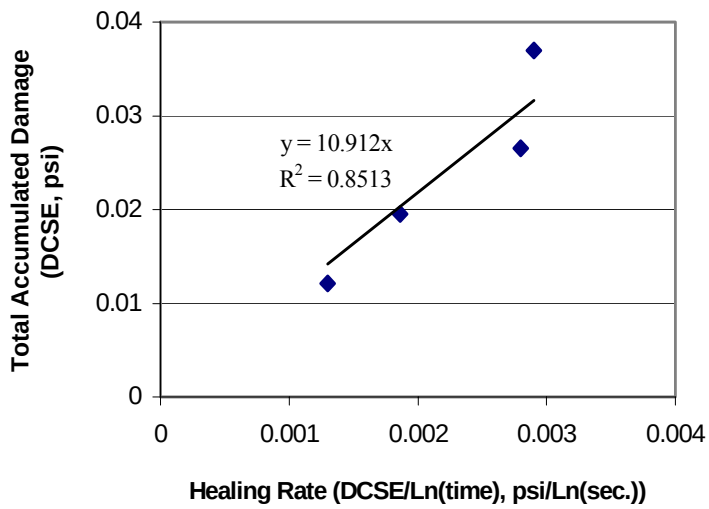

Figure 5.3 Relationship between total accumulated damage and healing rate (1000 cycles loading with 75 psi and healing at 15° C).

In order to confirm this relationship, three healing tests were conducted on the same mixture at the same condition, except for load. Cyclic loads of 55 psi were applied for three different loading times (540, 720, and 1000 seconds), which resulted in three different levels of DCSE at the start of the healing process, as shown in Figure 5.4. The test was conducted at 20° C. First of all, the healing rates in terms of DCSE were compared in Figure 5.5. As expected, the healing rate was proportional to the $DCSE_{applied}$. The normalized healing rate, a

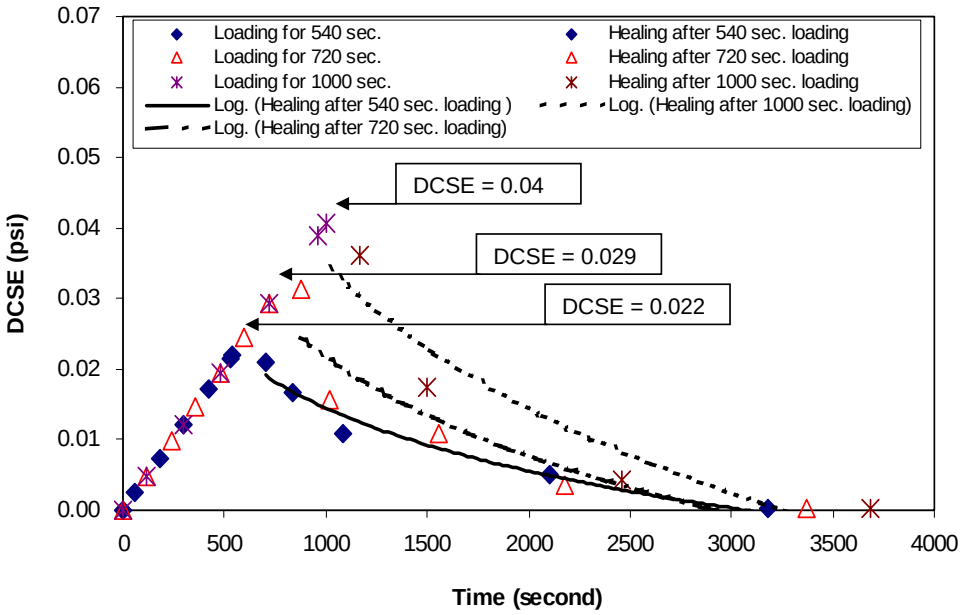

Figure 5.4 Healing test at different DCSE for modified mixtures with 6.1% AC (loading with 55 psi and healing at 20° C).

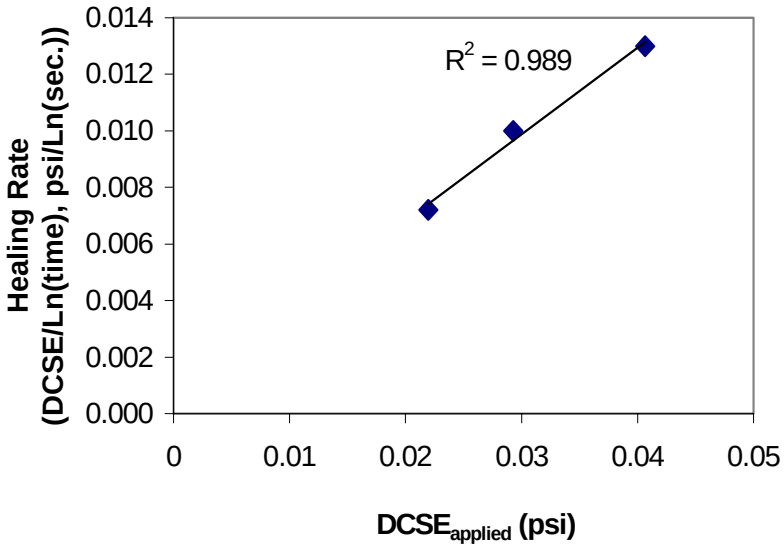

Figure 5.5 Healing rates in terms of DCSE with different $DCSE_{applied}$ on same mixtures (6.1SBS, loading with 55 psi and healing at 20° C).

slope of logarithmic function in the domain of $DCSE/DCSE_{applied}$ versus time, was then determined as shown in Figure 5.6. Figure 5.6 shows that the difference of normalized healing rates is so small as to be negligible. Thus, a normalized damage parameter ($DCSE/DCSE_{applied}$), which is DCSE divided by total accumulated DCSE, was defined to evaluate the rate of healing independently of the amount of damage incurred in the mixture.

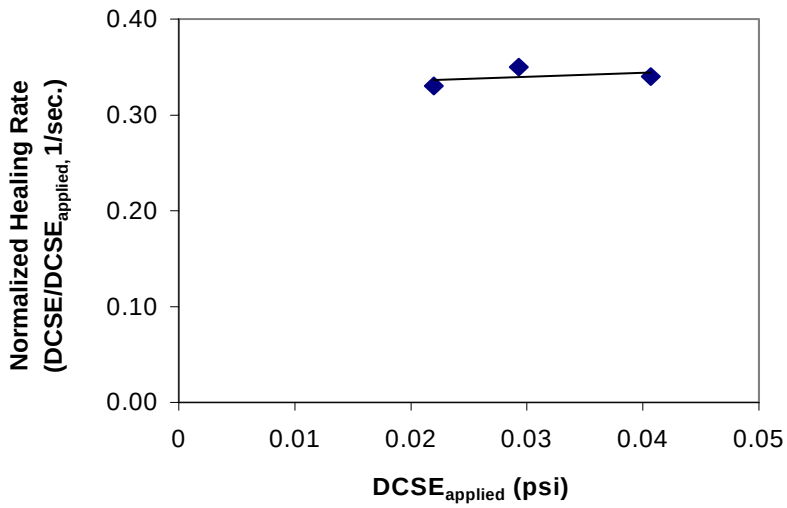

Figure 5.6 Healing rates in terms of $DCSE/DCSE_{applied}$ with different $DCSE_{applied}$ on same mixtures (6.1SBS, loading with 55 psi and healing at 20° C).

5.3 Healing Rates

Using the normalized damage parameter, $DCSE/DCSE_{applied}$, the healing test results were re-analyzed and plotted in Figure 5.7. From this analysis, the normalized healing rate was determined as shown in Figure 5.8. Lower asphalt content mixtures (6.1% for both the unmodified and the SBS modified) exhibit higher normalized healing rates than 7.2% asphalt content mixtures. This increased healing rate can be partially explained by the fact that these lower asphalt content mixtures were compacted more to reach 7.0% air void than the higher

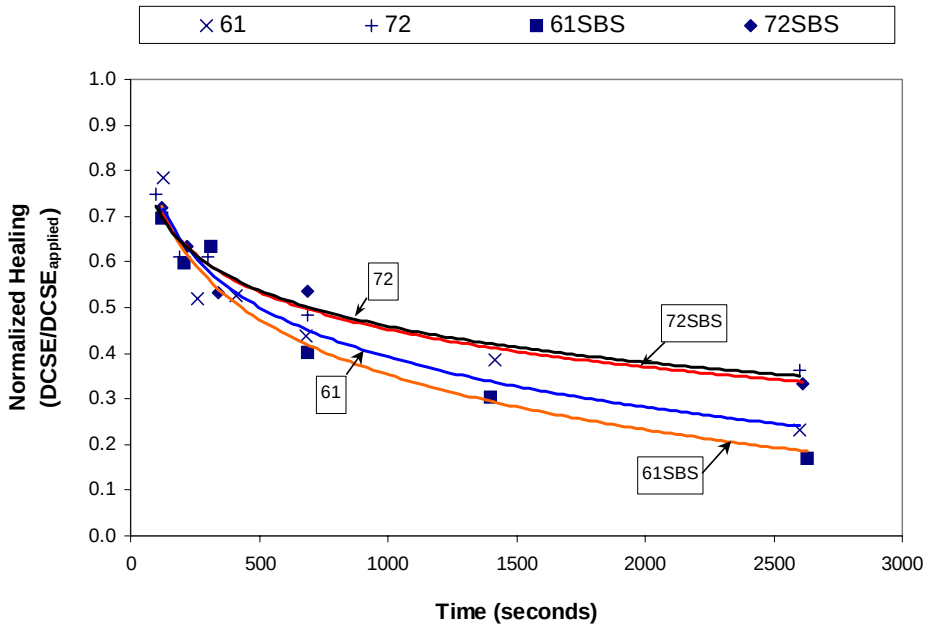

Figure 5.7 Normalized healing (after 1000 cycles of loading with 75 psi at 15° C).

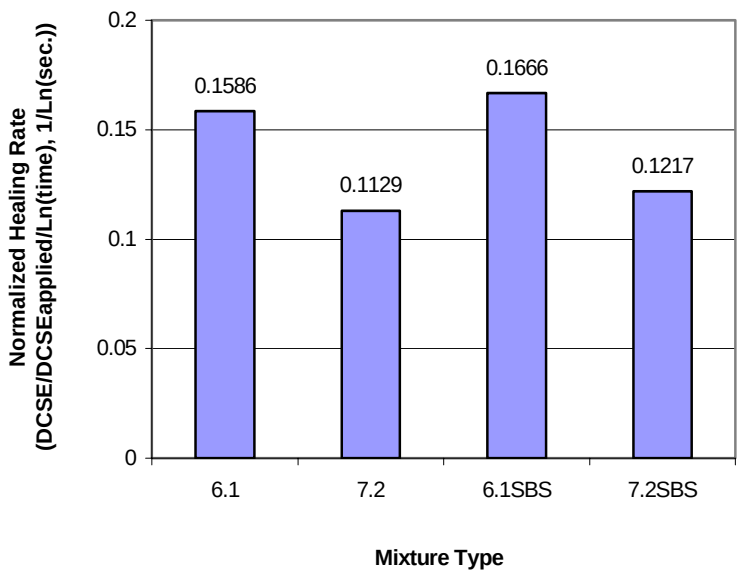

Figure 5.8 Comparison of normalized healing rates at 15° C.

asphalt content mixtures, which resulting in the increased capacity of healing. This trend is apparently related to the results of fracture tests where the mixtures with lower binder content exhibited greater resistance to fatigue-type crack growth for this particular type mixtures. On the other hand, SBS modification had relatively little effect on the normalized healing rate for both 6.1% and 7.2% asphalt content mixture. This effect of polymer on the healing rate can be partially explained by the work done by Little et al. (1999), who found that SBS polymer reduced a little of the healing rate of bitumen but retarded the crack growth of asphalt mixture. They hypothesized that the polymer acts as a filler system that interrupts the ability of pure bitumen to reestablish contact and heal.

The healing test was also conducted on these mixtures at three temperatures (0, 10, and 20° C) to evaluate the temperature sensitivity of the healing rate. The cyclic loads were 2000, 1200, and 500 lb at 0, 10, and 20° C, respectively, and repeated for 360 seconds. Loads were determined that would provide a horizontal strain between 100 to 200 micro-strain. The healing process was same as the previous healing tests, but the sample did not have a hole at the center, while the previous samples had a hole.

This designed hole might decrease the normalized healing rates as compared to those shown in Figure 5.9. On the other hand, as shown in Figure 5.9, the normalized healing rate of 6.1% asphalt content mixtures exhibited a higher normalized healing rate at all temperatures. Thus, it appears that the effect of polymer modification on the healing rate was negligible at all temperatures. As far as the asphalt binder, SBS polymer did not show an increase in the normalized healing rate for either 6.1% and 7.2 % asphalt contents. Figure 5.9 also showed that the healing rate increased as temperature increased. The increase in healing rate at higher temperature was greater than at lower temperature.

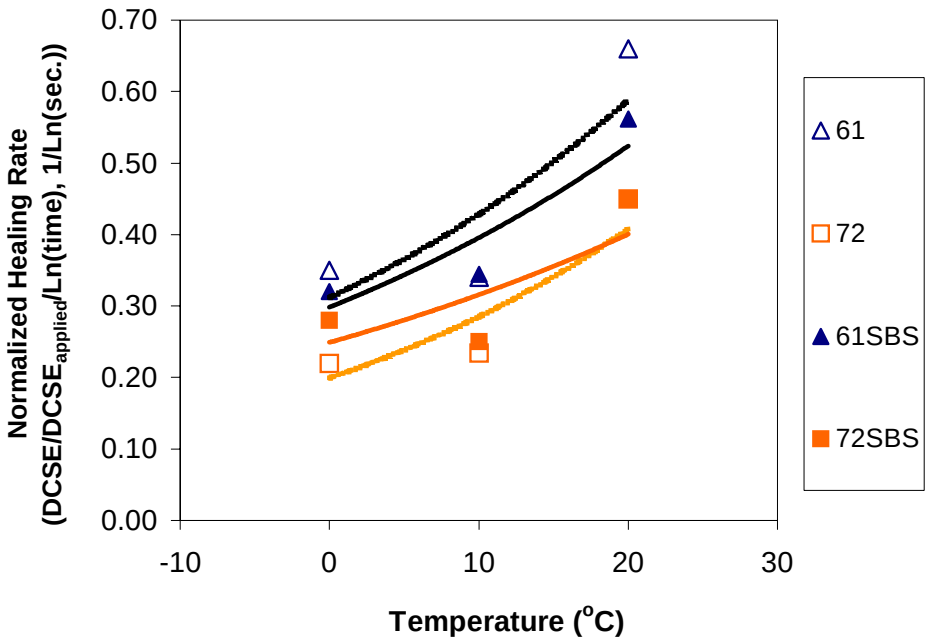

Figure 5.9 Temperature sensitivity of normalized healing rate.

In conclusion, it appears that the healing of these mixtures at low to intermediate temperature (0 to 20° C) are more affected by the structural characteristics of mixture such as asphalt content than the binder characteristics such as the polymer modification. Thus, SBS polymers appear to have no influence on the healing of asphalt mixtures. In addition, the temperature sensitivity of healing rate is non-linear but close to exponential function.

5.4 Damage Recovery

The first healing test of this study gave the overall healing characteristics of asphalt mixtures, but could not differentiate the damage-related healing from the overall healing. The second healing test was performed to identify the pure damage recovery from the overall healing by eliminating the effect of steric hardening and cooling. In contrast with the factors that increase

the resilient deformation during loading; damage, steric softening, and heating, the factors reducing resilient deformation during healing can be divided into three parts; damage recovery, steric hardening, and cooling. As described in Chapter 4.2, steric softening and probably heating can cause a rapid increase in resilient deformation during the initial stages of loading, but this increase of resilient deformation has no physical meaning from the damage point of view. Therefore, the total increase of resilient deformation (δ_D-δ_i) can be divided into two parts as shown in Figure 5.10: $\Delta\delta_D$ (= δ_D-δ_0) related to the damage, and $\Delta\delta ss$ (= δ_0-δ_i) related to the steric softening and heating. Then, the total decrease of resilient deformation in the healing process can be theoretically divided into two parts as shown in Figure 5.10; $\Delta\delta_{DR}$ that is damage recovery for $\Delta\delta_D$, and $\Delta\delta_{SH}$ that is steric hardening and cooling for $\Delta\delta ss$. In Figure 5.10, t_D is the time when the loading is stopped, t_{DR} is the time when the damage recovery is finished, t_H is the time when the mixture is fully healed, and $\dot{H}_N$ is the rate of damage recovery.

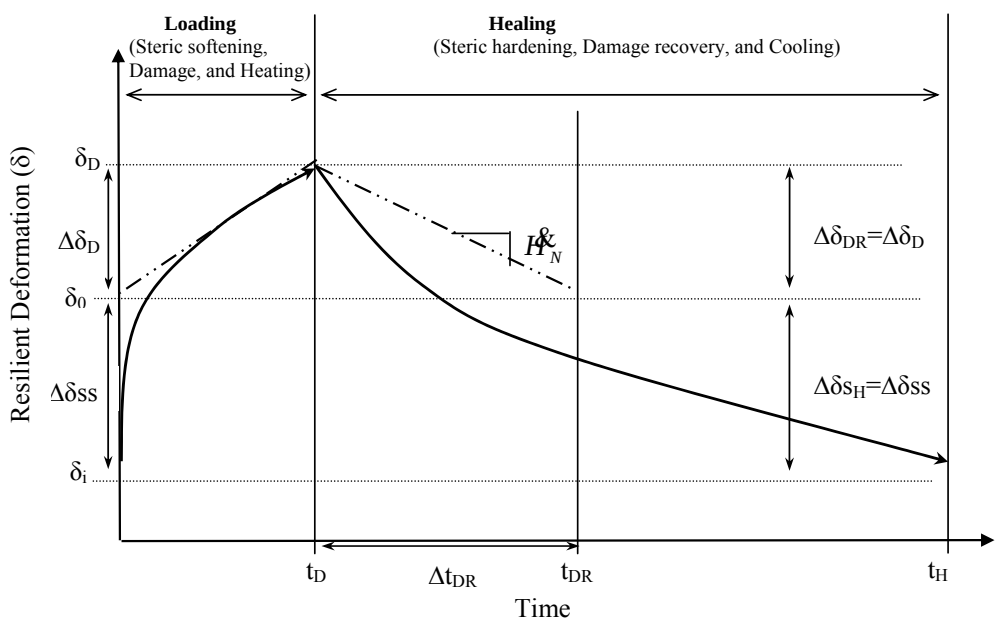

Figure 5.10 Resilient deformations during loading and healing.

The second healing test was performed to identify the pure damage recovery ($\Delta\delta_{DR}$) from the overall healing by eliminating the effect of steric hardening and cooling ($\Delta\delta_{SH}$). The test consisted of repeated loading sets having a rest period for healing between loading sets, as shown in Figure 5.11. The loading type was the same as for repeated fracture tests, and the loading time for each set was 6 minutes (360 loading cycles). After loading, the load was removed for healing. A second set of loading was then applied for 6 minutes followed by the second healing period. The loading and healing were repeated with healing time of around 4, 8, 12, 16, and 20 minute.

As described above, the original deformation (δ_0) theoretically represents the horizontal resilient deformation at the point that damage is started. This value was used to normalize damage and damage recovery in the second healing test such that the effect of stiffness was eliminated from the determination of the amount of damage and damage recovery. By the way, the damage was not fully recovered during rest periods in this test (i.e., part of damage remained in the specimen).

Thus, the normalized damage (D_N) was determined by adding the remaining normalized damage (D_{NR}) to the net normalized damage (D_{NN}). The relative damage recovery was defined as the ratio of the normalized damage recovery to the normalized damage. As expressed in the equations, parameters associated with damage and damage recoveries are presented as follows.

- Net normalized damage ($D_{NN,\,i}$) = ($\delta_{D,\,i}$ - $\delta_{0,\,i-1}$) / $\delta_{0,\,i-1}$, i=1~5
- Normalized damage ($D_{N,\,i}$) = $D_{NN,\,i}$ + $D_{NR,\,i-1}$ i=1~5, $D_{NR,\,0}$ = 0
- Remaining normalized damage ($D_{NR,\,i}$) = $D_{N,\,i}$ - $H_{N,\,i}$, i=1~5
- Normalized damage recovery ($H_{N,\,i}$) = ($\delta_{D,\,i}$ - $\delta_{0,\,i}$) / $\delta_{0,\,i-1}$, i=1~5
- Relative damage recovery = $H_{N,\,i}$ / $D_{N,\,i}$, i=1~5

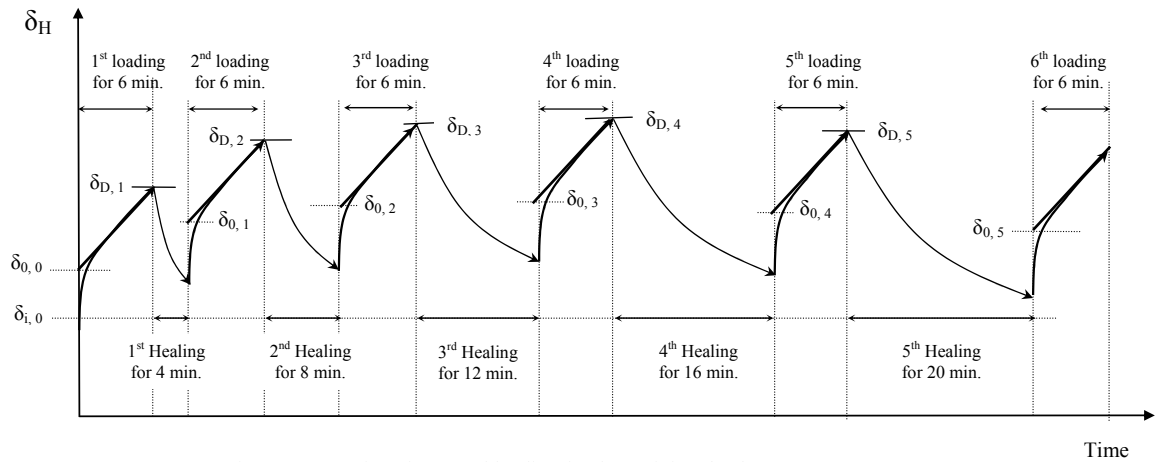

Figure 5.11 Series of repeated loading for determining the damage recovery rate.

The results of the second healing experiments are shown in Figure 5.12 and in Appendix D. By plotting the relative damage recovery with rest periods, the rate of normalized damage recovery ($\dot{H}_N$) was determined as a slope of linear regression curve. Time to the full recovery of damage (Δt_{DR}) was then calculated by extrapolating the regression curve (Figure 5.10).

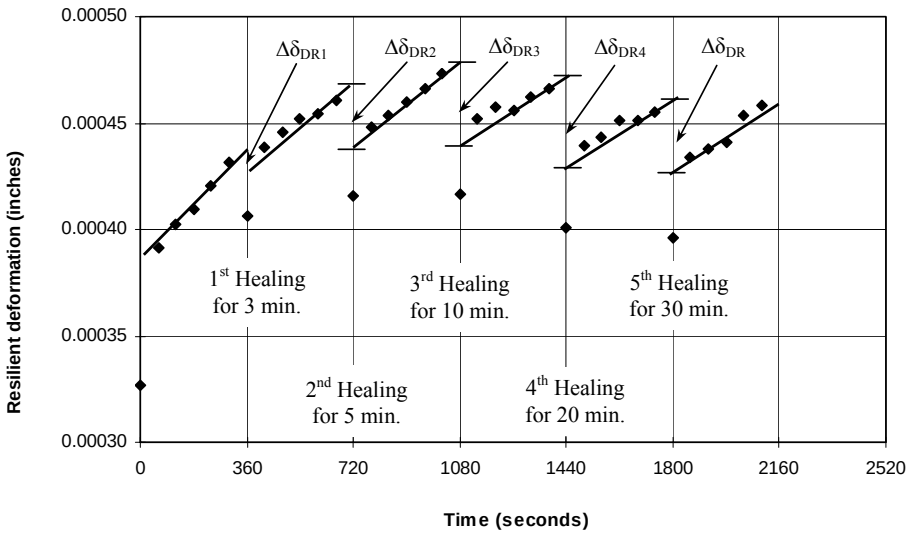

Figure 5.12 Typical healing test result for determining the rate of damage recovery (72SBS, 500 (lb) of cyclic loads at 20° C).

From the test and analysis, the rate of normalized damage recovery of mixtures at three temperatures (0, 10, and 20° C) is presented in Figure 5.13. As expected, 6.1% asphalt content mixtures exhibited the higher rate of damage recovery than those of 7.2% asphalt content mixtures at all ranges of temperatures. However, there was no difference in the rate of damage recovery between unmodified and SBS modified mixtures (both 6.1% and 7.2% asphalt content mixtures). Therefore, it appears that the overall healing rate as well as the rate of damage recovery of these mixtures is more affected by the structural characteristics of mixtures such as binder content, film thickness, VMA, etc., than by SBS polymer modification. SBS polymer

seems to have no effect on the rate of damage recovery of asphalt mixtures. It appears that the healing rate can replace the rate of damage recovery for the relative comparison of damage recovery between different mixtures.

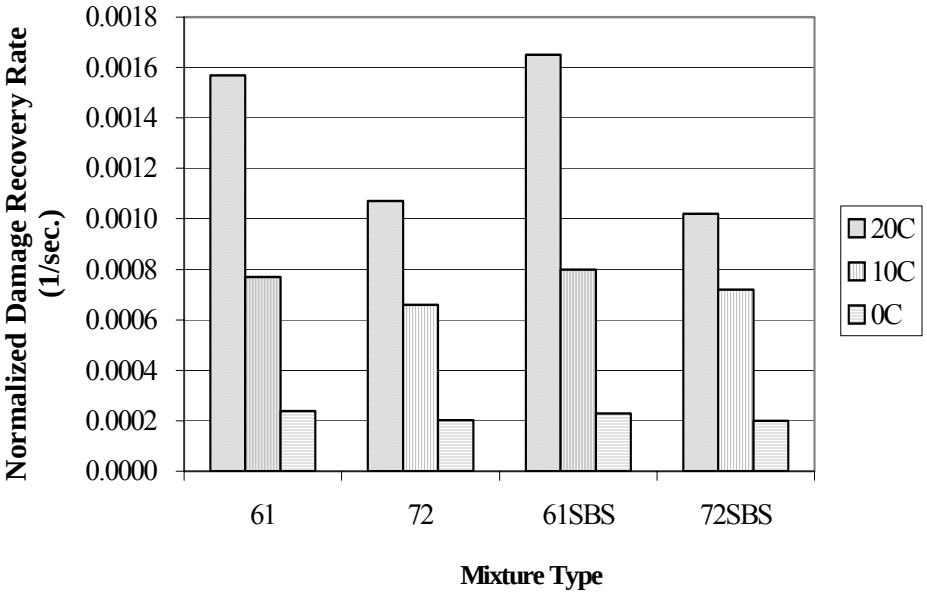

Figure 5.13 Normalized damage recovery rates of mixtures at three temperatures.

As far as the temperature sensitivity of damage recovery rates, the difference of damage recovery rates between 6.1% asphalt content mixture and 7.2% asphalt content mixture decreased as temperature decreased. This result is clearly shown in Figure 5.14, which is a plot of damage recovery rate versus temperature. The damage recovery rate increases exponentially with temperatures. As shown in Figure 5.14, the coefficients of the regression curve fitted in the exponential function of 6.1% unmodified mixture are identical to that of 6.1% SBS modified mixture. Similar results were obtained for mixtures with 7.2% asphalt content. Therefore, it appears that not only the rate of damage recovery but also the temperature sensitivity of the rate

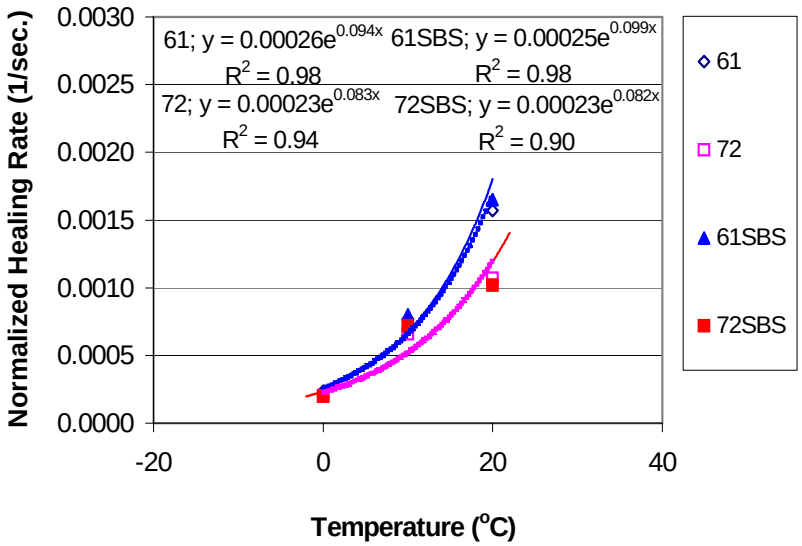

Figure 5.14 Temperature sensitivity of normalized damage recovery rate.

of damage recovery is mainly affected by the structure characteristics of mixtures. This result can be more clearly explained when the rate of damage recovery is compared with creep parameters (D_1 and m-value), as shown in Figure 5.15 and Figure 5.16. The rate of damage recovery is well correlated with D_1 at all range of temperatures tested, but not well with m-value. As IDT test results indicated that the structural characteristics of asphalt mixture could be well represented in D_1 and the binder characteristics of asphalt mixture could be well represented in m-value, the fact that the rate of damage recovery is mainly affected by the structure characteristics of mixtures than the binder properties appears to be clear in this study.

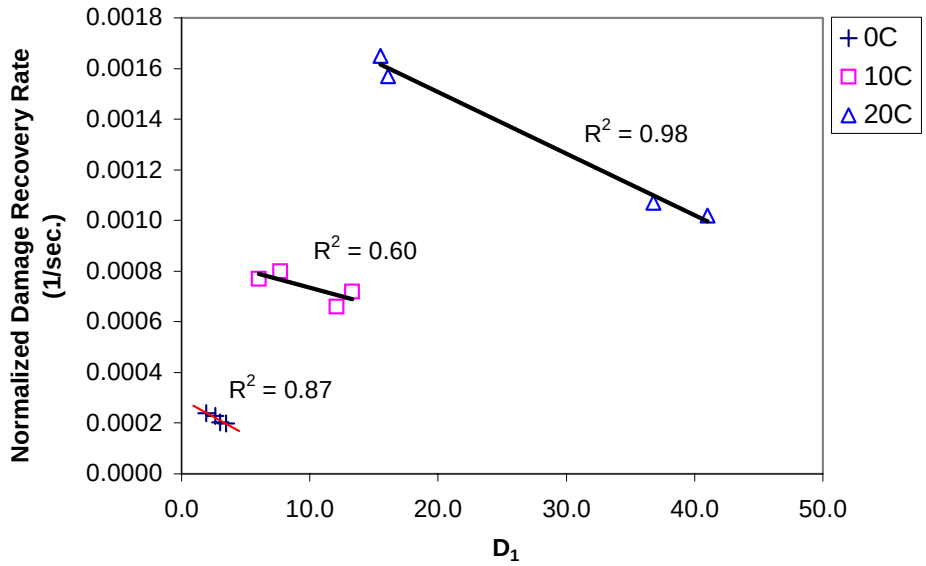

Figure 5.15 Relationship between normalized damage recovery rate and D_1.

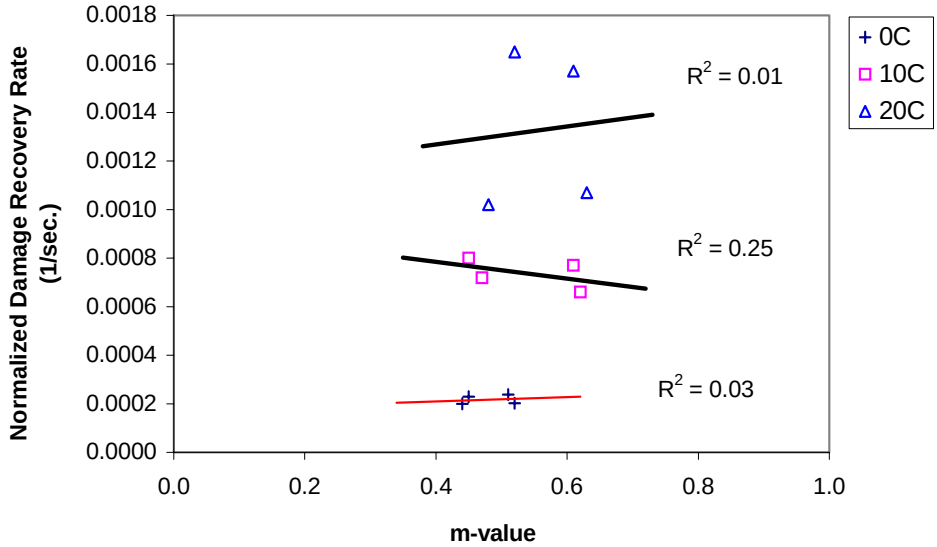

Figure 5.16 Relationship between normalized damage recovery rate and m-value.

CHAPTER 6
COST ANALYSIS FOR USE OF SBS MODIFIER

A parametric study was conducted to analyze the cost effectiveness for use of SBS polymer modified mixture in asphalt pavement. The study consisted of three steps: (1) design of three types of pavement structures (conventional asphalt pavement with crushed stone base, full depth asphalt pavement, and HMA overlay on the conventional asphalt pavement), (2) calculation of energy ratio as a fatigue cracking criterion for designed pavement structures, and (3) cost analysis for pavement structures with and without SBS modified mixture.

6.1 Pavement Design

For structural pavement design (layer thickness design), three typical asphalt pavement types (conventional asphalt pavement with crushed stone base, full depth asphalt pavement, and HMA overlay on the conventional asphalt pavement) were selected. Pavements were designed for three traffic levels, which represent low, medium, and high traffic levels. Based on the FDOT traffic data from 1997, 3 million or less ESALs which represent low traffic levels (traffic level 1 to 3 of Superpave mix design) cover 39.5% of total estimated design ESALs in Florida. Three to ten million ESALs which represent medium traffic levels (traffic level 4 to 5 of Superpave mix design) covers 58.9%, and 30 million or more ESAL which represent high traffic levels (traffic level 6 to 7 of Superpave mix design) covers 1.6% of total estimated design ESALs in Florida. Thus, three million ESAL as a upper limit of low traffic levels, 10 million ESAL as a average of medium traffic levels, and 30 million ESAL as a low limit of high traffic levels were selected for pavement design in this study.

For the selected pavement type and traffic levels, the AASHTO design guide (1993) was used for layer thickness design, and the design AC layer thickness was checked by AI (Asphalt

Institute) method. As input values, asphalt concrete (AC) modulus was determined from the Superpave IDT, and typical moduli of base and subgrade in Florida were selected. Structural coefficient (a_i) and drainage coefficient (m_i) were determined according to the AASHTO design guide as shown in Table 6.1. The following design inputs were assumed in all cases: 95% of reliability (R), 0.4 of standard deviation (S_o), and 2.0 of design serviceability loss (ΔPSI).

Table 6.1 Design Layer Thickness and Calculated Stresses

			Low Traffic	Medium Traffic	High Traffic
Conventional	Modulus (psi)	a_i & m_i	LAYER THICKNESS (inches)		
AC	1,200,000	0.40	6.0	7.0	8.5
Crushed stone base	40,000	0.14 & 1.2	8.5	10.5	10.0
Subgrade	10,000				
σ_t (psi) at the bottom of AC layer			204.0	165.0	129.0

			Low Traffic	Medium Traffic	High Traffic
HMA Full Depth	Modulus (psi)	a_i & m_i	LAYER THICKNESS (inches)		
AC	1,200,000	0.40	10.0	12.0	14.0
Subgrade	10,000				
σ_t (psi) at the bottom of AC layer			119.0	87.6	67.1

			Low Traffic	Medium Traffic	High Traffic
HMA Overlay	Modulus (psi)	a_i & m_i	LAYER THICKNESS (inches)		
AC Overlay	1,200,000	0.40	3.0	3.5	4.5
AC	1,200,000	0.40	6.0	7.0	8.5
Crushed stone base	40,000	0.14 & 1.2	8.5	10.5	10.0
Subgrade	10,000				
σ_t (psi) at the bottom of AC layer			121.0	94.7	68.0

Table 6.1 shows the resulting design layer thickness and the resulting tensile stresses at the bottom of AC layer. The tensile stresses were calculated for each design pavement structure using multi-layer elastic analysis program, BISAR using 9000 (lb) single axle loads with 6-inch radius. These stresses were used for calculating the energy ratio.

6.2 Calculation of Energy Ratio

A parameter, Energy Ratio (ER), which represents the fracture toughness of asphalt mixtures, was recently developed by Jajliardo (2003). This parameter allows for the evaluation of cracking performance for different pavement structures by incorporating the effects of mixture properties and pavement structural characteristics. In this study, the energy ratio was calculated for the design pavement structures as a fatigue cracking criterion. The energy ratio is expressed in Equation (6.1).

$$ER = \frac{a \times DCSE_f}{m^{2.98} \times D_1} \tag{6.1}$$

where $a = 0.0299\,\sigma^{-31}\,(6.36 - S_t) + 2.46 \times 10^{-8}$

σ is tensile stress of asphalt layer in psi

S_t is tensile strength in MPa

$DCSE_f$ is Dissipated Creep Strain Energy in KJ/m^3

D_1 and m are creep parameters in 1/psi.

The primary benefit of SBS polymer to mixture cracking resistance is derived from a reduced rate of micro-damage accumulation, which was reflected in a lower m-value for modified mixtures. Thus, by varying the variables in Equation (6.1), one can evaluate the effect of modifiers on the ER. The factorial design for the parametric study is shown in Table 6.2. Variables in Table 6.2 were selected based on the Superpave IDT results conducted at 10° C.

Table 6.2 Factorial Design for Parametric Study

m-value		0.60			0.45		
D_1*10^{-7} (1/psi)		14.0	10.0	6.0	14.0	10.0	6.0
$DCSE_f$ (KJ/m^3)	1.0						
	2.0						
	3.0						
	4.0						

For example, the typical m-value was 0.6 for unmodified mixtures, and 0.45 for modified mixtures. The ER calculated for each pavement structure and the selected factorial design are presented in Tables 6.3 through Table 6.5.

Table 6.3 Energy Ratios Calculated for Conventional Pavement Structures

(a) For low traffic

m-value		0.60			0.45		
D_1*10^{-7} (1/psi)		14.0	10.0	6.0	14.0	10.0	6.0
$DCSE_f$ (KJ/m^3)	1.0	0.11	0.16	0.26	0.26	0.37	0.61
	2.0	0.22	0.31	0.52	0.52	0.73	1.22
	3.0	0.33	0.47	0.78	0.78	1.10	1.83
	4.0	0.44	0.62	1.03	1.04	1.46	2.44

(b) For medium traffic level

m-value		0.60			0.45		
D_1*10^{-7} (1/psi)		14.0	10.0	6.0	14.0	10.0	6.0
$DCSE_f$ (KJ/m^3)	1.0	0.14	0.19	0.32	0.33	0.46	0.76
	2.0	0.28	0.39	0.65	0.65	0.92	1.53
	3.0	0.42	0.58	0.97	0.98	1.37	2.29
	4.0	0.56	0.78	1.30	1.31	1.83	3.05

Table 6.3–continued

(c) For high traffic level

m-value		0.60			0.45		
D_1*10^{-7} (1/psi)		14.0	10.0	6.0	14.0	10.0	6.0
$DCSE_f$ (KJ/m^3)	1.0	0.21	0.29	0.48	0.48	0.68	1.13
	2.0	0.41	0.58	0.96	0.97	1.36	2.26
	3.0	0.62	0.86	1.44	1.45	2.04	3.39
	4.0	0.82	1.15	1.92	1.94	2.71	4.52

Table 6.4 Energy Ratios Calculated for Full Depth AC Pavement

(a) For low traffic level

m-value		0.60			0.45		
D_1*10^{-7} (1/psi)		14.0	10.0	6.0	14.0	10.0	6.0
$DCSE_f$ (KJ/m^3)	1.0	0.24	0.34	0.56	0.57	0.80	1.33
	2.0	0.48	0.68	1.13	1.14	1.59	2.65
	3.0	0.72	1.01	1.69	1.70	2.39	3.98
	4.0	0.96	1.35	2.25	2.27	3.18	5.30

(b) For medium traffic level

m-value		0.60			0.45		
D_1*10^{-7} (1/psi)		14.0	10.0	6.0	14.0	10.0	6.0
$DCSE_f$ (KJ/m^3)	1.0	0.50	0.69	1.16	1.17	1.64	2.73
	2.0	0.99	1.39	2.31	2.34	3.27	5.45
	3.0	1.49	2.08	3.47	3.50	4.91	8.18
	4.0	1.98	2.78	4.63	4.67	6.54	10.90

(c) For high traffic level

m-value		0.60			0.45		
D_1*10^{-7} (1/psi)		14.0	10.0	6.0	14.0	10.0	6.0
$DCSE_f$ (KJ/m^3)	1.0	1.03	1.44	2.40	2.43	3.40	5.66
	2.0	2.06	2.88	4.80	4.85	6.79	11.32
	3.0	3.09	4.32	7.20	7.28	10.19	16.98
	4.0	4.12	5.76	9.61	9.70	13.58	22.64

Table 6.5 Energy Ratios Calculated for HMA Overlay

(a) For low traffic level

m-value		0.60			0.45		
D_1*10^{-7} (1/psi)		14.0	10.0	6.0	14.0	10.0	6.0
$DCSE_f$ (KJ/m^3)	1.0	0.23	0.33	0.54	0.55	0.77	1.28
	2.0	0.47	0.65	1.09	1.10	1.54	2.56
	3.0	0.70	0.98	1.63	1.65	2.31	3.84
	4.0	0.93	1.31	2.18	2.20	3.08	5.13

(b) For medium traffic level

m-value		0.60			0.45		
D_1*10^{-7} (1/psi)		14.0	10.0	6.0	14.0	10.0	6.0
$DCSE_f$ (KJ/m^3)	1.0	0.41	0.57	0.95	0.96	1.34	2.24
	2.0	0.81	1.14	1.90	1.92	2.68	4.47
	3.0	1.22	1.71	2.85	2.87	4.02	6.71
	4.0	1.63	2.28	3.79	3.83	5.37	8.94

(c) For high traffic level

m-value		0.60			0.45		
D_1*10^{-7} (1/psi)		14.0	10.0	6.0	14.0	10.0	6.0
$DCSE_f$ (KJ/m^3)	1.0	0.99	1.39	2.31	2.34	3.27	5.45
	2.0	1.98	2.77	4.62	4.67	6.54	10.90
	3.0	2.97	4.16	6.94	7.01	9.81	16.35
	4.0	3.96	5.55	9.25	9.34	13.08	21.80

On the other hand, Jajliardo (2003) recommended a minimum required ER (ER_{min}) for various traffic levels. He recommended an ER_{min} of 1.1 for 3 million ESAL, 1.3 for 10 million ESAL, and 1.7 for 30 million ESAL. Comparing the ER in Table 6.3 with the ER_{min}, most of AC layers in conventional pavement structures with unmodified binder (typically m-value of 0.6) could not meet the ER_{min} for all traffic levels. Even though AC layers modified with polymer

(typically m-value of 0.45) having low $DCSE_f$ or high D_1 (generally means low quality mixtures) could not meet the ER_{min}, the modified AC layer with high $DCSE_f$ or low D_1 (generally means high quality mixtures) met the ER_{min} for all traffic levels.

As far as full depth AC pavement structures, the ER of modified AC was enough to meet the criteria, while the ER of unmodified AC layers was not enough to meet the criteria for low traffic level as shown in Table 6.4. However, the ER for medium and high traffic levels was over the ER_{min} regardless of modification, except for the cases of low $DCSE_f$. Very similar trends resulted in HMA overlay pavement structures as shown in Table 6.5.

In summary, when the ER is considered as a criterion of fatigue cracking, it appears that conventional pavements, which consists of AC surface, crushed stone base, and subgrade, designed according to the AASHTO procedure, do not have a sufficient resistance against fatigue cracking, even though SBS polymer modified asphalt mixtures are used in AC layer, except for the pavement structures with a very high quality asphalt mixture, which has a higher $DCSE_f$ and lower creep. Thus, a thicker AC layer than that designed according to the AASHTO procedure is necessary to have the sufficient fatigue cracking resistance. Conversely, unmodified AC layers with higher quality asphalt mixtures (higher $DCSE_f$ and lower creep) and polymer modified AC layers have sufficient fatigue cracking resistance in full depth and HMA overlay pavement structures, while unmodified AC layers with lower quality asphalt mixtures (lower $DCSE_f$ and higher creep) are not sufficient to tolerate the fatigue cracking.

6.3 Cost Analysis

A parametric study was conducted to compare the construction costs of AC layers with and without SBS polymer modifier. Based on the FDOT Item Average Unit Costs (item no. 2334 and 2337), the unit cost of unmodified HMA and polymer modified HMA are assumed at

50 dollars per ton and 70 dollars per ton, respectively. The cost analysis was performed for two cases as follows:

- Calculated ER ≥ Minimum Required ER
- Calculated ER of Unmodified HMA ≥ Calculated ER of Modified HMA

Case 1 ($ER_{HMA} \geq ER_{min}$)

In this case, the minimum required ER (ER_{min}) was used as a criterion to determine the construction cost. The ER_{min} criteria were presented in the previous section (i.e., 1.1 for 3 million ESAL, 1.3 for 10 million ESAL, and 1.7 for 30 million ESAL). When the calculated ER, which is based on the thickness designed according to the AASHTO procedure, is less than the ER_{min}, the ER was increased to meet the ER_{min} by increasing the thickness of AC layer resulting in the decreased tensile stress at the bottom of AC layer. Otherwise, the designed thickness was use to calculate the construction cost. In other words, the design thickness of AC layer meeting the ER_{min} was maintained, regardless of redundant margin between the ER_{min} and the ER calculated, since the thickness designed according to AASHTO procedure was assumed as the minimum allowable thickness.

Table 6.6 and Figure 6.1 shows the cost of AC layer meeting the ER_{min} for conventional pavement structures. AC layer thickness and resulting tensile stress meeting the ER_{min} are presented in Appendix E. Table 6.7 and Table 6.8 show the cost of AC layer for HMA full depth

Table 6.6 Cost of AC Layer to Meet ER_{min} in Conventional Pavement

(a) Low traffic (unit: $)

m-value		0.60 (unmodified)			0.45 (modified)		
$D_1 * 10^{-7}$ (1/psi)		14	10	6	14	10	6
$DCSE_f$ (KJ/m^3)	1.0	37.8	35.3	31.0	33.3	30.5	26.2
	2.0	32.4	29.6	25.7	27.6	24.5	19.2
	3.0	29.3	27.1	21.7	23.7	19.2	19.2
	4.0	26.8	24.0	18.0	20.0	19.2	19.2

Table 6.6–continued

(b) Medium traffic

m-value		0.60 (unmodified)			0.45 (modified)		
D_1*10^{-7} (1/psi)		14	10	6	14	10	6
$DCSE_f$ (KJ/m^3)	1.0	38.6	36.7	32.4	34.4	31.6	27.4
	2.0	33.3	31.0	26.8	29.1	25.7	22.0
	3.0	29.6	27.6	23.1	25.4	22.0	22.0
	4.0	27.9	25.1	19.7	22.0	22.0	22.0

(c) High traffic

m-value		0.60 (unmodified)			0.45 (modified)		
D_1*10^{-7} (1/psi)		14	10	6	14	10	6
$DCSE_f$ (KJ/m^3)	1.0	40.9	38.1	34.1	37.2	33.8	29.6
	2.0	35.3	32.7	28.8	31.0	28.2	26.2
	3.0	32.4	29.6	25.4	27.6	26.2	26.2
	4.0	29.9	27.4	24.0	26.2	26.2	26.2

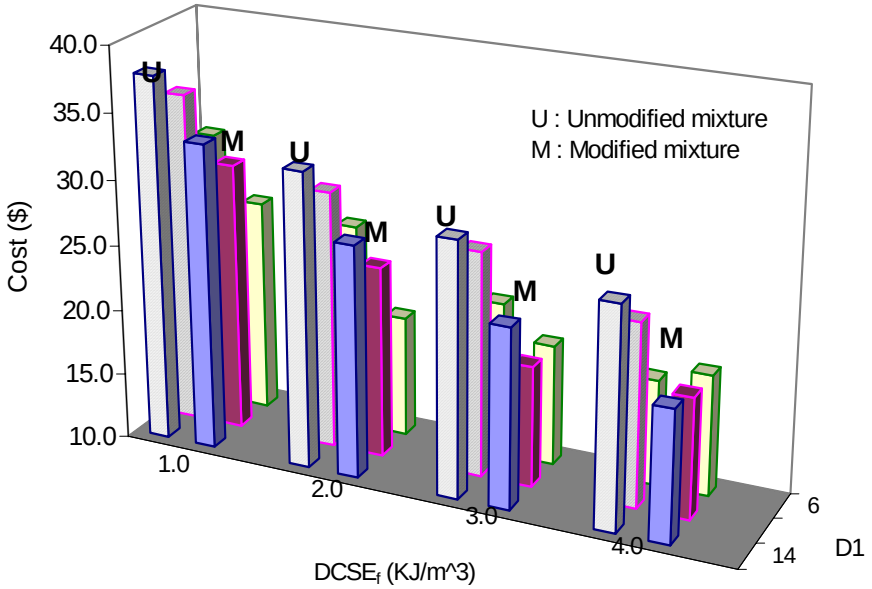

Figure 6.1 Comparison of construction cost of AC layer depending on mixture properties for conventional pavement and low traffic level.

Table 6.7 Cost of AC Layer to Meet ER_{min} in HMA Full Depth Pavement

(a) Low traffic (unit: $)

m-value		0.60 (unmodified)			0.45 (modified)		
D_1*10^{-7} (1/psi)		14	10	6	14	10	6
$DCSE_f$ (KJ/m^3)	1.0	40.0	37.5	33.6	35.5	32.7	30.5
	2.0	34.7	31.9	28.2	30.5	30.5	30.5
	3.0	31.6	29.0	28.2	30.5	30.5	30.5
	4.0	29.3	28.2	28.2	30.5	30.5	30.5

(b) Medium traffic

m-value		0.60 (unmodified)			0.45 (modified)		
D_1*10^{-7} (1/psi)		14	10	6	14	10	6
$DCSE_f$ (KJ/m^3)	1.0	41.5	38.6	34.7	36.9	36.1	36.1
	2.0	35.8	33.8	33.8	36.1	36.1	36.1
	3.0	33.8	33.8	33.8	36.1	36.1	36.1
	4.0	33.8	33.8	33.8	36.1	36.1	36.1

(c) High traffic

m-value		0.60 (unmodified)			0.45 (modified)		
D_1*10^{-7} (1/psi)		14	10	6	14	10	6
$DCSE_f$ (KJ/m^3)	1.0	43.7	40.9	39.5	41.7	41.7	41.7
	2.0	39.5	39.5	39.5	41.7	41.7	41.7
	3.0	39.5	39.5	39.5	41.7	41.7	41.7
	4.0	39.5	39.5	39.5	41.7	41.7	41.7

Table 6.8 Cost of AC Layer to Meet ER_{min} in HMA Overlay Pavement

(a) Low traffic (unit: $)

m-value		0.60 (unmodified)			0.45 (modified)		
D_1*10^{-7} (1/psi)		14	10	6	14	10	6
$DCSE_f$ (KJ/m^3)	1.0	20.9	18.3	14.1	16.4	13.5	10.7
	2.0	15.5	12.7	8.7	10.7	10.7	10.7
	3.0	12.4	10.2	8.5	10.7	10.7	10.7
	4.0	9.9	8.5	8.5	10.7	10.7	10.7

Table 6.8–continued

(b) Medium traffic

m-value		0.60 (unmodified)			0.45 (modified)		
D_1*10^{-7} (1/psi)		14	10	6	14	10	6
$DCSE_f$ (KJ/m^3)	1.0	18.9	16.9	12.7	14.7	12.1	12.1
	2.0	13.5	11.3	9.9	12.1	12.1	12.1
	3.0	9.9	9.9	9.9	12.1	12.1	12.1
	4.0	9.9	9.9	9.9	12.1	12.1	12.1

(c) High traffic

m-value		0.60 (unmodified)			0.45 (modified)		
D_1*10^{-7} (1/psi)		14	10	6	14	10	6
$DCSE_f$ (KJ/m^3)	1.0	16.9	14.1	12.7	15.0	15.0	15.0
	2.0	12.7	12.7	12.7	15.0	15.0	15.0
	3.0	12.7	12.7	12.7	15.0	15.0	15.0
	4.0	12.7	12.7	12.7	15.0	15.0	15.0

and HMA overlay pavement structures, respectively. AC layer thickness and resulting tensile stress are also presented in Appendix E.

As shown in Table 6.6, the cost was reduced by up to 30% for conventional pavements by using polymers. However, the cost reduction was decreased as traffic level increased. Therefore, the result indicates that if AC layer of conventional asphalt pavement should have the minimum fatigue cracking toughness, using SBS modifiers in AC layer, as compared with unmodified AC layer, can reduce the construction cost by around 5% to 30%, in depending on traffic level. On the other hand, in some cases of, presented in Table 6.6 (for example, D_1 is 6 and $DCSE_f$ is 4 for low traffic), the cost of modified AC layer was increased. This increased cost is because the design thickness determined in Table 6.1 is used as a minimum thickness in this analysis.

Conversely, Table 6.7 shows that by using modifiers, the cost of AC layer was decreased by 10% for HMA full depth pavement with mixtures having lower $DCSE_f$ and higher D_1 (lower quality asphalt mixtures). Even though the cost was increased by 8% for higher $DCSE_f$ and lower D_1 (higher quality asphalt mixtures), the increased cost is not the cost loss incurred from the use of modifiers, as described above. However, it was found that the thicker AC layer of HMA full depth pavements caused a relatively small cost reduction, compared to that of conventional pavement.

As far as the HMA overlay shown in Table 6.8, the variation of the cost difference was from 30% of reduction in AC layers with lower $DCSE_f$ and higher D_1 (lower quality asphalt mixtures) to 27% of increase in AC layers with higher $DCSE_f$ and lower D_1 (higher quality asphalt mixtures). Therefore, in the pavement with a thick AC layer such as HMA full depth and HMA overlay, it appears that the cost effectiveness largely depends on the quality of asphalt mixtures. In other words, if a relatively lower quality asphalt mixture is used, the construction cost of AC layer can be largely saved by using modifiers.

In summary, if the minimum energy ratio is required for asphalt pavement, using the SBS polymer in AC layer can reduce the construction cost up to by 30%, depending on pavement structure and traffic level, as shown in Figure 6.2. In addition to that, the amount of cost reduction also depends on the mixture quality.

Case 2 ($ER_{HMA} \geq ER_{PMHMA}$)

In this case, the ER of modified HMA (ER_{PMHMA}) was used as the criterion to determine the construction cost of AC layer. The typical m-value of polymer modified and straight asphalt mixture is 0.45 and 0.6, respectively as presented in the factorial design. As shown in Tables 6.3 through Table 6.5, the resulting ER_{PMHMA} is higher than that of the ER of unmodified HMA

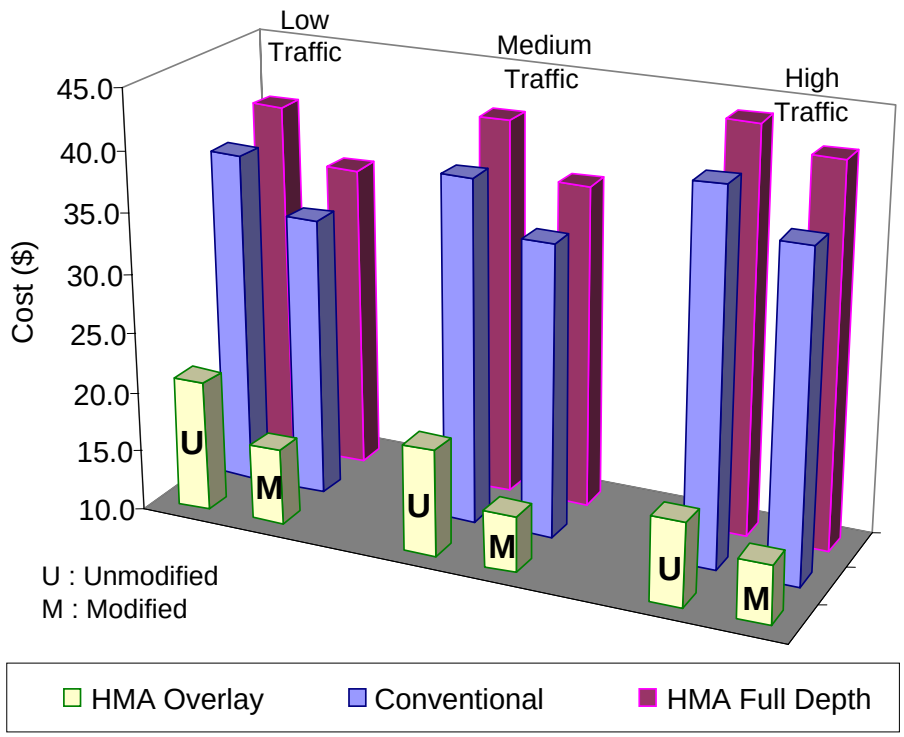

Figure 6.2 Comparison of construction cost of AC layer depending on pavement structure and traffic level for the mixtures with $DCSE_f$= 1.0 (KJ/m^3) and D_1=14 × 10^{-7} (1/psi).

(ER_{HMA}) at the same conditions. Therefore, in this case, the ER_{HMA} was increased to meet the ER_{PMHMA} by increasing the thickness of AC layer resulting in the decreased tensile stress at the bottom of AC layer, which gives an equivalent fatigue cracking resistance of modified AC layer.

Table 6.9 shows the cost of unmodified AC layer and modified AC layer having the equivalent ER. The cost of modified AC layer was calculated in two cases to identify how much cost was reduced by varying the thickness of modified mixture: (1) the case where whole AC layer was constructed with modified mixture, and (2) the case where top two inches of AC layer

was constructed with modified mixture. AC layer thickness and resulting tensile stresses meeting the ER of modified AC layer are shown in Appendix E.

Table 6.9 Costs of AC Layer with the Equivalent ER

(Unit: $)

		Traffic		
		Low	Medium	High
Conventional Structure	Unmodified	26.8	28.2	31.0
	Modified (2" replacement)	19.2	22.0	26.2
	Modified (Full depth replacement)	23.7	27.7	33.6
HMA Full Depth	Unmodified	34.7	40.6	46.5
	Modified (2" replacement)	30.5	36.1	41.7
	Modified (Full depth replacement)	39.5	47.4	55.3
HMA Overlay	Unmodified	15.5	16.9	18.3
	Modified (2" replacement)	10.7	12.1	15.0
	Modified (Full depth replacement)	11.9	13.8	17.8

As shown in Table 6.9, there is little difference in cost for conventional pavement structures. The cost of modified AC layer (full depth replacement) is 12% lower for low traffic level and 8% higher for high traffic level than those of unmodified AC layer. However, in HMA full depth pavement structures, the cost of modified AC layer (full depth replacement) is 14% to 19% higher for all traffic levels than those of unmodified AC layer. For HMA overlay structures, modified mixture resulted in lower cost (3% to 24% lower cost of modified AC layer than those of unmodified AC layer). These results are due to the thickness of AC layer. That is, the thinner the AC layer, the higher the cost reduction by applying SBS polymer modifier in this analysis. These results indicate that there is a break point below which the construction cost of AC layer can be saved by using modifiers. As shown in Table 6.1 and Table 6.9, the positive cost

reduction appears to happen below 7 inches of AC layer thickness in conventional pavement structures, and 4.5 inches of HMA overlay thickness.

Another cost comparison was performed to identify how much cost was reduced by varying the thickness of modified mixtures. That is, the case when the top two inches of AC layer is replaced by the modified mixture and the pavement still has an equivalent ER. The top two inches of AC layer were selected, since top-down cracking is the most prevalent type of cracking and two inches is the typical length of cracks in Florida. As shown in Table 6.9, the construction cost was reduced for all cases and up to 30% cost reduction was induced by the use of SBS polymer in this case. Thus, the parametric analysis in this study showed that the use of SBS modifier to mitigate fatigue cracking in asphalt pavement was clearly justified with respect to the reduction of construction cost.

CHAPTER 7
FINDINGS AND CONCLUSIONS

7.1 Findings

It may not be possible to produce Superpave mixtures with conventional asphalt cement for certain levels of traffic and environment that to have both adequate rutting and cracking resistance. Mixtures designed for high traffic may be susceptible to cracking due to the lower design asphalt content. One way to achieve sufficient fracture resistance is through the use of asphalt modifiers. Styrene Butadiene Styrene (SBS) polymer modifiers have become increasingly popular because of their apparent success in mitigating cracking of pavements in the field. However, the specific effect of SBS polymer on the cracking resistance and healing characteristics of Superpave mixtures is not clear yet.

This study was conducted to evaluate the effects of SBS polymer modification on cracking resistance and healing characteristics of Superpave mixtures. The investigation also focused on identifying mixture properties and/or characteristics, as well as specific test methods that can be used to uniquely characterize the presence and beneficial effect of SBS modifiers in asphalt mixtures. The findings of this study may be summarized as follows:

SBS polymer modification appears to improve the cracking performance of asphalt mixtures by reducing the rate of creep accumulation, which has been shown to be directly related to the rate of micro damage development, without reducing the threshold fracture energy of the mixture. Therefore, one must determine both the creep properties and the fracture energy limit of mixtures to reveal the beneficial effect of SBS polymer modification on cracking performance.

The reduced rate of creep accumulation in modified mixtures appears to be mainly and perhaps almost exclusively, reflected in a lower m-value.

The HMA fracture model developed at the University of Florida appears to accurately reflect the beneficial effects of SBS polymer modification on the cracking performance of asphalt mixtures. The model uses creep compliance parameters determined from a 1000-second creep test and the threshold fracture energy determined from a tensile strength test, both of which are performed with the Superpave IDT, to predict crack initiation and growth in asphalt mixtures.

It is possible to uniquely characterize the presence of SBS polymer modification in mixtures by evaluating the post-peak stress-strain behavior of the mixture during a tensile strength test performed with the Superpave IDT. SBS modified mixtures exhibited higher post-peak fracture energies than unmodified mixtures. This finding is particularly useful for quality-control purposes, where relatively simple test is required to assure that the right type and level of modification was used during production.

Time to crack initiation determined from creep tests appears to provide another parameter that is uniquely related to the presence and benefit of SBS modification. Failure limits ($DCSE_f$) obtained in this manner were identical to failure limits obtained from conventional Superpave IDT strength tests.

The relative effect of SBS modifiers was increased at higher binder contents and temperatures. It implies that the effect of SBS polymer would be increased in the mixtures with higher asphalt contents such as open graded friction courses.

SBS modifiers do not appear to influence aging of asphalt mixtures. However, long-term oven aging makes mixtures stiffer and may result in higher number of cycles to failure, which is well represented in the decreased D_1 of long-term oven aged specimens.

SBS modification does not appear to improve or to adversely affect the healing characteristics of asphalt mixtures. The healing characteristics appear to be affected by the structure of asphalt mixture rater than the base binder.

The results of cost analysis indicated that if AC layer should have the minimum energy ratio, using SBS modifiers in AC layer, as compared with unmodified AC layer, could reduce the construction cost by around 5% to 30%, in depending on traffic level.

However, the cost analysis for the cases where both unmodified and modified mixtures had an equivalent energy, indicated that the thinner the AC layer, the higher the cost reduction by applying SBS polymer modifier. Thus, it appeared that there was a break point below which the construction cost of the AC layer could be saved by using SBS modifiers: 7 inches of AC layer thickness in conventional pavement structures, and 4.5 inches of HMA overlay thickness.

Thus, the parametric analysis in this study showed that it was clearly justified with respect to the reduction of construction cost for use of SBS modifier to mitigate fatigue cracking in asphalt pavement.

7.2 Conclusions

Conclusions from this study may be summarized as follows:

The key to characterizing the presence and beneficial effects of SBS modifier on the cracking resistance of asphalt mixture is in the evaluation of the combined effects of creep and failure limits. This may be accomplished in one of two ways: (1) By performing a short-term creep followed by a strength test to obtain the mixture's m-value and DCSE, whose combined effect can be evaluated using the HMA fracture model, and (2) By performing a longer-term creep test to assure crack initiation by creep. The failure limits and m-value can also be determined from this test. In addition, the time to crack initiation provides a parameter that can

be used directly to evaluate the relative cracking resistance of mixtures without further modeling. However, the longer-term creep test will generally be more time-consuming than the short-term creep and strength test.

Residual dissipated energy might provide a quick way to make relative comparisons of mixture cracking performance suitable for the polymer-modified asphalt mixtures.

The modifier would not only allow the use of higher asphalt contents in open graded friction courses, as does the ground tire rubber, but it would also reduce the rate of micro damage development in these mixtures.

APPENDIX A
AGGREGATE BATCH WEIGHT SHEETS

Table A.1 Cumulative Batch Weight (IDT Samples)

Coarse 1 (Cumulative weights, g)

Sieve size (mm)	S1a	S1b	Screen	Filler
12.5	116	459	3306	4454
9.5	318	630	3306	4454
4.75	429	2011	3306	4454
2.36	445	2987	3472	4454
1.18	449	3127	3804	4454
0.6	450	3149	4054	4454
0.3	451	3158	4230	4454
0.15	452	3192	4376	4454
0.075	454	3226	4424	4459
< 0.075	459	3306	4454	4500

Fine 1 (Cumulative weights, g)

Sieve size (mm)	S1a	S1b	Screen	Filler
12.5	231	914	2056	4454
9.5	633	983	2056	4454
4.75	853	1536	2056	4454
2.36	886	1928	2404	4454
1.18	893	1984	3097	4454
0.6	895	1993	3619	4454
0.3	897	1997	3986	4454
0.15	900	2010	4291	4454
0.075	903	2024	4392	4459
< 0.075	914	2056	4454	4500

Table A.2 Cumulative Batch Weight (MTD Samples)

Coarse 1 (Cumulative weights, g)

Sieve size (mm)	S1a	S1b	Screen	Filler
12.5	39	153	1102	1485
9.5	106	210	1102	1485
4.75	143	670	1102	1485
2.36	148	996	1157	1485
1.18	150	1042	1268	1485
0.6	150	1050	1351	1485
0.3	150	1053	1410	1485
0.15	151	1064	1459	1485
0.075	151	1075	1475	1486
< 0.075	153	1102	1485	1500

Fine 1 (Cumulative weights, g)

Sieve size (mm)	S1a	S1b	Screen	Filler
12.5	77	305	685	1485
9.5	211	328	685	1485
4.75	284	512	685	1485
2.36	295	643	801	1485
1.18	298	661	1032	1485
0.6	298	664	1206	1485
0.3	299	666	1329	1485
0.15	300	670	1430	1485
0.075	301	675	1464	1486
< 0.075	305	685	1485	1500

APPENDIX B
ASPHALT MIX DESIGN AND VOLUMETRIC PROPERTIES OF MIXTURES

Table B.1 Volumetric Properties for Asphalt Mix Design (Coarse 1)

Nominal maximum aggregate size = 12.5mm

AGGREGATE			S1A	S1B	SCREEN	FILLER
	Individual % by mass		10.200	63.267	25.511	1.022
	Individual specific gravity		2.425	2.451	2.527	2.690
	Gsb		2.469	2.469	2.469	2.469
SPECIFIC GRAVITY	%AC		6.0	6.5	7.0	
	Gb		1.035	1.035	1.035	
	Gmm(measured)		2.347	2.329	2.311	
	Gse(calculated)		2.553	2.550	2.547	
	Gmb	Ni=7	1.942	1.946	1.942	
		Ni=8	1.956	1.959	1.955	
		Ni=9	1.968	1.971	1.968	
	Gmb	Nd=75	2.198	2.199	2.203	
		Nd=100	2.228	2.231	2.231	
		Nd=125	2.250	2.253	2.253	
	Gmb	Nmax=115	2.241	2.244	2.245	
		Nmax=160	2.270	2.275	2.275	
		Nmax=205	2.291	2.296	2.296	
VOLUMETRIC PROPERTY	VMA	Nd=75	16.322	16.721	17.052	
		Nd=100	15.176	15.515	15.983	
		Nd=125	14.349	14.692	15.163	
	Va	Nd=75	6.316	5.540	4.672	
		Nd=100	5.034	4.172	3.444	
		Nd=125	4.107	3.238	2.502	
	VFA	Nd=75	61.302	66.866	72.598	
		Nd=100	66.831	73.107	78.450	
		Nd=125	71.375	77.958	83.497	
% of Gmm	N_i	7	82.8	83.6	84.0	
		8	83.4	84.1	84.6	
		9	83.9	84.7	85.2	
	N_{des}	75	93.7	94.5	95.3	
		100	95.0	95.8	96.6	
		125	95.9	96.8	97.5	
	N_{max}	115	95.5	96.4	97.2	
		160	96.8	97.7	98.5	
		205	97.6	98.6	99.4	
MIXTURE PROPERTY AT 4% AIR VOID	N_d	75	100	125	Requirement	
	%AC	7.2	6.6	6.1		
	Va	4.0	4.0	4.0		
	VMA	17.2	15.6	14.5	>14	
	VFA	75.0	74.0	73.0	65-78	
% of Gmm	N_i	84.2	84.3	84.1	=< 89	
	N_{max}	97.4	97.9	97.8	=< 98	

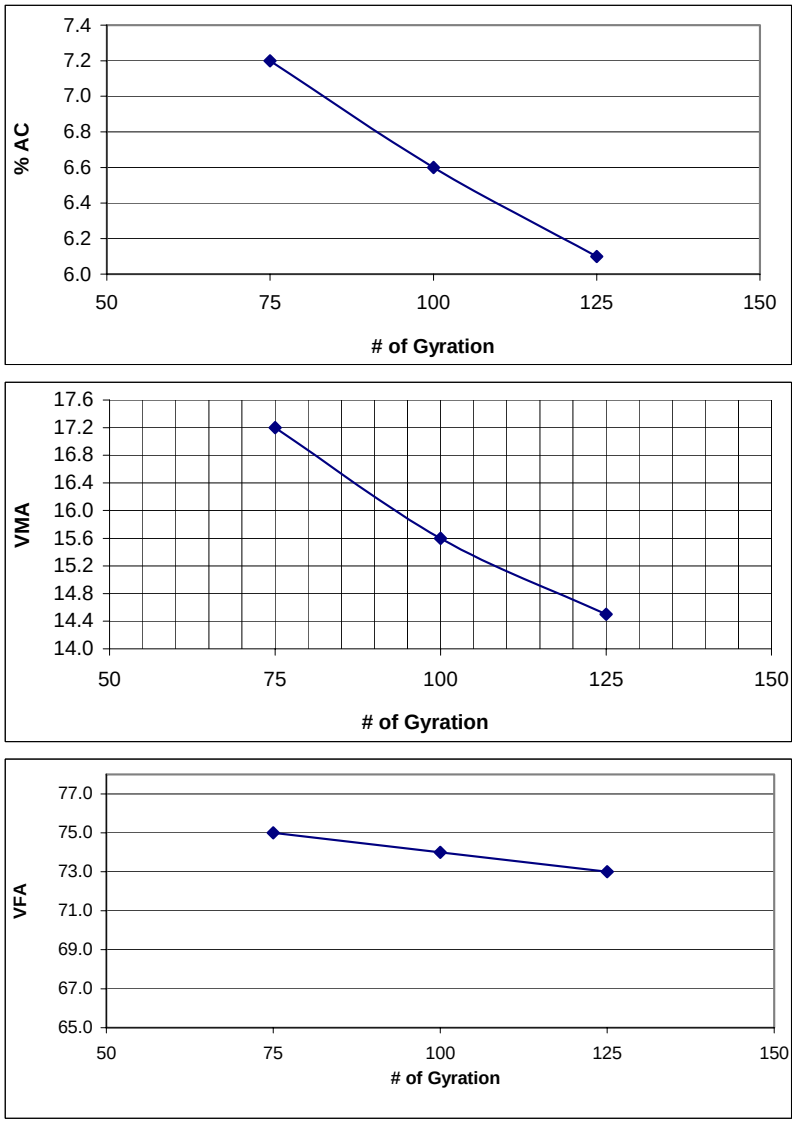

Figure B.1 Volumetric properties with number of gyrations at 4% air voids (Coarse 1).

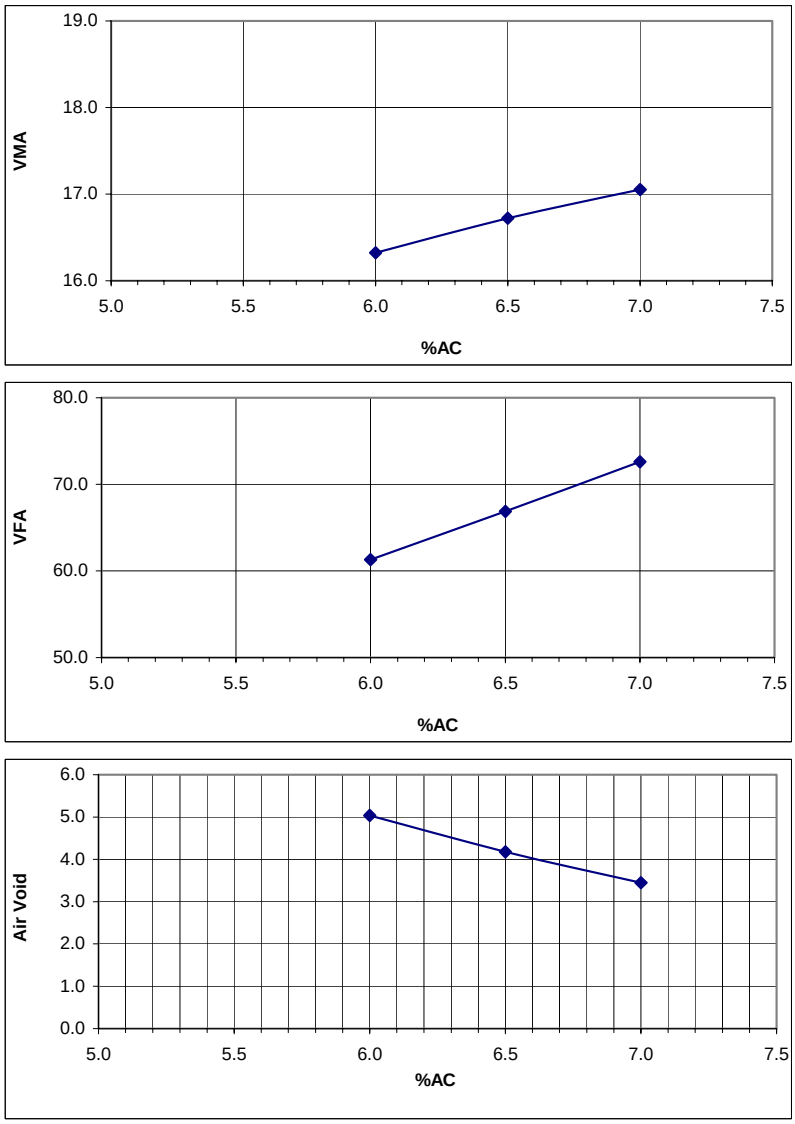

Figure B.2 Volumetric properties with asphalt contents at N_d = 75 (Coarse 1).

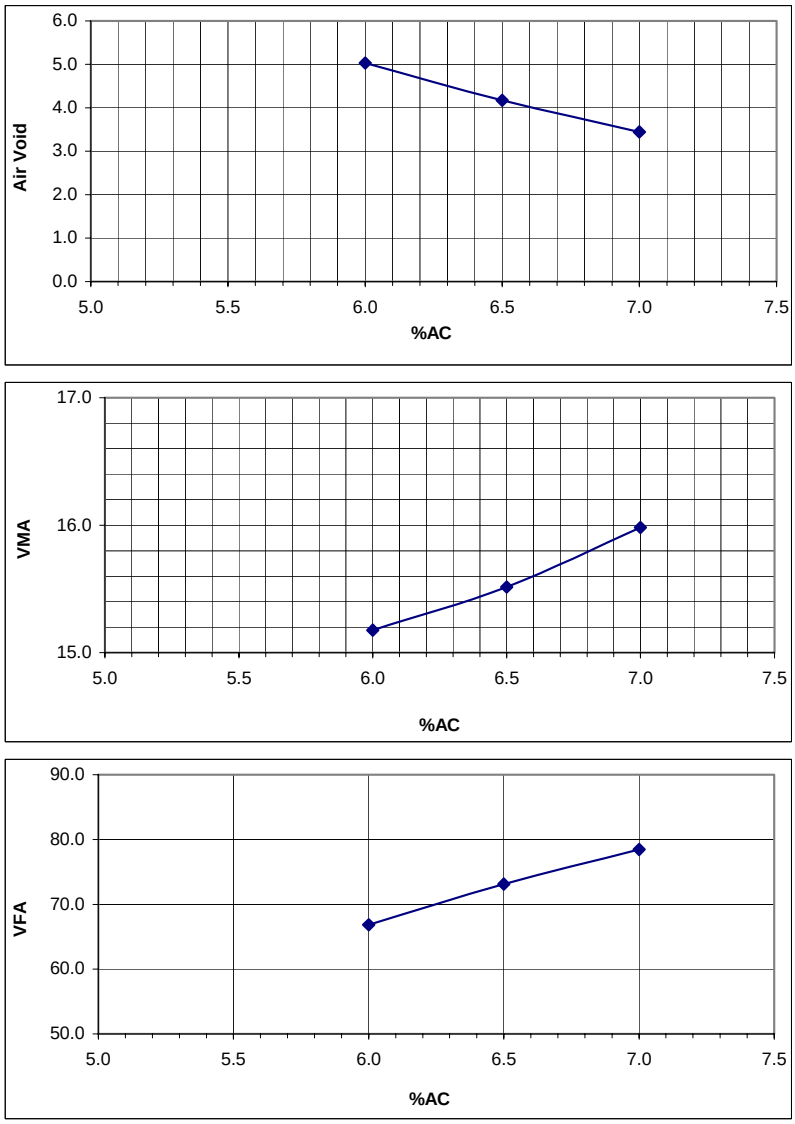

Figure B.3 Volumetric properties with asphalt contents at N_d = 100 (Coarse 1).

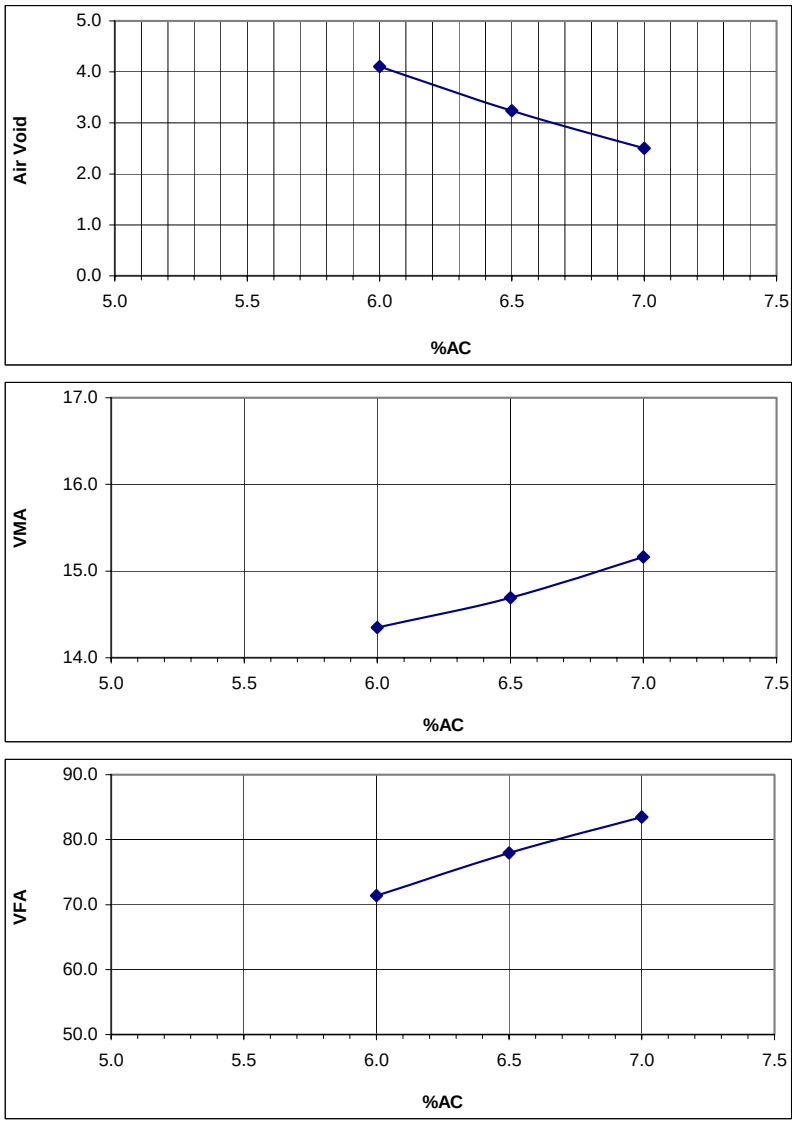

Figure B.4 Volumetric properties with asphalt contents at N_d = 125 (Coarse 1).

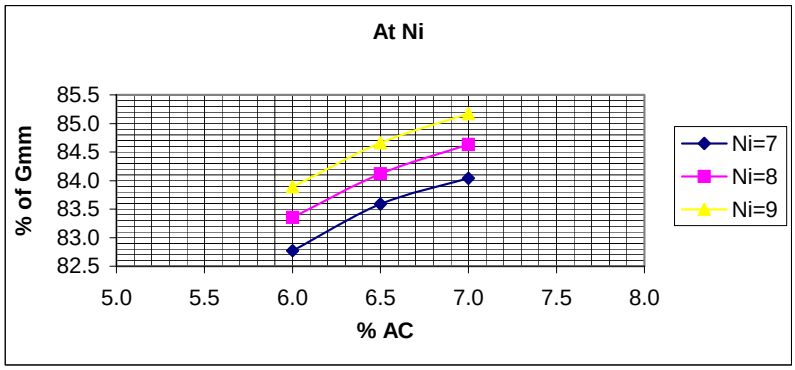

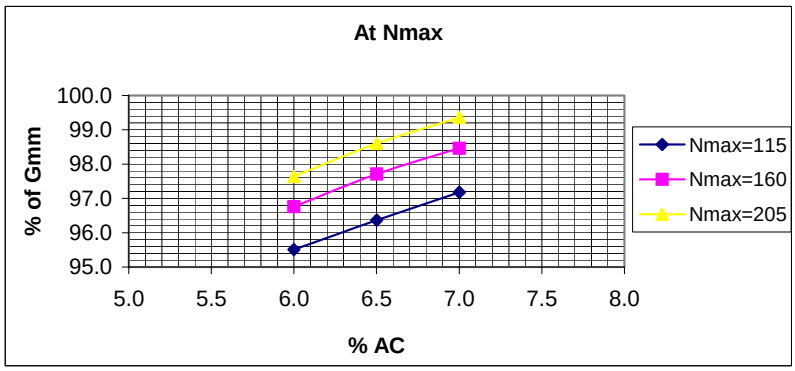

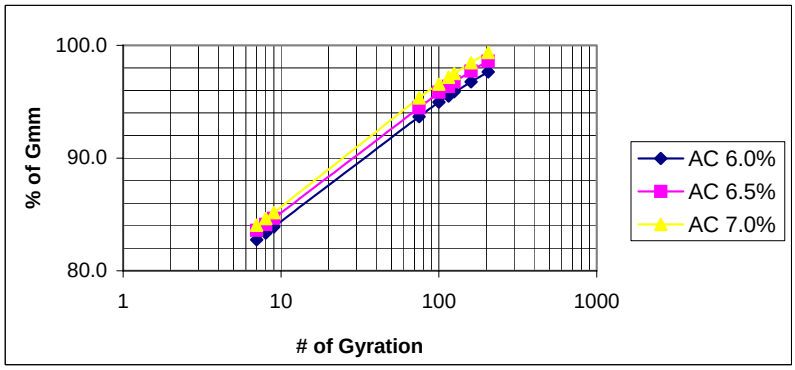

Figure B.5 Percentage of Gmm (Coarse 1).

Table B.2 Volumetric Properties for Asphalt Mix Design (Fine 1)

						Nominal maximum aggregate size = 12.5mm
AGGREGATE			S1A	S1B	SCREEN	FILLER
	Individual % by mass		20.311	25.378	53.289	1.022
	Individual specific gravity		2.425	2.451	2.527	2.690
	Gsb		2.488	2.488	2.488	2.488
SPECIFIC GRAVITY	%AC		5.8	6.3	6.8	
	Gb		1.035	1.035	1.035	
	Gmm		2.3645	2.3448	2.3250	
	Gse		2.568	2.563	2.558	
	Gmb	Ni=7	2.012	2.027	2.035	
		Ni=8	2.024	2.039	2.047	
		Ni=9	2.033	2.048	2.058	
		Nd=75	2.207	2.225	2.243	
		Nd=100	2.228	2.247	2.265	
		Nd=125	2.243	2.263	2.280	
		Nmax=115	2.237	2.258	2.274	
		Nmax=160	2.258	2.280	2.297	
		Nmax=205	2.273	2.295	2.310	
VOLUMETRIC PROPERTY	VMA	Nd=75	16.445	16.202	15.971	
		Nd=100	15.629	15.382	15.144	
		Nd=125	15.076	14.757	14.584	
	Va	Nd=75	6.677	5.117	3.529	
		Nd=100	5.766	4.188	2.580	
		Nd=125	5.149	3.480	1.937	
	VFA	Nd=75	59.395	68.419	77.901	
		Nd=100	63.106	72.772	82.961	
		Nd=125	65.849	76.419	86.715	
% of Gmm	Ni=7		85.1	86.4	87.5	
	Ni=8		85.6	86.9	88.0	
	Ni=9		86.0	87.3	88.5	
	Nmax=115		94.6	96.3	97.8	
	Nmax=160		95.5	97.2	98.8	
	Nmax=205		96.1	97.9	99.4	
MIXTURE PROPERTY AT 4% AIR VOID	Nd	75	100	125	Requirement	
	%AC	6.6	6.4	6.2		
	Va	4.0	4.0	4.0		
	VMA	16.2	15.3	15.0	>14	
	VFA	75.0	75.0	74.0	65-78	
% of Gmm	Ni	87.1	87.2	87.1	=< 89	
	Nmax	97.5	97.6	97.6	=< 98	

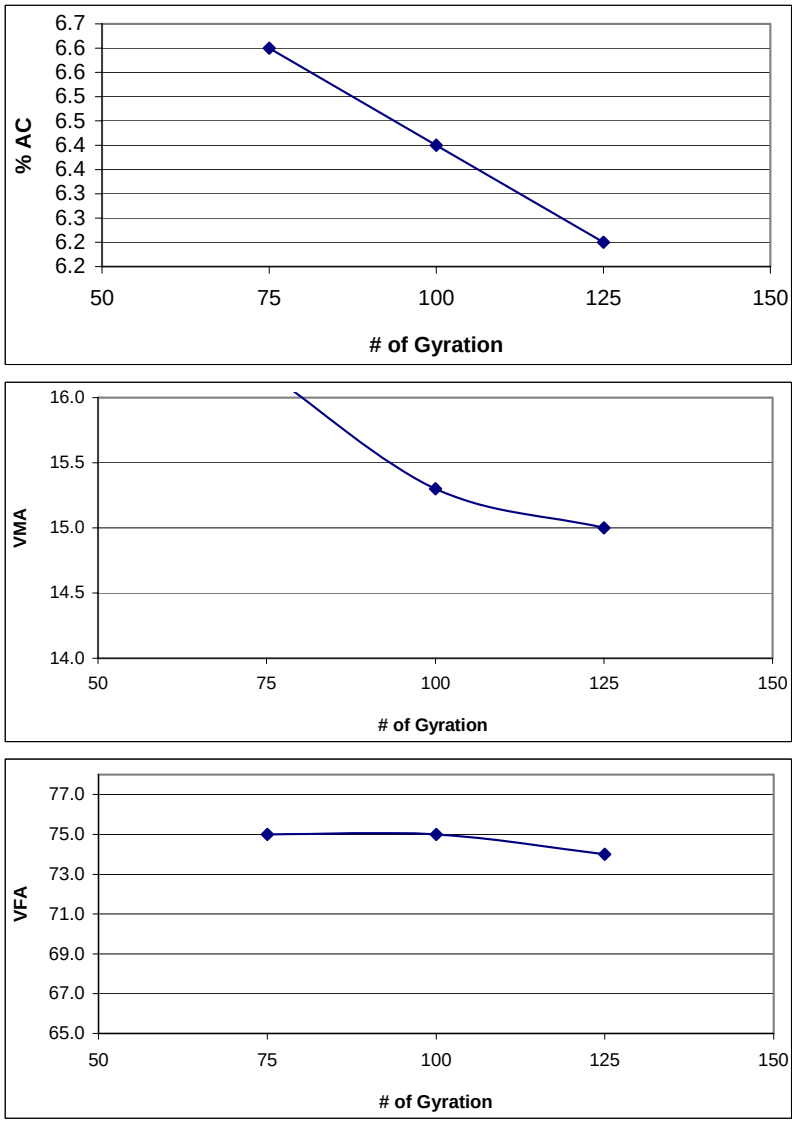

Figure B.6 Volumetric Properties with Number of Gyrations (Fine 1).

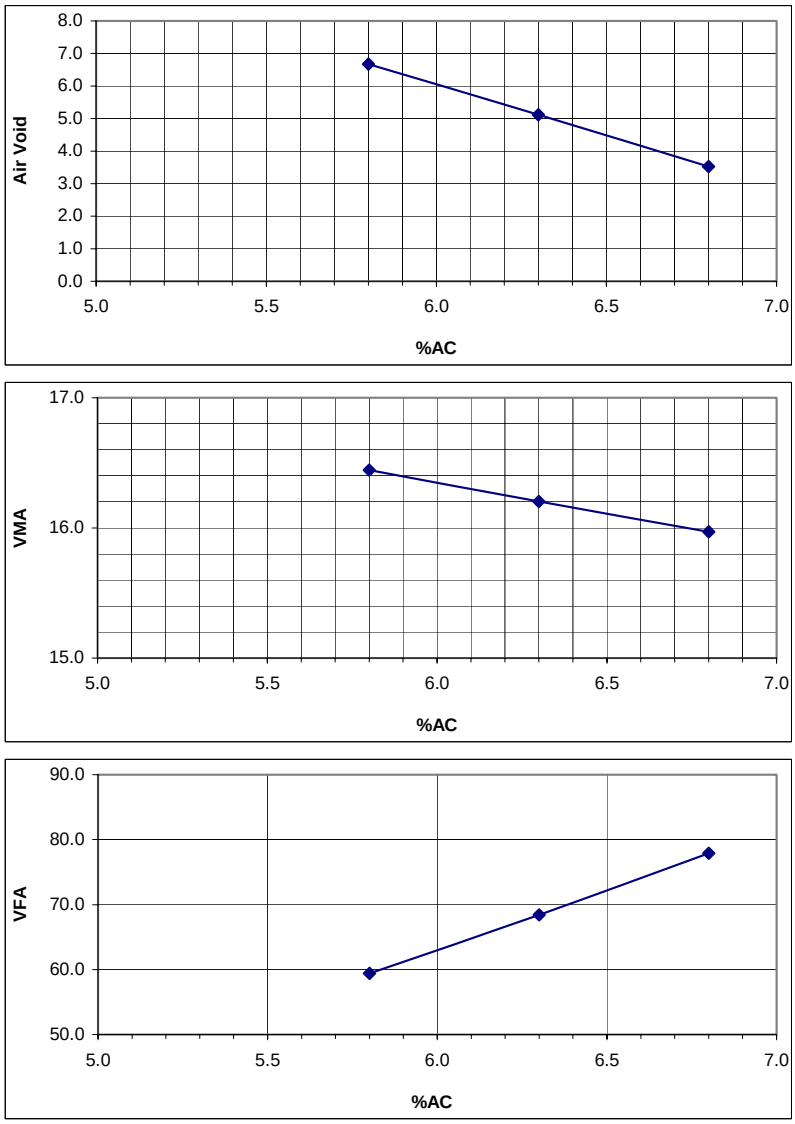

Figure B.7 Volumetric Properties with Asphalt Contents at N_d = 75 (Fine 1).

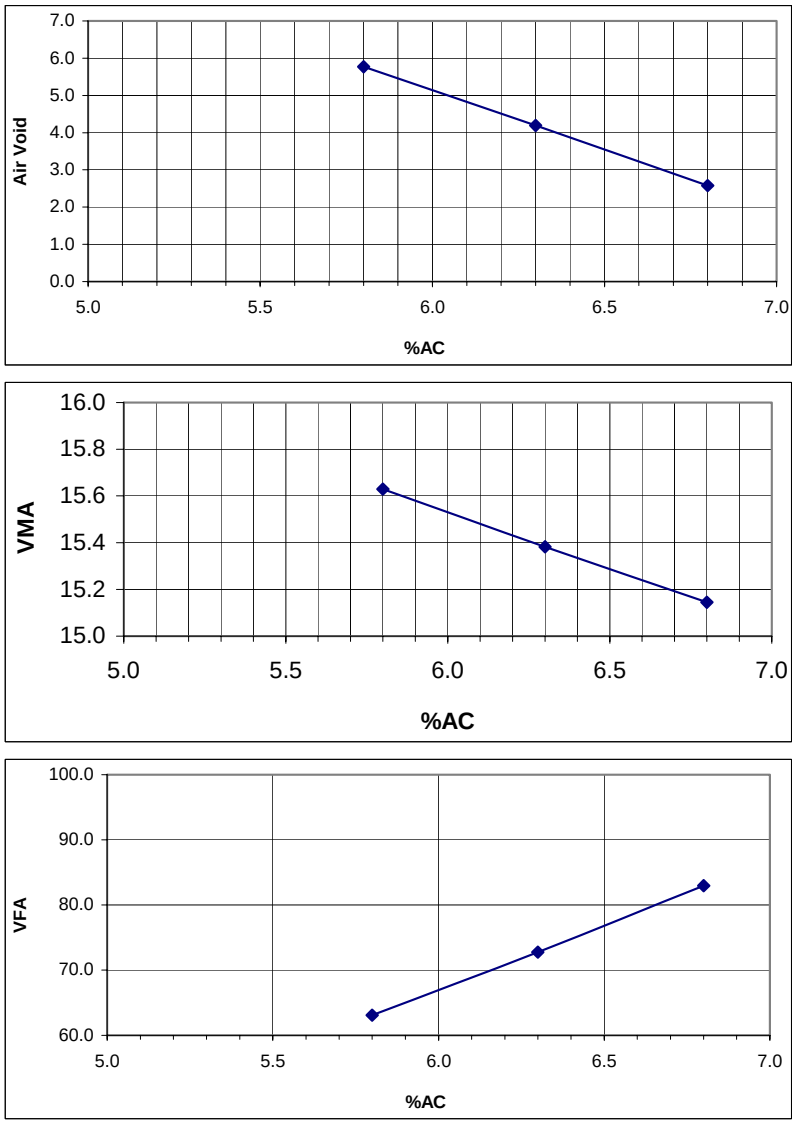

Figure B.8 Volumetric properties with asphalt contents at N_d = 100 (Fine 1).

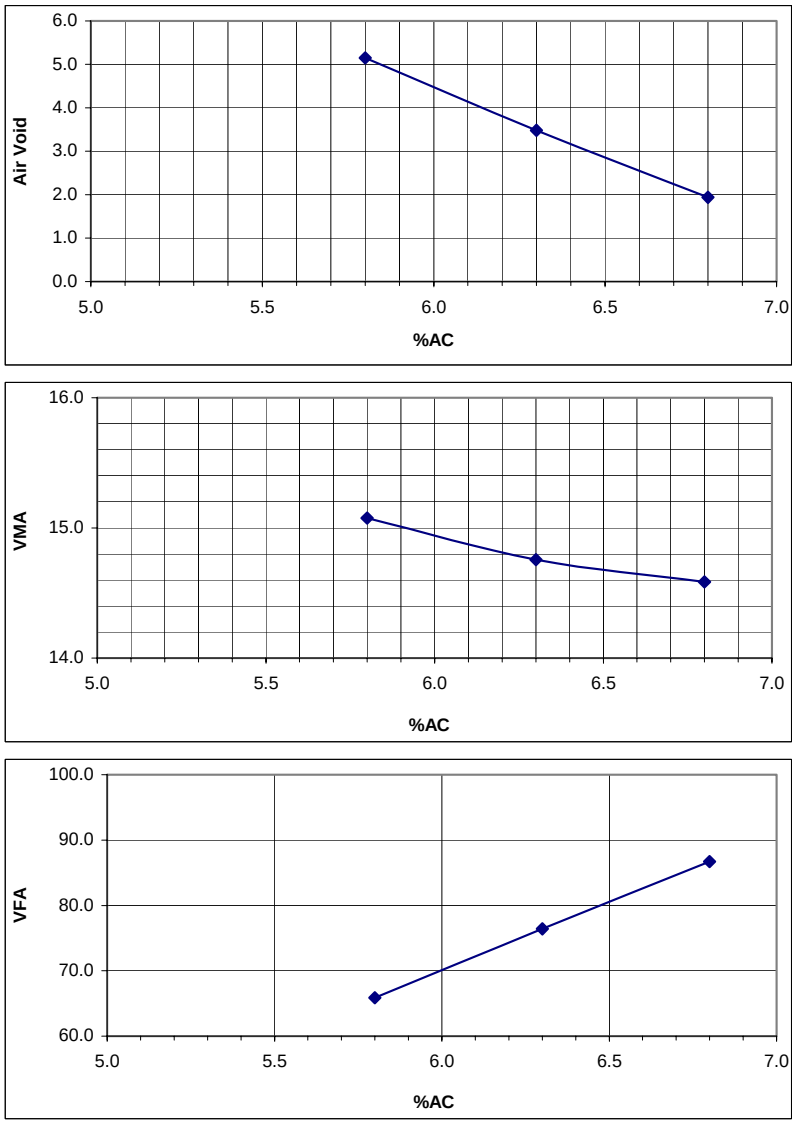

Figure B.9 Volumetric properties with asphalt contents at N_d = 125 (Fine 1).

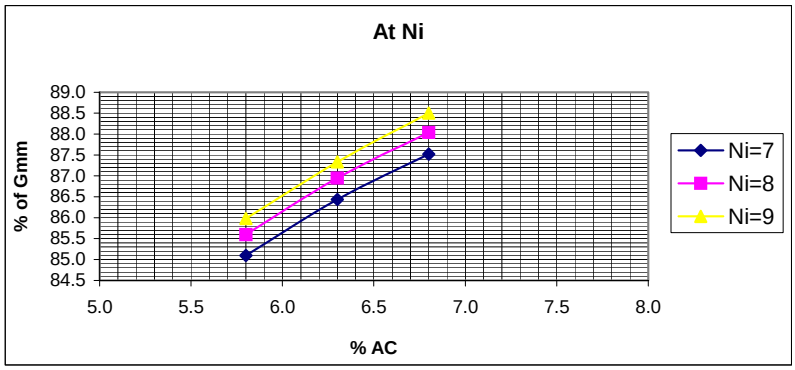

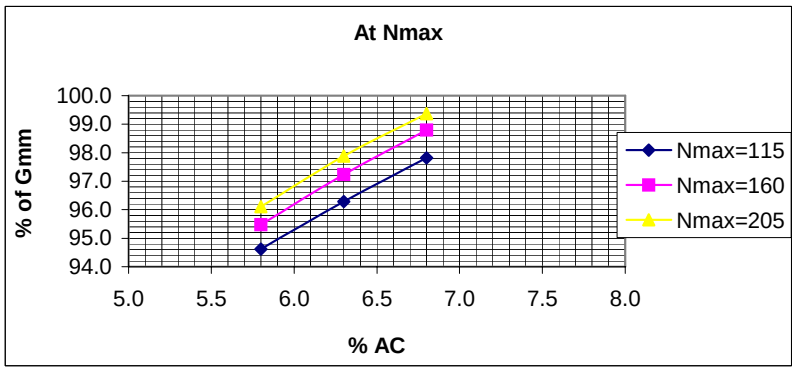

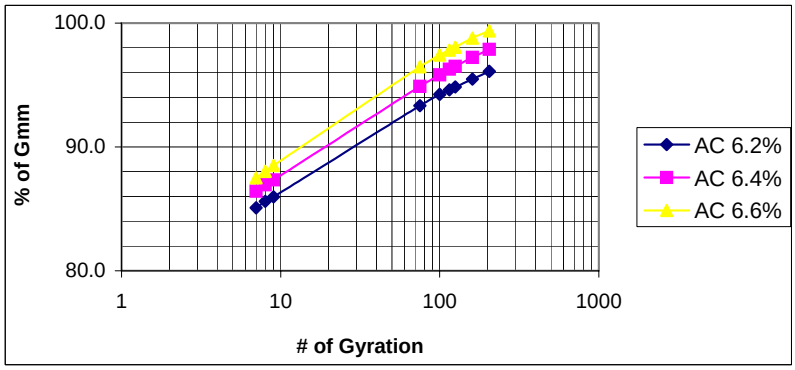

Figure B.10 Percentage of Gmm (Fine 1).

APPENDIX C
INDIRECT TENSILE TEST (IDT) DATA

Table C.1 Superpave IDT Results (Coarse 1, LTOA)

Temperature: 10° C

Sample	Property							
	Resilient Modulus (Gpa)	Creep compliance at 1000 sec. (1/Gpa)	Tensile Strength (Mpa)	Fracture Energy (kJ/m^3)	Failure Strain (10^{-6})	m-value	D_1	$DCSE_f$ (kJ/m^3)
Straight Asphalt Binder								
6.1	10.76	4.29	2.13	3.45	2368.50	0.621	3.94E-07	3.24
7.2	8.75	9.72	1.60	4.10	2988.71	0.581	1.18E-06	3.95
SBS Modified Binder								
6.1s	11.21	1.85	2.23	3.15	1736.19	0.46	3.99E-07	2.93
7.2s	8.80	2.46	2.02	3.75	2619.69	0.45	9.07E-07	3.52

Table C.2 Superpave IDT Results (Fine 1, STOA)

Temperature: 10° C

Sample	Properties							
	Resilient Modulus (Gpa)	Creep compliance at 1000 sec. (1/Gpa)	Tensile Strength (Mpa)	Fracture Energy (kJ/m^3)	Failure Strain (10^{-6})	m-value	D_1	$DCSE_f$ (kJ/m^3)
Straight Asphalt Binder								
6.2	7.72	6.97	2.17	7.00	4010.45	0.55	1.03E-06	6.70
6.6	7.56	7.89	2.23	7.90	4406.48	0.59	1.39E-06	7.57
SBS Modified Binder								
6.2SBS	8.15	4.70	2.06	5.70	3607.81	0.47	1.06E-06	5.44
6.6SBS	8.34	4.30	2.32	6.00	3382.54	0.54	1.29E-06	5.68

APPENDIX D
HEALING TEST RESULTS

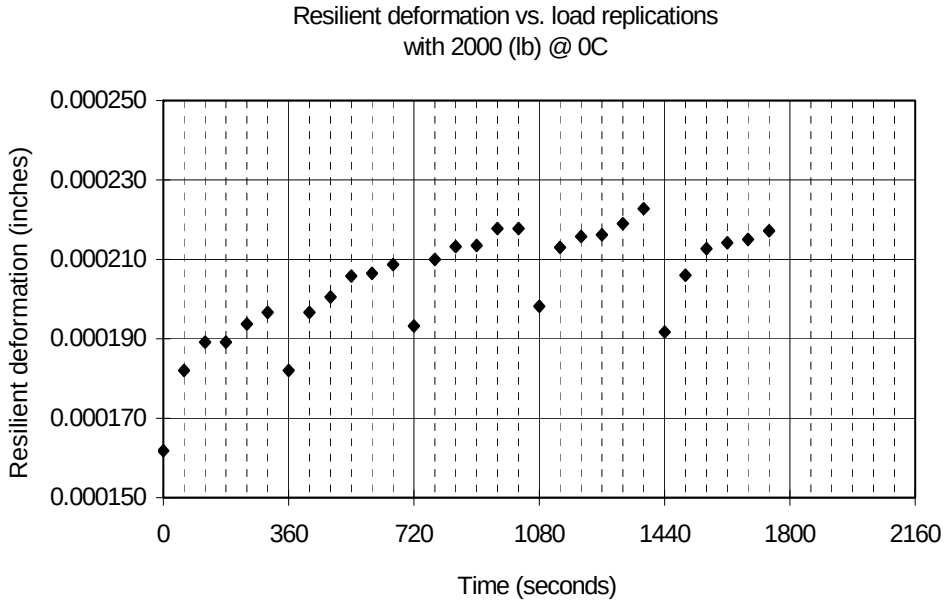

Figure D.1 Healing test (6.1% unmodified asphalt, Coarse 1, 2000 (lb) cyclic load at 0° C).

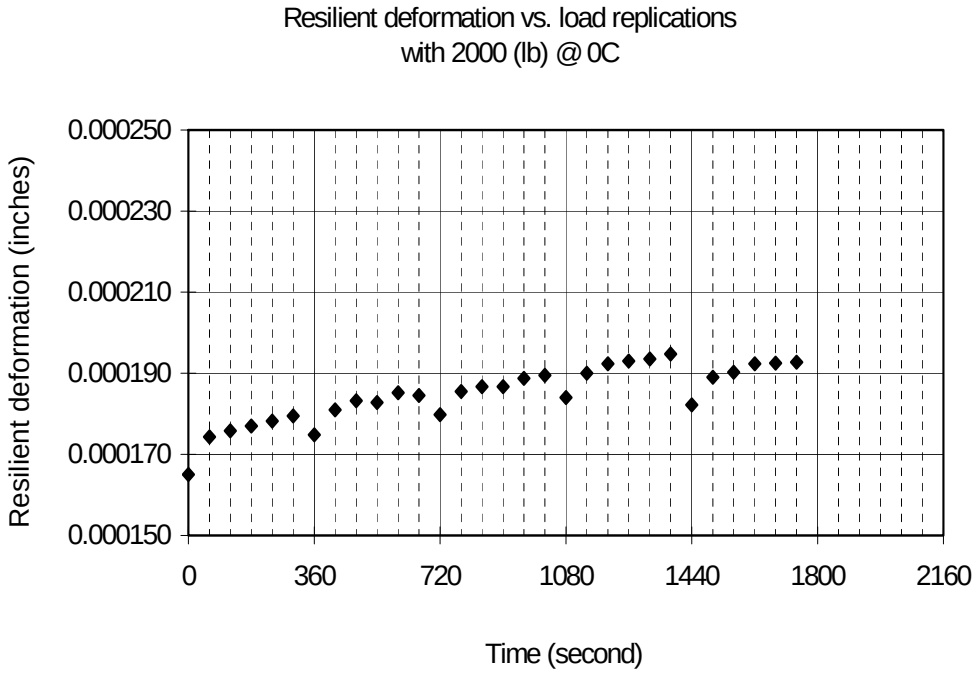

Figure D.2 Healing test (6.1% modified asphalt, Coarse 1, 2000 (lb) cyclic load at 0° C).

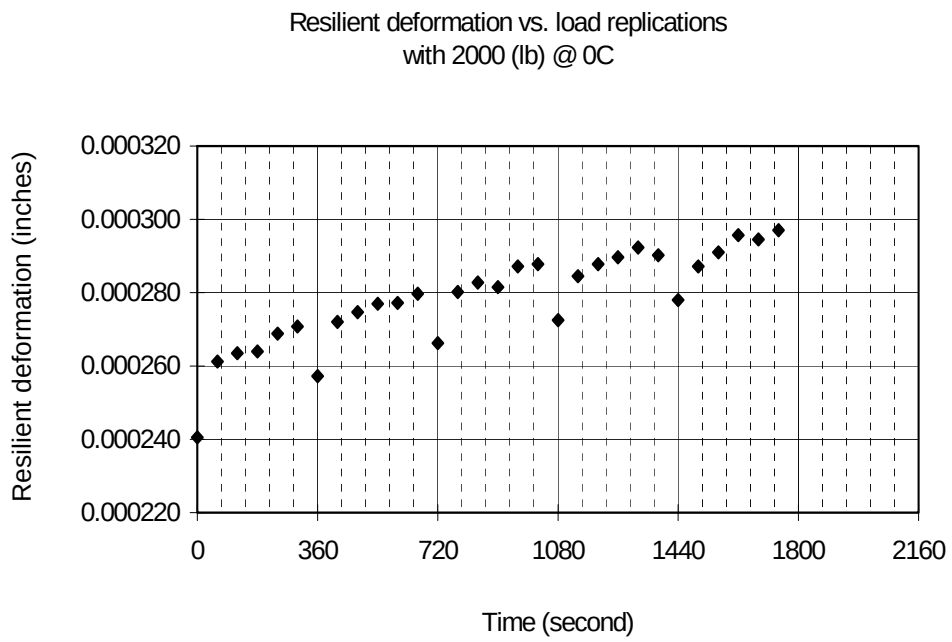

Figure D.3 Healing test (7.2% modified asphalt, Coarse 1, 2000 (lb) cyclic load at 0° C).

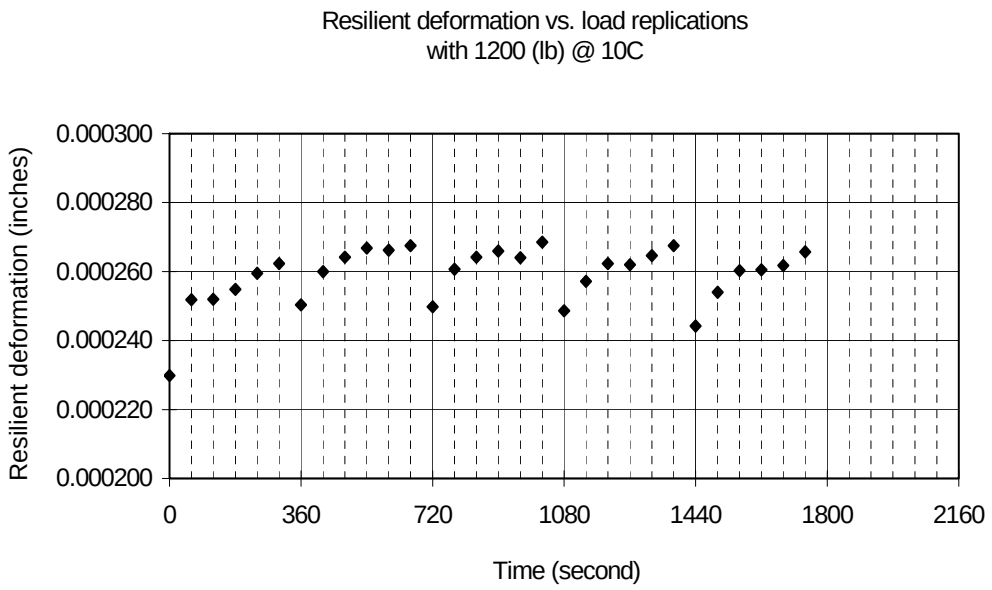

Figure D.4 Healing test (6.1% unmodified asphalt, Coarse 1, 1200 (lb) cyclic load at 10° C).

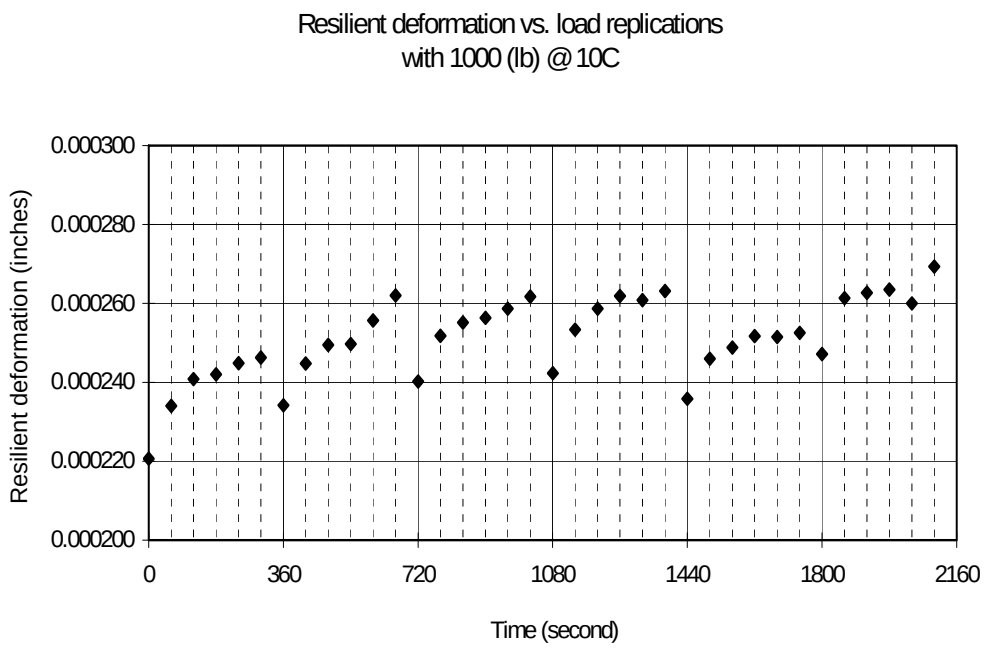

Figure D.5 Healing test (7.2% unmodified asphalt, Coarse 1, 1000 (lb) cyclic load at 10° C).

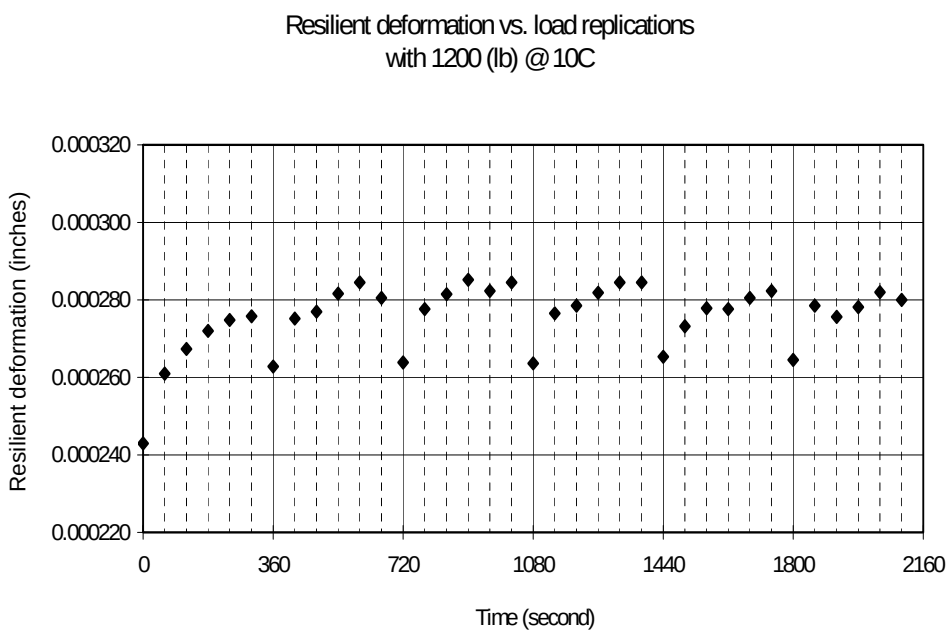

Figure D.6 Healing test (6.1% modified asphalt, Coarse 1, 1200 (lb) cyclic load at 10° C).

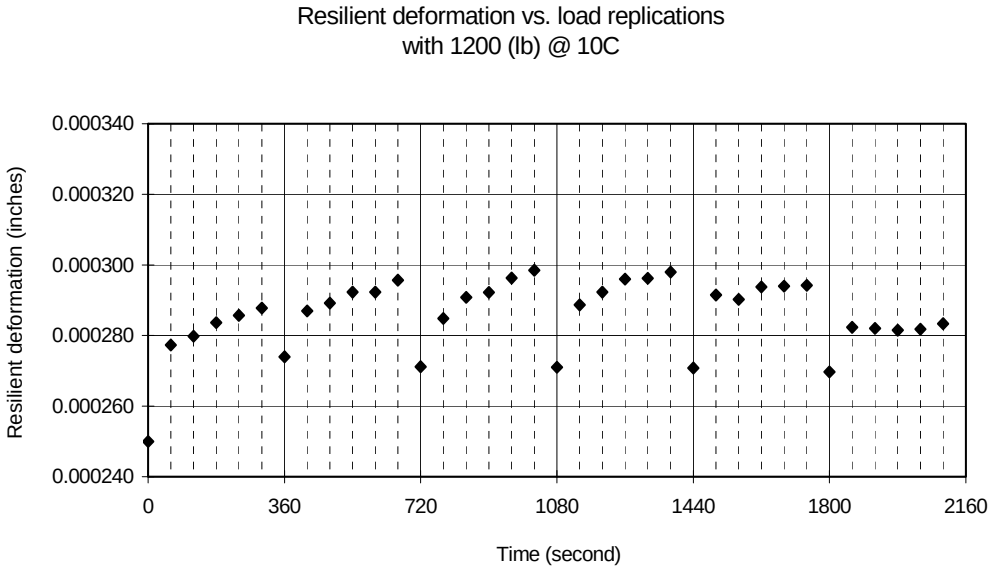

Figure D.7 Healing test (7.2% modified asphalt, Coarse 1, 1200 (lb) cyclic load at 10° C).

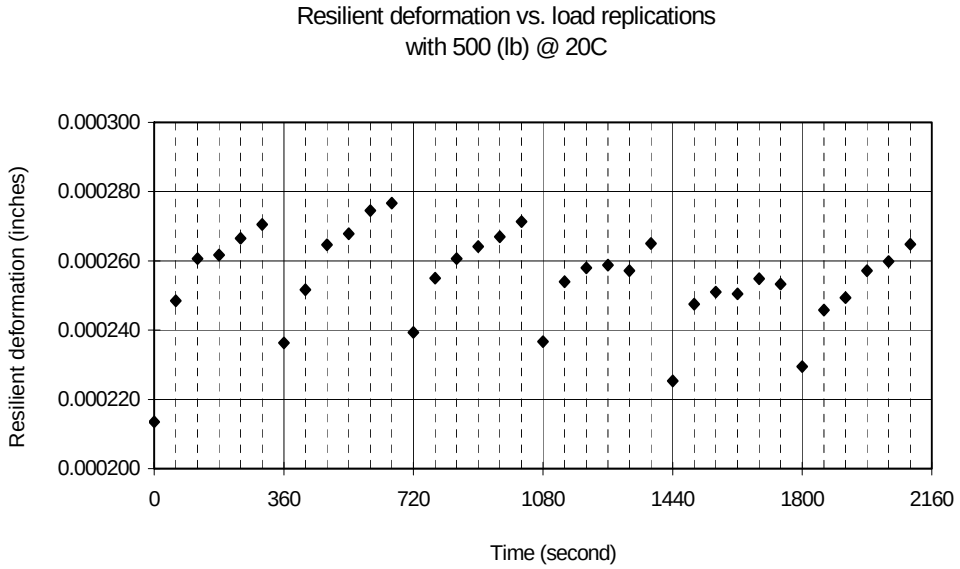

Figure D.8 Healing test (6.1% unmodified asphalt, Coarse 1, 500 (lb) cyclic load at 20° C).

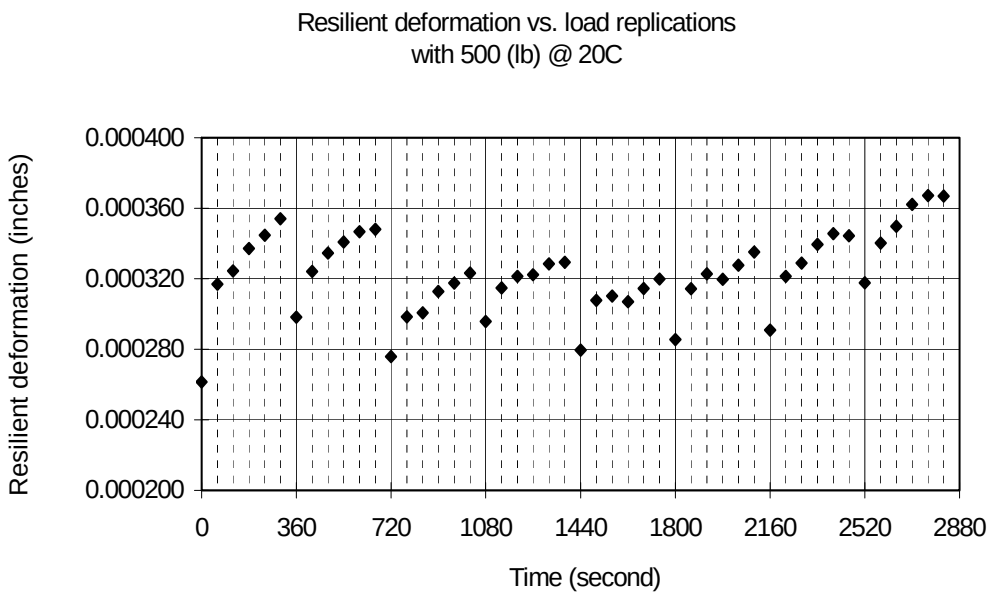

Figure D.9 Healing test (7.2% unmodified asphalt, Coarse 1, 500 (lb) cyclic load at 20° C).

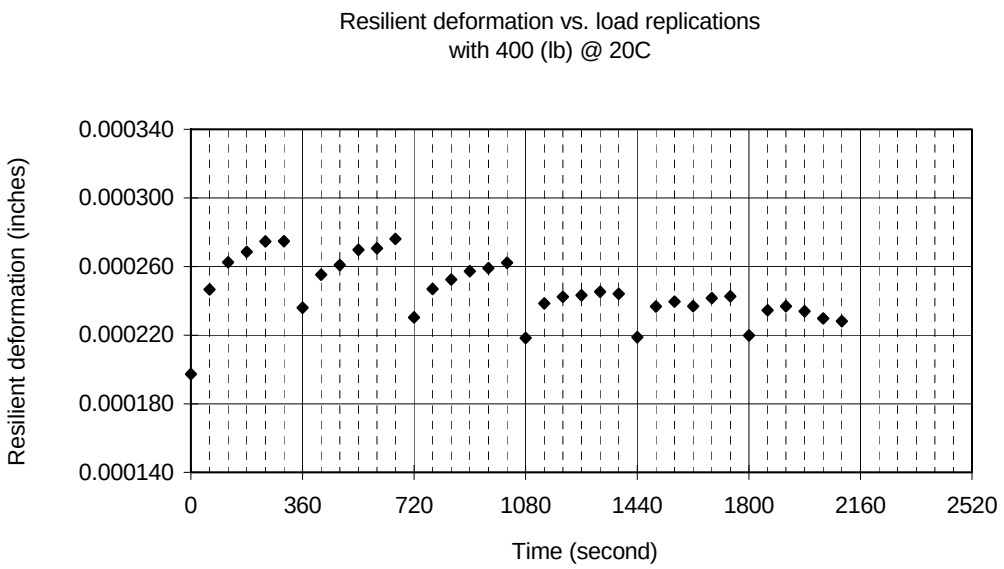

Figure D.10 Healing test (6.1% modified asphalt, Coarse 1, 400 (lb) cyclic load at 20° C).

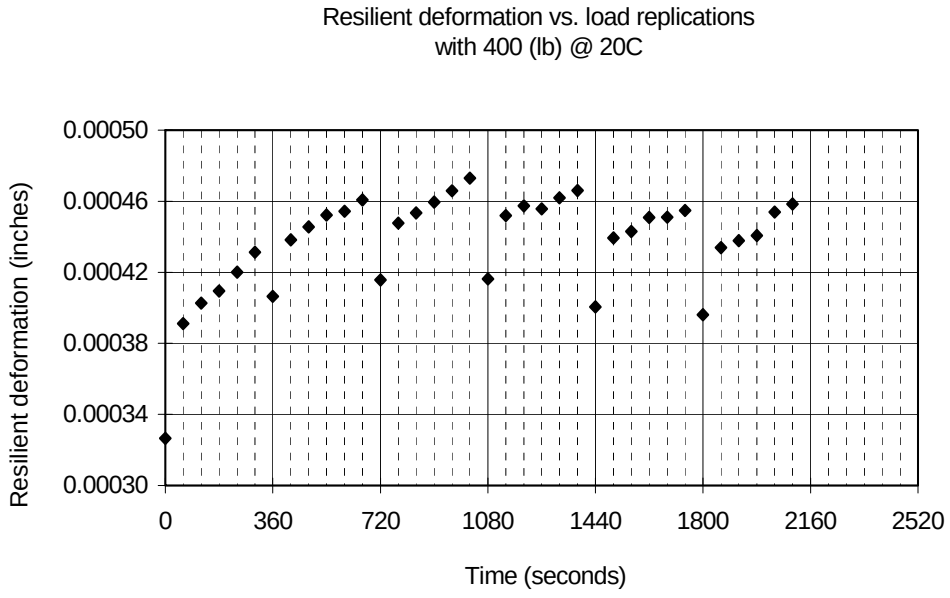

Figure D.11 Healing test (7.2% modified asphalt, Coarse 1, 400 (lb) cyclic load at 20° C).

APPENDIX E
AC LAYER THICKNESS FOR COST ANALYSIS

Table E.1 Tensile Stress at the Bottom of AC Layer to Meet ER_{min} for Conventional Pavement

(a) Low traffic ERmin = 1.1

m-value		0.60			0.45		
D_1*10^{-7} (1/psi)		14	10	6	14	10	6
$DCSE_f$ (KJ/m^3)	1.0	33.3	37.2	44.0	30.3	33.8	40.0
	2.0	17.1	19.0	22.4	15.5	17.3	20.4
	3.0	11.5	12.9	15.2	10.5	11.7	13.8
	4.0	8.8	9.8	11.5	8.0	8.9	10.5

(b) Medium traffic ERmin = 1.3

m-value		0.60			0.45		
D_1*10^{-7} (1/psi)		14	10	6	14	10	6
$DCSE_f$ (KJ/m^3)	1.0	31.5	35.2	41.6	28.7	32.0	37.9
	2.0	16.2	18.0	21.3	14.7	16.4	19.4
	3.0	10.9	12.2	14.4	10.0	11.1	13.1
	4.0	8.3	9.3	10.9	7.6	8.4	9.9

(c) High traffic ERmin = 1.7

m-value		0.60			0.45		
D_1*10^{-7} (1/psi)		14	10	6	14	10	6
$DCSE_f$ (KJ/m^3)	1.0	28.9	32.3	38.1	26.3	29.4	34.7
	2.0	14.8	16.5	19.5	13.5	15.1	17.8
	3.0	10.0	11.2	13.2	9.1	10.2	12.0
	4.0	7.6	8.5	10.0	6.9	7.7	9.1

Table E.2 AC Layer Thickness to Meet ER_{min} for Conventional Pavement

(a) Low traffic

m-value		0.60			0.45		
D_1*10^{-7} (1/psi)		14	10	6	14	10	6
$DCSE_f$ (KJ/m^3)	1	13.4	12.5	11.0	11.0	10.0	8.5
	2	11.5	10.5	9.1	9.0	7.9	5.3
	3	10.4	9.6	7.7	7.6	6.5	6.0
	4	9.5	8.5	6.4	6.3	6.0	6.0

(b) Medium traffic

m-value		0.60			0.45		
D_1*10^{-7} (1/psi)		14	10	6	14	10	6
$DCSE_f$ (KJ/m^3)	1	13.7	13.0	11.5	11.4	10.4	8.9
	2	11.8	11.0	9.5	9.5	8.3	7.0
	3	10.5	9.8	8.2	8.2	7.0	7.0
	4	9.9	8.9	7.0	7.0	7.0	7.0

(c) High traffic

m-value		0.60			0.45		
D_1*10^{-7} (1/psi)		14	10	6	14	10	6
$DCSE_f$ (KJ/m^3)	1	14.5	13.5	12.1	12.4	11.2	9.7
	2	12.5	11.6	10.2	10.2	9.2	8.5
	3	11.5	10.5	9.0	9.0	8.5	8.5
	4	10.6	9.7	8.5	8.5	8.5	8.5

Table E.3 AC Layer Thickness to Meet ER_{min} for HMA Full Depth Pavement

(a) Low traffic

m-value		0.60			0.45		
D_1*10^{-7} (1/psi)		14	10	6	14	10	6
$DCSE_f$ (KJ/m^3)	1	14.2	13.3	11.9	11.8	10.8	10.0
	2	12.3	11.3	10.0	10.0	10.0	10.0
	3	11.2	10.3	10.0	10.0	10.0	10.0
	4	10.4	10.0	10.0	10.0	10.0	10.0

(b) Medium traffic

m-value		0.60			0.45		
D_1*10^{-7} (1/psi)		14	10	6	14	10	6
$DCSE_f$ (KJ/m^3)	1	14.7	13.7	12.3	12.3	12.0	12.0
	2	12.7	12.0	12.0	12.0	12.0	12.0
	3	12.0	12.0	12.0	12.0	12.0	12.0
	4	12.0	12.0	12.0	12.0	12.0	12.0

(c) High traffic

m-value		0.60			0.45		
D_1*10^{-7} (1/psi)		14	10	6	14	10	6
$DCSE_f$ (KJ/m^3)	1	15.5	14.5	14.0	14.0	14.0	14.0
	2	14.0	14.0	14.0	14.0	14.0	14.0
	3	14.0	14.0	14.0	14.0	14.0	14.0
	4	14.0	14.0	14.0	14.0	14.0	14.0

Table E.4 AC Layer Thickness to Meet ER_{min} for HMA Overlay

(a) Low traffic

m-value		0.60			0.45		
D_1*10^{-7} (1/psi)		14	10	6	14	10	6
$DCSE_f$ (KJ/m^3)	1	7.4	6.5	5.0	5.0	4.0	3.0
	2	5.5	4.5	3.1	3.0	3.0	3.0
	3	4.4	3.6	3.0	3.0	3.0	3.0
	4	3.5	3.0	3.0	3.0	3.0	3.0

(b) Medium traffic

m-value		0.60			0.45		
D_1*10^{-7} (1/psi)		14	10	6	14	10	6
$DCSE_f$ (KJ/m^3)	1	6.7	6.0	4.5	4.4	3.5	3.5
	2	4.8	4.0	3.5	3.5	3.5	3.5
	3	3.5	3.5	3.5	3.5	3.5	3.5
	4	3.5	3.5	3.5	3.5	3.5	3.5

(c) High traffic

m-value		0.60			0.45		
D_1*10^{-7} (1/psi)		14	10	6	14	10	6
$DCSE_f$ (KJ/m^3)	1	6.0	5.0	4.5	4.5	4.5	4.5
	2	4.5	4.5	4.5	4.5	4.5	4.5
	3	4.5	4.5	4.5	4.5	4.5	4.5
	4	4.5	4.5	4.5	4.5	4.5	4.5

Table E.5 AC Layer Thickness and Tensile Stress of Unmodified AC Layer to Meet ER of Modified Mixture

			TRAFFIC 1	TRAFFIC 2	TRAFFIC 3
Conventional	Modulus(psi)	a & m	AC layer thickness to meet $ER_{PM\text{-}HMA}$		
AC (unmodified)	1,200,000	0.40	9.5	10.0	11.0
CRUSHED STONE BASE	40,000	0.14 & 1.2	8.5	10.5	10.0
SUBGRADE	10,000				
σ_t (psi) at the bottom of AC layer			114.6	103.6	88.4

			TRAFFIC 1	TRAFFIC 2	TRAFFIC 3
Full Depth	Modulus(psi)	a & m	AC layer thickness to meet $ER_{PM\text{-}HMA}$		
AC (unmodified)	1,200,000	0.40	12.3	14.4	16.5
SUBGRADE	10,000				
σ_t (psi) at the bottom of AC layer			83.2	64.2	50.1

			TRAFFIC 1	TRAFFIC 2	TRAFFIC 3
HMA Overlay	Modulus(psi)	a & m	AC layer thickness to meet $ER_{PM\text{-}HMA}$		
AC (unmodified) Overlay	1,200,000	0.40	5.5	6.0	6.5
AC (unmodified)	1,200,000	0.40	6.0	7.0	8.5
CRUSHED STONE BASE	40,000	0.14 & 1.2	8.5	10.5	10.0
SUBGRADE	10,000				
σ_t (psi) at the bottom of AC layer			84.2	68.8	50.8

REFERENCES

Aglan, H. A. 1997. "Polymer Modifiers for Improved Performance of Asphalt." *Asphalt Science and Technology*, Usmani, Marcel Dekker, pp. 197-216.

AASHTO. 1993. AASHTO Guide for Design of Pavement Structures. Washington, DC.

Bazin, P., and J. B. Saunier. 1967. "Deformability, Fatigue and Healing Properties of Asphalt Mixes." *Proceedings*, Second International Conference on the Structural Design of Asphalt Pavements, Ann Arbor, MI, pp. 553-569.

Button, J. W., D. N. Little, Y. Kim, and J. Ahmed. 1987. "Mechanistic Evaluation of Selected Asphalt Additives." *Proceedings*, Association of Asphalt Paving Technologists, Vol. 56, pp. 62-90.

Chomton, G., and P. J. Valayer. 1972. "Applied Rheology of Asphalt Mixes, Practical Applications." *Proceedings*, Third International Conference on the Structural Designing of Asphalt Pavements, London, Vol. I, pp. 241-232.

Collins, J. H., M. G. Bouldin, R. Gellens, and A. Berker. 1991. "Improved Performance of Paving Asphalt by Polymer Modification." *Proceedings*, Association of Asphalt Paving Technologists, Vol. 60, pp. 43-79.

Diani, E., M. Da Via, and M.Grazia Cavaliere. 1997. "Chemistry and Technology of SBS Modifier." *Asphalt Science and Technology*, Marcel Dekker Inc., New York, pp. 279-295.

Florida Department of Transportation. 2001. "Standard Specifications for Road and Bridge Construction 2000." State of Florida, Tallahassee, Section 334-4.2.1.

Grant, T. P. 2001. "Determination of Asphalt Mixture Healing Rate Using the Superpave Indirect Tensile Test." *Master's Thesis* (ME), University of Florida.

Jacobs, M. M. J., P. C. Hopman, and A. A. A. Molenaar. 1996. "Application of Fracture Mechanics Principles to Analyze Cracking in Asphalt Concrete." *Journal of the Association of Asphalt Paving Technologists*, Vol. 65, pp. 1-39.

Jajliardo, P. A. 2003. "Development of Specification Criteria to Mitigate Top-Down Cracking." *Master's Thesis* (ME), University of Florida.

Jones, S. D., K. C. Mahboub, R. M. Anderson, and H. U. Bahia. 1998. "Applicability of Superpave to Modified Asphalts–A Mixture Study." *Transportation Research Record 1630*, TRB, National Research Council, Washington, DC, pp. 42-50.

Khattak, M. J., and G. Y. Baladi. 1998. "Engineering Properties of Polymer Modified Asphalt Mixture." *Transportation Research Record 1638*, TRB, National Research Council, Washington, DC, pp.12-22.

Khattak, M. J., and G. Y. Baladi. 2001. "Fatigue and Permanent Deformation Models for Polymer-Modified Asphalt Mixtures." *Proceedings*, 80th Transportation Research Board, TRB ID No. 01-2813, Washington DC, January.

Kim, Y. R., D. N. Little, and F. C. Benson. 1990. "Chemical and Mechanical Evaluation on Healing Mechanism of Asphalt Concrete." *Journal of the Association of Asphalt Paving Technologists*, Vol. 59, pp. 240-275.

Kim, Y. R., S. L. Whitmoyer, and D. N. Little. 1994. "Healing in Asphalt Concrete Pavements: Is It Real?" *Transportation Research Record 1454*, Transportation Research Board, National Research Council, Washington, DC.

Kim, Y. R., and R. P. Wool. 1983. "A Theory of Healing at a Polymer-Polymer Interface." *Macromolecules*, Vol. 16, pp. 1115-1120.

Lee, H. J., and Y. R. Kim. 1998. "Viscoelastic Continuum Damage Model of Asphalt Concrete with Healing." *Journal of Engineering Mechanics*, Vol. 124, No. 11, pp. 1224-1232.

Little, D. N., R. L. Lytton, D. Williams, and Y. R. Kim. 1999. "An Analysis of the Mechanics of Microdamage Healing Based on the Application of Micromechanics First Principles of Fracture and Healing." *Journal of the Association of Asphalt Paving Technologists*, Vol. 68, pp. 501-542.

Lytton, R. L., C. W. Chen, and D. N. Little. 2001. "Microdamage Healing in Asphalt and Asphalt Concrete; Volume III: A Micromechanics Fracture and Healing Model for Asphalt Concrete." *Report FHWA-RD-98-143*, Texas Transportation Institute, Texas A&M University, College Station.

Monismith, C. L. 1981. "Fatigue Characteristics of Asphalt Paving Mixtures and Their Use in Pavement Design." *Proceedings*, Eighteenth Paving Conference, East Lansing, MI.

Monismith, C. L., J. A. Epps, and F. N. Finn. 1985. "Improved Asphalt Mix Design." *Proceedings*, Association of Asphalt Paving Technologists, Vol. 55, pp. 347-406.

Myers, L. A. 1997. "Mechanism of Wheel Path Cracking That Initiates at the Surface of Asphalt Pavements." *Master's Thesis*, University of Florida.

Myers, L. A. 2000. "Development and Propagation of Surface-Initiated Longitudinal Wheel Path Cracks in Flexible Highway Pavements." *Ph.D. Dissertation*, University of Florida.

Paris, P. C., and F. Erdogan. 1963. "A Critical Analysis of Crack Propagation Laws." Transactions of the ASME, *Journal of Basic Engineering*, Series D, 85, No. 3.

Read, J. M., and A. C. Collop. 1997. "Practical Fatigue Characterization of Bituminous Paving Mixtures." *Journal of the Association of Asphalt Paving Technologists*, Vol. 66, pp. 74-108.

Roque, R., W. G. Buttlar, B. E. Ruth, M. Tia, S. W. Dickson, and B. Reid. 1997. "Evaluation of SHRP Indirect Tension Tester to Mitigate Cracking in Asphalt Pavements and Overlays." *Final Report* for Florida Department of Transportation, University of Florida, Gainesville, August.

Roque, R., Z. Zhang, and B. Sankar. 1999. "Determination of Crack Growth Rate Parameter of Asphalt Mixtures Using the Superpave IDT." *Journal of the Association of Asphalt Paving Technologists*, Vol. 68, pp. 404-433.

Rouse, M. W. 1997. "Production, Identification, and Application of Crumb Rubber Modifier for Asphalt Pavements." *Asphalt Science and Technology*, Marcel Dekker Inc., New York, pp. 279-295.

Schapery, R. A. 1984. "Correspondence Principles and a Generalized J-integral for Large Deformation and Fracture Analysis of Viscoelastic Media." *International Journal of Fracture*, Vol. 25, pp. 195-223.

Sebaaly, P. E. 1997. "Rheological Properties of Polymer-Modified Asphalt Binders." *Asphalt Science and Technology*, Marcel Dekker Inc., New York, pp. 235-247.

Tayebali, A., J. A. Deacon, J. S. Coplantz, J. T. Harvey, and C. L. Monismith. 1994. "Mix and Mode-of Loading Effects on Fatigue Response of Asphalt-Aggregate Mixes." *Proceedings*, Association of Asphalt Paving Technologists, Vol. 63, pp. 118-151.

Tayebali, A., G. Rowe, and J. Sousa. 1992. "Fatigue Response of Asphalt-Aggregate Mixtures." Paper Presented at the Annual Meeting of the Association of Asphalt Paving Technologists.

Usmani, A. M. 1997. "Polymer Science and Technology." *Asphalt Science and Technology*, Marcel Dekker Inc., New York, pp. 307-336.

van Dijk, W. 1975. "Practical Fatigue Characterization of Bituminous Mixes." *Proceedings*, Association of Asphalt Paving Technologists, Vol. 44, pp. 38-75.

van Dijk, W., and W. Visser. 1977. "The Energy Approach to Fatigue for Pavement Design." *Journal of the Association of Asphalt Paving Technologists*, Vol. 46, pp. 1-38.

Wegon, V., and B. Brûlé. 1999. "The Structure of Polymer Modified Binders and Corresponding Asphalt Mixtures." *Proceedings*, Association of Asphalt Paving Technologists, Vol. 68, pp. 64-88.

Wool, R. P., and K. M. O'Connor. 1981. "A Theory of Crack Healing in Polymers." *Journal of Applied Physics*, Vol. 52, No. 10, pp. 5953-5963.

Zhang, Z. 2000. "Identification of Crack Growth Law for Asphalt Mixtures Using the Superpave Indirect Tensile Test (IDT)." *Ph.D. Dissertation*, University of Florida.

Zhang, Z., R. Roque, and B. Birgisson. 2001. "Identification and Verification of a Suitable Crack Growth Law." *Journal of the Association of Asphalt Paving Technologists*, Vol. 70, pp. 206-241.